การวิเคราะห์เอเมอร์จีและเอกเซอร์จีของนิคมอุตสาหกรรมเชิงนิเวศน์ฐานชีวภาพ

นางสาวปรารถนา นิมมานเทอดวงศ์

วิทยานิพนธ์นี้เป็นส่วนหนึ่งของการศึกษาตามหลักสูตรปริญญาวิทยาศาสตรดุษฎีบัณฑิต
สาขาวิชาเคมีเทคนิค ภาควิชาเคมีเทคนิค
คณะวิทยาศาสตร์ จุฬาลงกรณ์มหาวิทยาลัย
ปีการศึกษา 2559

EMERGY AND EXERGY ANALYSES OF A BIO-BASED ECO-INDUSTRIAL PARK

Miss Prathana Nimmanterdwong

A Dissertation Submitted in Partial Fulfillment of the Requirements
for the Degree of Doctor of Philosophy Program in Chemical Technology
Department of Chemical Technology
Faculty of Science
Chulalongkorn University
Academic Year 2016

Thesis Title	EMERGY AND EXERGY ANALYSES OF A BIO-BASED ECO-INDUSTRIAL PARK
By	Miss Prathana Nimmanterdwong
Field of Study	Chemical Technology
Thesis Advisor	Professor Dr. Pornpote Piumsomboon
Thesis Co-Advisor	Associate Professor Dr. Benjapon Chalermsinsuwan

---

Accepted by the Faculty of Science, Chulalongkorn University in Partial Fulfillment of the Requirements for the Doctoral Degree

....Dean of the Faculty of Science
(Associate Professor Dr. Polkit Sangvanich)

THESIS COMMITTEE

....Chairman
(Associate Professor Dr. Prasert Reubroycharoen)

....Thesis Advisor
(Professor Dr. Pornpote Piumsomboon)

....Thesis Co-Advisor
(Associate Professor Dr. Benjapon Chalermsinsuwan)

....Examiner
(Professor Dr. Somkiat Ngamprasertsith)

....Examiner
(Associate Professor Dr. Prapan Kuchonthara)

....External Examiner
(Associate Professor Dr. Thumrongrut Mungcharoen)

ปรารถนา นิมมานเทอดวงศ์ : การวิเคราะห์เอเมอร์จีและเอกเซอร์จีของนิคมอุตสาหกรรมเชิงนิเวศน์ฐานชีวภาพ (EMERGY AND EXERGY ANALYSES OF A BIO-BASED ECO-INDUSTRIAL PARK) อ.ที่ปรึกษาวิทยานิพนธ์หลัก: ศ. ดร. พรพจน์ เปี่ยมสมบูรณ์, อ.ที่ปรึกษาวิทยานิพนธ์ร่วม: รศ. ดร. เบญจพล เฉลิมสินสุวรรณ, 186 หน้า.

ปัจจุบันกระบวนการใช้ประโยชน์จากชีวมวลเพื่อลดการพึ่งพาทรัพยากรใช้แล้วหมดไปเป็นกลยุทธ์สำคัญในการจัดการปัญหาสิ่งแวดล้อม โดยการพัฒนากระบวนการผลิตจำเป็นต้องดำเนินการแบบเป็นองค์รวม "นิคมอุตสาหกรรมเชิงนิเวศน์" เพื่อลดมลภาวะและใช้ทรัพยากรภายในระบบให้เกิดประสิทธิภาพสูงสุด งานวิจัยนี้มีเป้าหมายเพื่อพัฒนาเครื่องมือประเมินความยั่งยืนของระบบเพื่อใช้ในการตัดสินใจ โดยการพัฒนาอัลกอริทึมในการคำนวณเอเมอร์จีด้วยภาษา MATLAB ซึ่งมีส่วนประมวลผลสองส่วน ได้แก่ 1) ส่วนการค้นหาเส้นทางของเอเมอร์จี และ 2) ส่วนการคำนวณปริมาณเอเมอร์จี ซึ่งจากการทดสอบพบว่าอัลกอริทึมที่พัฒนาขึ้นสามารถคำนวณเอเมอร์จีได้อย่างแม่นยำ จากนั้นจะนำอัลกอริทึมที่ได้ไปประเมินระบบนิเวศน์อุตสาหกรรมฐานชีวภาพที่สร้างขึ้นด้วยโปรแกรม ASPEN PLUS โดยใช้หญ้าเนเปียร์ที่ปลูกในไทยมาเป็นตัวแทนชีวมวล จากการวิเคราะห์พบว่าเอเมอร์จีส่วนใหญ่ที่ใช้ไปในขั้นการปลูกคือแรงงานคนและน้ำมันดีเซล ค่าความยั่งยืน (ESI) ของภาคการปลูกกับความยั่งยืนของทั้งระบบอยู่ที่ 0.29 และ 0.10 ตามลำดับ ทั้งนี้เนื่องจากภาคอุตสาหกรรมมีการใช้ทรัพยากรจากภายนอกระบบและเป็นทรัพยากรที่ไม่หมุนเวียน แต่เมื่อนำเอเมอร์จีต่อหน่วยผลิตภัณฑ์ทั้ง 4 ชนิด ได้แก่ เชื้อเพลิงเหลว เมทานอล ไอน้ำ และไฟฟ้า ที่ได้จากการผลิตแบบบูรณาการเทียบกับระบบที่มีอยู่ในปัจจุบัน พบว่าระบบแบบบูรณาการใช้เอเมอร์จีอย่างมีประสิทธิภาพกว่าระบบปัจจุบัน สุดท้ายทำการวิเคราะห์เอเมอร์จีเปรียบเทียบกับเอเซอร์จี พบว่าทั้งสองวิธีให้แนวโน้มที่ต่างกันเนื่องจากทั้งสองทฤษฎีมีมุมมองคนละด้าน เอกเซอร์จีเหมาะที่จะใช้อธิบายประสิทธิภาพของระบบแต่ละหน่วยย่อย ในขณะที่เอเมอร์จีจะอธิบายการใช้ทรัพยากรของระบบตั้งแต่ต้นทางไปถึงผลิตภัณฑ์สุดท้ายซึ่งเป็นภาพที่กว้างกว่า สะท้อนภาพความยั่งยืนของกระบวนการได้ดีกว่า

ภาควิชา	เคมีเทคนิค	ลายมือชื่อนิสิต	....
สาขาวิชา	เคมีเทคนิค	ลายมือชื่อ อ.ที่ปรึกษาหลัก	....
ปีการศึกษา	2559	ลายมือชื่อ อ.ที่ปรึกษาร่วม	....

5572862323 : MAJOR CHEMICAL TECHNOLOGY
KEYWORDS: EMERGY ANALYSIS / EXERGY ANALYSIS / BIOREFINERY

PRATHANA NIMMANTERDWONG: EMERGY AND EXERGY ANALYSES OF A BIO-BASED ECO-INDUSTRIAL PARK. ADVISOR: PROF. DR. PORNPOTE PIUMSOMBOON, CO-ADVISOR: ASSOC. PROF. DR. BENJAPON CHALERMSINSUWAN, 186 pp.

The recent development of biomass utilization systems to reduce the dependence on non-renewable resources is an effective strategy to achieve a sustainable solution. The evolution of bio-production requires industrial symbiosis strategies called 'eco-industrial park' to achieve lower pollution emission and resource consumption. The aim of this study is to provide a sustainability decision tool called emergy accounting analysis using MATLAB language which consists of two components; 1) the search of emergy pathways and 2) the computation of emergy flow. The algorithm has been validated and found to be accurate. Then, the algorithm was applied to a bio-based eco-industrial park model which was developed using ASPEN PLUS. Napier grass (Pennisetum purpureum) grown in Thailand was used as a representative feedstock. The main emergy support the cultivation were human labor resources and diesel consumption. The sustainability indicator (ESI) of the cultivation and the entire system were 0.29 and 0.10, respectively. The reason is that the industrial section relied on imported and non-renewable resources. The integrated biorefinery system with four main products (liquid fuels, methanol, steam and electricity) achieves higher performance in terms of the emergy compared to the existing alternative processes. Finally, emergy and exergy analyses were compared. The exergy analysis provides an insight view mainly on the efficiency of the specific process, while the emergy analysis gives a broader view of the resource supporting to the entire system.

Department:	Chemical Technology	Student's Signature	....
Field of Study:	Chemical Technology	Advisor's Signature	....
Academic Year:	2016	Co-Advisor's Signature	....

ACKNOWLEDGEMENTS

I would like to express my deep gratitude to Professor Dr. Pornpote Piumsomboon, my research supervisor, for his patient guidance, enthusiastic encouragement and all valuable knowledges. I would also like to thank Associate Professor Dr. Benjapon Chalermsinsuwan, my research co-advisor, for his advice and assistance in keeping my progress on schedule. I also would like to express my appreciation to Professor Hanne Østergård and her students, Andreas and Lise, who had opened my mind to emergy and sustainable livings. Also, thanks to Watchara for all supports and always being a good friend. Thanks to all Cybernetics Laboratory colleagues for a joyful atmosphere that always encouraged my work. I would also like to extend my gratitude to the staff member of the Chemical Technology department for their help in offering me the resources to complete this work.

Finally, I am eternally grateful to my beloved parents and sisters for their supports and encouragement.

This study was financially supported by the 60/40 Support for Tuition Fee and Overseas Research Experience Scholarship for Graduate Student, Chulalongkorn University.

CONTENTS

Page

CHAPTER I: INTRODUCTION

1.1.Background

Natural resources are utilized for supporting human life. It formulates by natural processes and forces persistent in natural environment. Renewable resources are resources that can be replenished or reformed either by nature or by systemic recycling of used resources. Non-renewable resources, known as a finite resource, do not renew itself at a sufficient rate leading to resource depletion. Nowadays, the industry has grown enormously with the support of new technologies. The growth of industry gives advantages in economic viewpoint. As industry populations and consumption growing faster, greater waste volumes are generated. Such technologies also produce more complex waste where traditional treatment becomes particularly difficult. Therefore, practical application of sustainable development strategies in activities of industrial enterprises is becoming an important aspect. To evaluate sustainable development in both economic and environmental terms, two major issues must be realized. The first one is, do natural resources sufficient to drive the human society. The second one is, how to deal with the environmental issues which become more severe due to higher amount of waste generated and larger resource consumptions. In the recent years, the idea of eco-industrial park becomes one of the most common concrete applications of industrial development. With the close loop concept of material and energy through reuse and recycling, the used materials and energy become optimal use; also, waste generation is minimized.

The purpose of this study is to evaluate the process sustainability based on exergy and emergy theories of the bio-based eco-industrial park which can reduce the environmental burden, minimize material consumptions and waste, maximize energy efficiency and provides sustainable and economical perspectives for further development.

1.2. Objectives

1.2.1. Develop computational tool based on emergy theory for process sustainability analysis.

1.2.2. Develop process models for a bio-based eco-industrial park focused on chemical and biofuel production based on napier grass

1.2.3. Perform exergy and emergy analyses of the developed eco-industrial park

1.2.4. Analyze the results of exergy and emergy analyses in the aspect of the proper sustainability indicators.

1.3. Scope of dissertation

1.3.1. Achieve a bio-based eco-industrial park model developed using ASPEN PLUS which provide sustainable perspective for further development.

1.3.2. Achieve the computational tool based on emergy algebra using MATLAB for process sustainability analysis.

1.3.3. Achieve the results of exergy and emergy analyses in the aspect of the proper sustainability indicators.

CHAPTER II: THEORY AND LITERATURE REVIEWS

The industrial production of chemicals and energy carriers has grown enormously with the support of new technologies. This growth has advantages from an economic viewpoint, but as industrial production expands, driven by increased populations, then greater waste volumes are generated. Considering only one side of the coin cannot lead us for long-term sustainability. A proper assessment is needed to provide broader aspects.

2.1. Biorefinery

The issues about resource depletion and environmental degradation have driven us for rapid shift to alternative production from renewable feedstock. To achieve the energy and climate goals, the idea of extracting energy from biomass-biological materials has been introduced. The facility that converts those materials into fuels, energy, chemicals and materials is what we call biorefinery (see Figure II.1). A variety of different inputs/feedstocks and conversion technologies can be employed to biorefineries system. The recent improvement of biomass utilization systems to reduce the dependence on fossil fuels has been encouraged to provide a sustainable development for the near future. Where a *sustainable development* was defined as "development that meets the needs of the present without compromising the ability of future generations to meet their own needs" (Brundtland, 1987). To achieve the context, effective strategies should fully integrate three relative dimensions including; economic, social and environmental.

2.1.1. Sustainability in Terms of Socio-Economic Aspect

The expansion of bioenergy seems to have substantial impact on social and economic development. After the fossil fuels crisis, global raises awareness to the fluctuation of oil prices due to dependent upon fossil fuels. Diversification of fuel sources obviously provides advantages strategy for reducing the risks from fossil fuels dependency. It can solve long term fuel price fluctuations which have huge impacts to global economy (Neff, 1997). Moreover, supporting the use of biomass for industrial production can increase employment and rural development (Berndes and Hansson, 2007).

However, increased demand for bioenergy can be both advantages and disadvantages. It is important to clearly determine the magnitude of the following variables; (1) the competitiveness of alternative fuels (other than biofuels), (2) the labor intensity of the bioenergy system and (3) rural wages affected from increased bioenergy demand. If the bioenergy costs higher than alternative fuels (other than biofuels), the demand will shift away from bioenergy. This will lead to negative effects on rural labor employment. Even though the bioenergy has been supported by subsidies, it will make government spending away from health, education and other social services. Also, changes in bioenergy prices affects the nation economy. Since Thailand is a major exporter in agricultural goods, if increased bioenergy can reduce net energy imports and increase domestic exports, bioenergy can be socio-economically competitive.

2.1.2. Sustainability in Terms of Environmental Aspect

Regarding to the environmental aspect, bioenergy promises to decrease the fossil greenhouse gas (GHG) emissions dominated by fossil-based fuels from the transportation sector. Therefore, the ideal biofuels must be drawn from the feedstock that provides lower greenhouse gas emission than conventional fossil fuels through their life cycle. There are many options available as shown in Figure II.2 such as first-generation ethanol from sugar or carbohydrates (food crops) or biodiesel from vegetable oil.

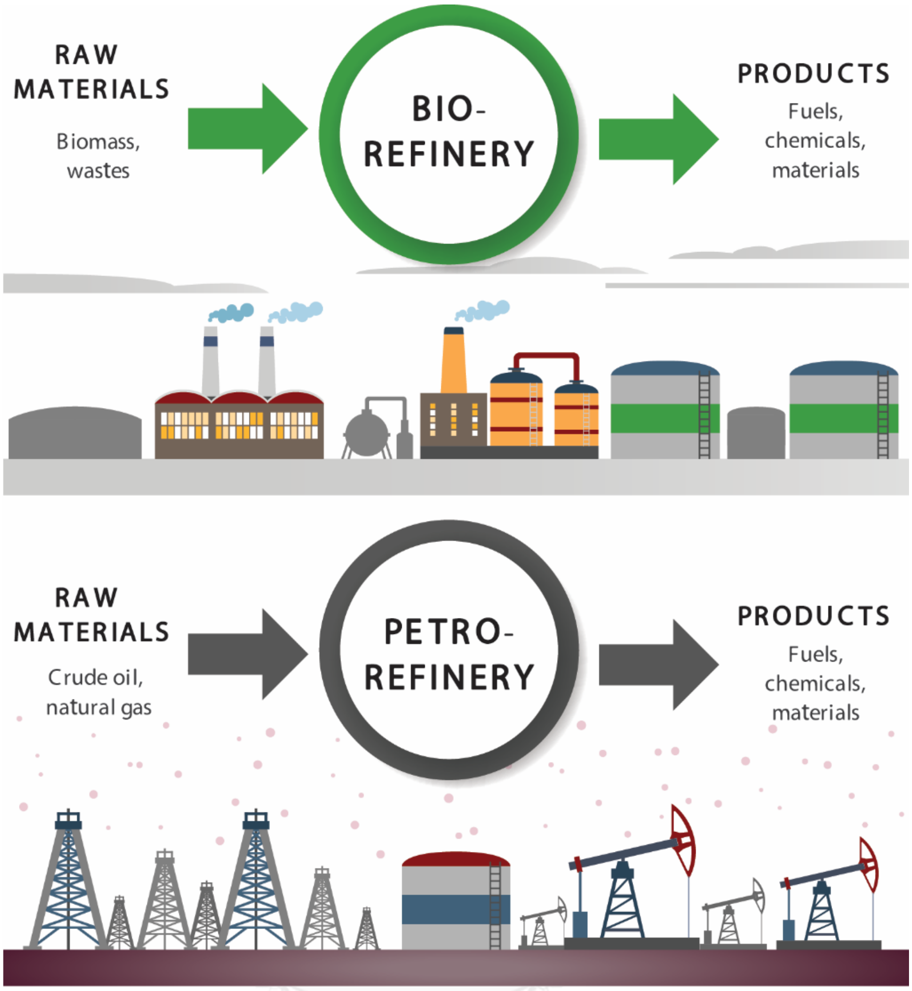

Figure II.1. Bio-based refinery and petrol-based refinery

However, using biomass as a feedstock in a biorefinery to convert the biological materials into fuels and chemicals is still in a nascent state. The promotion of non-edible crops as the main feedstock to produce bio-energy may replace arable land with biofuel crops. Also, growing the biomass requires large area of land to provide sufficient feed rate to the biorefinery. In this case, industries can either directly use food crops as feedstock or replace existing land for food crops with energy crops which would cause higher food prices and triggers the farmers to clearing more forest to grow more food crops (Tilman et al., 2009). Alternatively, biomass residues, such as straw, husk and other agricultural co-products is one type of promising feedstock for advanced biofuels. Another is perennial warm-season grasses, such as Napier grass (Pennisetum purpureum), Miscanthus (Morandi et al., 2016), Indiangrass and switchgrass (Felix and Tilley, 2009), could be alternative energy crops on marginal or degraded lands abandoned from agricultural use since they could be produced reasonable yields even under these conditions with low maintenance (Campbell et al., 2008). Napier grass, which has been widely used to feed local cattle in Thailand and recently promoted as a bioenergy crop by the Thai government, is studied here as an example of a lignocellulosic bioenergy feedstock.

An important concern for utilizing biomass as a substitution for primary fuel is that biomass production at present indirectly involves consumption of non-renewable resources (Giampietro et al., 1997). The question arises whether the present bio-based technologies can potentially replace the existing fossil-based processes in both economic and environmental aspects.

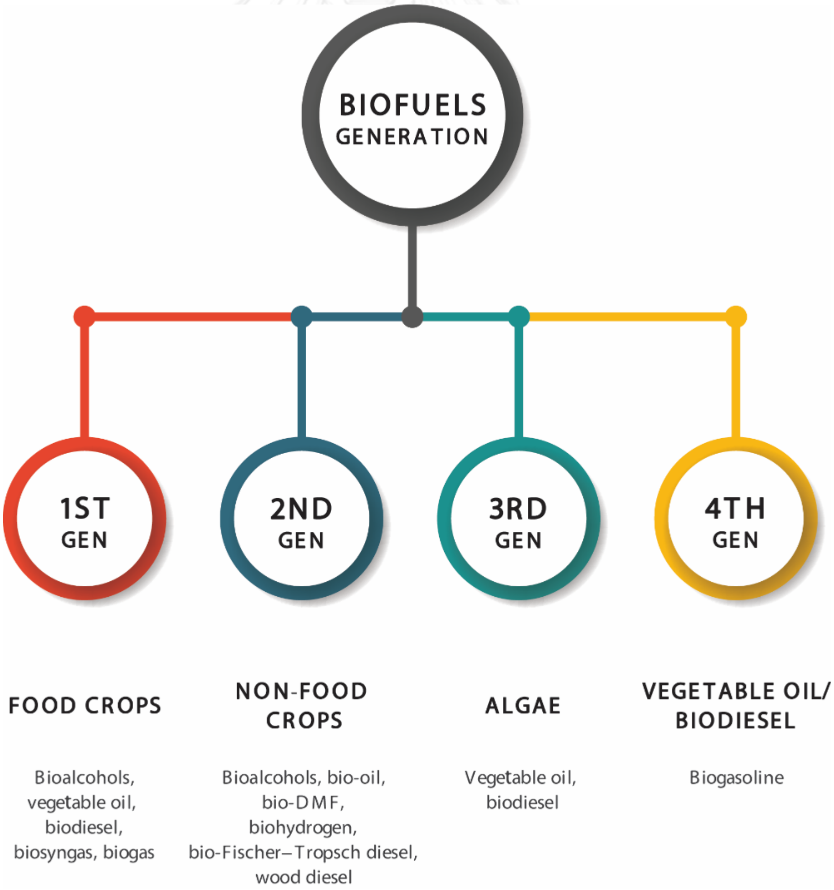

Figure II.2. Biofuels generation (Pandey, 2011)

2.2. Emergy at First Glance

The original definition of emergy is "the available energy of one kind previously used up directly and indirectly to make a product or service." (Odum 1996). Unlike energy which indicates the present amount of available work. Its concept is to express the record of all resources used by the biosphere in earlier steps to produce a product or service. By tracing back every form of energy and matters that utilized along the transformation process into one kind of energy, which is solar energy in this case. This idea provides the quantitative indicators involving the resource use and the percent renewability of the systems. It also gives us broader viewpoint of how the resources utilized in the processes and how systems interacted with each other. As the engineers, we do research to find every feasible way to create the better technology to support our need. However, as everybody knows, due to fossil fuel depletion and environmental degradation, we cannot look for only the technologies that gives higher economic benefits. From all those inventions we created, we have to decide how to choose the solution from them, the one with the most sustainable process. But considering only one side of the coin cannot lead us for long-term sustainability. Two major issues on sustainable industrial development must be concerned; (1) do we still have enough resources for the future production processes? and (2) how can the industries deal with crucial environmental issues caused by the production processes? So, in this dissertation, the emergy analysis will be introduced as a tool for sustainable decision-making.

2.2.1. Development of Emergy Analysis

Over the past decades, several tools and methods have been proposed to provide comprehensive criteria guidance for decision-making, such as techno-economic (Swanson et al., 2010), life cycle analysis (Owens, 1997), exergy (Dincer and Rosen, 2012) and emergy analyses (Odum, 1996). The techno-economic studies provide the economic feasibility aspect whether the production process gives benefits in the range of the given time. By using feasibility analysis, Fontoura (Fontoura et al., 2015) found that converting an Elephant grass into a biorefinery adds value is economically feasible. However, the value of the present products is temporary and inverse to real wealth. Thus, the economic benefit does not reflect long term sustainability. The life cycle analysis (LCA) is a method defined to analyze the environmental impacts of the production system by focusing on emission throughout the life cycle of the analyzed product. By using LCA, Chang (Chang et al., 2017) two bioethanol production schemes (using Napier grass and short rotated Eucalyptus as feedstocks) were compared and the analysis could identify the process that provided lower environmental impact. Thus, the LCA could provide the guidance for process improvement in the aspect of environment. However, the LCA analysis does not take the aspect of economics into consideration.

In the mid-1900s, Howard Odum defined the word 'EMERGY' which stands for 'embodied energy' to represent the real value of energies (materials, heat, electricity, fuels, chemicals, information, etc.) through their transformation processes. As the ecologist, he employed his knowledge into the concept by using the system connections in the ecology to explain how things created and traced back into their original energy source. Thus, every form of energy can be converted into one energy equivalent form. It includes the amount of free natural inputs (solar, wind, rain, geothermal, etc.) and economic inputs (materials, man-made energy, and labors) to the system and is expressed in units of solar equivalent joule (sej).

Emergy approach has been applied to various systems, such as crop cultivations (Morandi et al., 2016; Nimmanterdwong et al., 2015), biorefineries (Kamp and Østergård, 2013; Patrizi et al., 2015), power production (Sha and Hurme, 2012) and waste treating systems (Londoño et al., 2017). In the previous work, the feasibility of two agricultural crops, oil palm and Jatropha, as bioenergy feedstocks in Thailand was evaluated to identify suitable species for energy sources (Nimmanterdwong et al., 2015). By using emergy accounting, it was found that oil palm required less emergy input per unit biomass and had a higher renewability than Jatropha. Thus, oil palm was the preferable choice for the biorefinery. Moreover, by using emergy analysis, we could point out that large portion of human labor required for harvesting and transporting in the biomass cultivation stage. Neglecting this portion of energy may probably cause a misleading conclusion. The study on cultivating Miscanthus as energy crop reveals that different logistic strategies affect the emergy used or the environmental cost of the entire process (Morandi et al., 2016). The recent emergy study was done on the bioethanol production in Siena, Italy. It was found that using local resources (straw and residual geothermal heat) to produce bioethanol provided an appropriate solution for fossil fuels substitution (Patrizi et al., 2015). Nevertheless, by using emergy assessment, it was also found that the biorefineries do not completely use renewable resources. Most bioenergy such as bioethanol (Pereira and Ortega, 2010) and biodiesel (Cavalett and Ortega, 2010) production processes still require supplemental non-renewable resources. Emergy accounting methodology has been developed over decades as an alternative tool for decision making, and it provides a more comprehensive view of sustainability than that provided by other methods. However, there are many criticisms on the practical aspects of emergy approach due to its uncertainties of the calculation data. Since the procedure involved with large amount of data and lots of assumptions had been made through the calculations. Thus, many researches attempted to make emergy analysis be more consistence by created rules, constraints or alternative procedures for the calculations e.g. (Kamp and Østergård, 2013; Tennenbaum, 2015; Zarbá and Brown, 2015). Nevertheless, novel concepts about emergy has not been steady. It needs to be studied further to make the idea be more consistent and more accepted. Still, many researches, this dissertation also, followed the early emergy concept in Odum's book (Odum, 1996). However, besides conserving the original emergy rules, this dissertation also provided some discussions about the novel emergy concepts and suggestions about how to implement emergy assessment to the industrial production processes.

2.3. Basic Theory for Emergy Evaluation

The concept of emergy is to express the record of all resources used by the biosphere in earlier steps to produce a product or service. Unlike energy which indicates the present amount of available energy, emergy provides all the past record of energy required to produce product stream(s). Sometimes it is called energy memory. The unit emergy value (UEV, its unit was sej/J, or sej/kg or sometimes sej/$, depending on the unit of the considered stream) indicates the amount of emergy required to produce a unit of product(s). A higher UEV value means a larger amount of emergy input is required for the process to obtain the product(s). When comparing products or processes, the UEV can be used to reveal the resource use efficiency of the system, where the product with a lower UEV has a higher production efficiency.

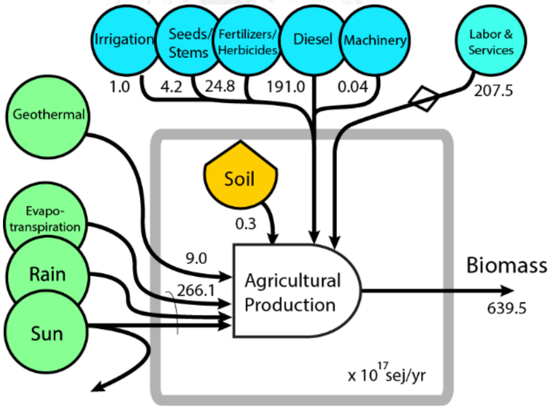

Figure II.3. An example of emergy diagram for agricultural production process.

*Remark: some literatures called UEV as ‘transformity’, ‘specific emergy’ or ‘emergy per unit Money’.

With the existence of the input UEVs from previous literatures, the given data such as mass, energy, money flow can be converted to emergy by multiplying them with relevant UEVs. For example, Figure II.3 represents the emergy diagram for napier grass cultivation in this study. Each number on the stream line indicates the amount of emergy input to the cultivation. Table II.1 is constructed from the diagram (full information of the table was shown in the supplementary section). Where resource flow, labor and energy in the third column are converted into emergy unit (in the sixth column) by using the UEVs from the literatures (in the fifth column). In the table, column 3 indicates the amount of energy flow (J), material flow (kg) and manpower (US$). The unit emergy value (UEV) in column 5 was obtained from previous studies, and is the amount of emergy required by the system per one unit of product(s), typically as sej/J, or sometimes sej/kg, depending on the unit of the input (Odum, 1996). In this study, the UEVs based on the early solar emergy baseline were corrected using Eq. (2.1);

$$UEV = UEV_e \times (Em_{global} / Em_{global,e}), \qquad (2.1)$$

where UEV_e and $Em_{global,e}$ indicate the un-updated UEV and global emergy from early years and Em_{global} is the latest global emergy (1.20×10^{25} sej/y; baseline year 2016) obtained from (Brown and Ulgiati, 2016).

The emergy flow was then estimated by Eq. (2.2);

$$Em_i = UEV_i \times En_i, \qquad (2.2)$$

where Em and UEV are the emergy and unit emergy value, respectively, and En is the amount of raw data, such as energy flow, mass flow or manpower. The subscript i represents the index of input stream i. By using Eq. (2.2), the emergy of the input streams in column 3 was calculated by multiplying the input with the UEV per unit input in column 5. For example, the emergy of diesel consumption in the Napier grass cultivation accounted for 1.91×10^{19} sej/y, obtained by multiplication of the diesel annual energy consumption (1.35×10^{14} J/y) and diesel UEV (1.41×10^{5} sej/J). After every emergy input in column 6 was calculated, the total emergy required for the system to accomplish the task was obtained.

Table II.1 Emergy accounting table of Napier grass cultivation

Note	Item	Amount	Units	UEV* (sej/unit)	Emergy flow (sej/y)
1	Agricultural phase				
	Natural renewable resources (R)				
1.1	Solar insolation**	2.30×10^{17}	J/y	1	2.30×10^{17}
1.2	Rain (Chemical potential)**	2.60×10^{14}	J/y	2.31×10^{4}	6.01×10^{18}
1.3	Geothermal	5.64×10^{13}	J/y	1.60×10^{4}	9.04×10^{17}
1.4	Evapotranspiration	3.48×10^{14}	J/y	6.10×10^{4}	2.12×10^{19}
	Natural non-renewable resources (N)				
1.5	Net loss of top soil	1.92×10^{11}	J/y	1.58×10^{5}	3.03×10^{16}
	Imported resource (F)				
1.6	Water (irrigation)	1.18×10^{12}	J/y	8.76×10^{4}	1.03×10^{17}
1.7	Initial napier stem	1.72×10^{6}	kg/y	2.43×10^{11}	4.18×10^{17}
1.8	Fertilizers	1.47×10^{6}	kg/y	1.68×10^{12}	2.48×10^{18}
1.9	Diesel consumption	1.35×10^{14}	J/y	1.41×10^{5}	1.91×10^{19}
1.10	Machinery	6.01×10^{4}	kg/y	6.90×10^{10}	4.15×10^{15}
	Labor and services (L)				
1.11	Direct labor (man-hour UEV)	1.49×10^{6}	h/y	9.06×10^{12}	1.35×10^{19}
1.12	Indirect labors (global EMR as UEV)	3.56×10^{6}	$/y	1.73×10^{12}	7.25×10^{18}
	Product:				
1.13	Napier grass	2.63×10^{8}	kg/y	2.43×10^{11}	6.39×10^{19}
		4.73×10^{15}	J/y	1.35×10^{4}	

*References for the UEVs were given in the appendix.

**Total used emergy is calculated without double counting of co-products, according to the emergy algebra.

2.3.1. Emergy and Energy Hierarchy

Understanding how energy involves with our system and how it reacts between other systems would give us broader view and explain how it affects to the surrounding environment. This complexity can be understood by a simple illustration, the energy system diagram. The system diagramming will help us easily to recognize and visualize the flows and behaviors of the systems. It shows how energy or other forms of energy such as materials, money, electricity or human power interacts to produce outputs to the ecosystem. The hierarchy also explains the way emergy accounted and how much energy of each kind required for another. Figure II.4 depicts symbols representing each type used in construction of an emergy diagram for a system.

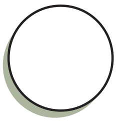

Emergy source: A source of energy input to the system outside the boundary.

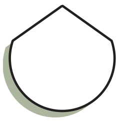

Emergy storage tank: An energy that stored within the system boundary such as nutrient in soil, minerals.

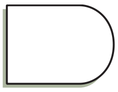

Producer: Unit that collects and transforms low-quality energy under control interactions of high-quality flows.

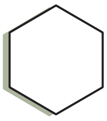

Consumer: Unit that transforms energy quality, stores it, and feeds it back autocatalytically to improve inflow.

Miscellaneous symbol to use for whatever unit or function is labeled.

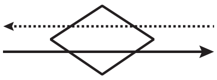

Transaction: A unit that indicates a sale of goods or services (solid line) in exchange for payment of money (dashed line). Price is shown as an external source.

Figure II.4. Symbols used in the emergy diagrams (Odum, 1996)

An example for system diagramming of the basic biorefinery process was shown in Figure II.5. The system consists of biomass cultivation and crop transportation in the first boundary and biomass produced from the first boundary will be sent to the second boundary, biorefinery, as feedstock.

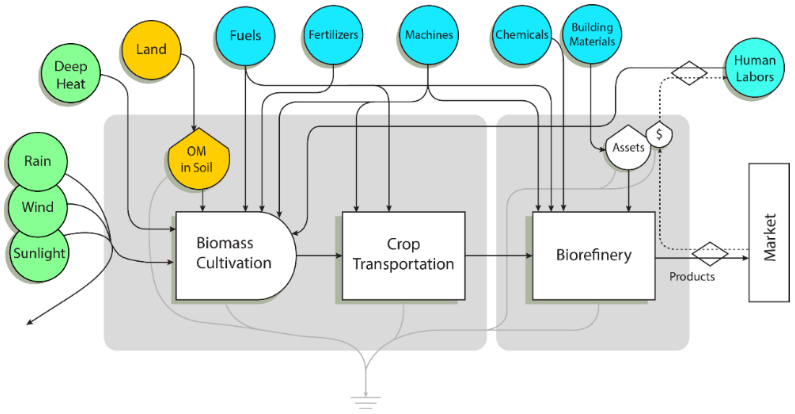

Figure II.5. Energy flow diagram of a system included biomass cultivation, transportation and biorefinery

2.3.2. Emergy Global Budget

As already mentioned, emergy was originally defined to use as a measure of energy (of one kind) that consumed by nature to build an ecosystem. For example, to obtain 1 Joule of organic matter, it required energy stored 1000 Joule in term of sunlight or 39,200 Joule sunlights to produce 1 Joule of coal. If we considered our planet as a system where materials and energy cycle within the biosphere. There are three sources that driven the process inside our planet; the energy from solar radiation, geothermal heat (deep heat) and tidal. These energy sources were considered as the global emergy budget or in some literatures called geobiosphere emergy baseline (GEB). Where the boundary of the system included 100 km above to 100 km below the Earth's surface and one year transient domain.

In Figure II.6, the components within the system boundary including; atmosphere, ocean and earth crust which consists of land storage (minerals and fuels) and human society received the energy from the three renewable inputs (Table II.2). Among the three-main global renewable resources, solar energy was used as a basis form of energy. So, here, the unit emergy value for the solar energy is equal to 1 and for the geothermal and tidal was calculated (Table II.3).

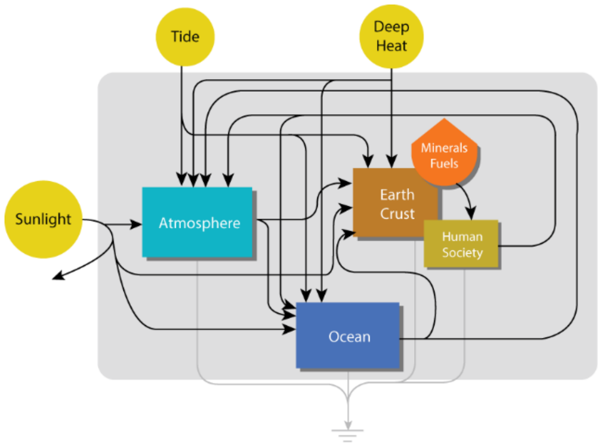

Figure II.6. Diagram of global energy flow (Odum et al., 2000)

Table II.2. Energy flow of the three-main global renewable resources.

Sources	Energy[1] (J/yr)	Energy[2] (J/yr)
Sunlight	3.93×10^{24}	3.6×10^{24}
Geothermal	6.72×10^{20}	9.78×10^{20}
Tidal	0.52×10^{20}	1.17×10^{20}

[1] baseline year 1996 (Odum et al., 2000)

[2] baseline year 2016 (Brown and Ulgiati, 2016)

Table II.3. Annual global emergy budget (baseline year 1996). (Odum et al., 2000)

Note	Sources	Energy (J/yr)	UEV (sej/J)	Emergy (sej/yr)
1	Sunlight	3.93×10^{24}	1	3.93×10^{24}
2	Deep heat	6.72×10^{20}	11,981	8.06×10^{24}
3	Tidal	0.52×10^{20}	73,923	3.84×10^{24}
	Total			*15.83×10^{24}*

Notes: (1) Sunlight exergy = (solar constant) × (earth cross section facing sun) × (% absorbed on earth) = (2 Langley/min) × (1.27×10^{14} m^2) × (70% absorbed) × (10 kcal/m^2/Langley) × (4,186 J/kcal) = 3.93×10^{24} J/yr. Solar UEV is 1 sej/J by definition.

(2) and (3) Heat to the earth's crust is equal to 13.21×10^{20} J/yr (Sclater et al., 1980). By subtracting heat released by crustal radioactivity (1.98×10^{20} J/yr) plus heat flowing up from mantle (4.74×10^{20} J/yr) from total crustal heat outflow, the remaining 6.72×10^{20} J/yr can be considered as deep heat contributed from solar-driven atmosphere, ocean and earth crust. The following equations expressed; the balance of crustal heat or heat generated by surface processes (Figure II.7a) and the balance of oceanic geopotential (Figure II.7b).

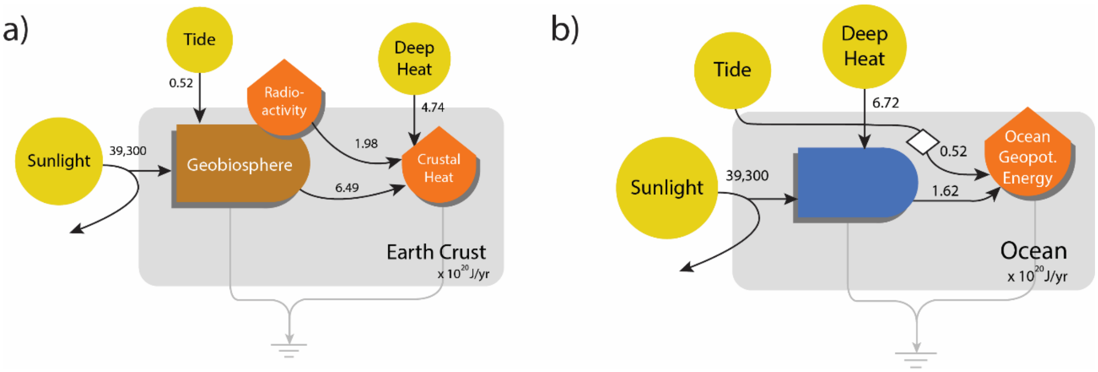

Figure II.7. Diagram for heat generated by

a) surface processes and b) oceanic geopotential (Odum et al., 2000)

Solar emergy + Tidal emergy = Emergy of heat generated by surface processes

$$(3.93 \times 10^{24}\ \mathrm{J/yr}) \times (1\ \mathrm{sej/J}) + (0.52 \times 10^{20}\ \mathrm{J/yr}) \times \mathrm{UEV}_{\mathrm{tidal}} = (6.49 \times 10^{20}\ \mathrm{J/yr}) \times \mathrm{UEV}_{\mathrm{deep\ heat}}$$

Solar emergy + Tidal emergy + Deep Earth emergy = Oceanic geopotential emergy

$$(3.93 \times 10^{24}\ \mathrm{J/yr}) \times (1\ \mathrm{sej/J}) + (0.52 \times 10^{20}\ \mathrm{J/yr}) \times \mathrm{UEV}_{\mathrm{tidal}} + (6.49 \times 10^{20}\ \mathrm{J/yr}) \times \mathrm{UEV}_{\mathrm{deep\ heat}}$$

$$= (2.14 \times 10^{20}\ \mathrm{J/yr}) \times \mathrm{UEV}_{\mathrm{tidal}}$$

Combining these equations gives the UEV of Deep heat and Tidal as follow;

$$\mathrm{UEV}_{\mathrm{deep\ heat}} = 11{,}981\ \mathrm{sej/J}$$

$$\mathrm{UEV}_{\mathrm{tidal}} = 73{,}923\ \mathrm{sej/J}$$

These UEVs of three main emergy sources were used as a starting point for the energy hierarchy on earth to provide UEVs for another smaller scale. Following section relates to the basic theory for emergy accounting.

2.3.3. Emergy Sustainability Indicators

Typically, the input emergy of the systems can be classified as free natural resources available within system boundary or economic inputs. Free natural resources are separated into renewable resources (R) and non-renewable resources (N). For example, renewable resources include solar radiation, wind and rain, while non-renewable resources include minerals and soil. Only the largest emergy flow among solar radiation, wind and rain is counted in order to avoid double counting of renewable resource (Odum, 1996). Economic inputs can be classified into two types, i.e., purchased energy and materials (F) and human labor (L). Labor may contribute directly to the process (DL) or indirectly as service external labor coming from the economic sector or larger scale outside the system boundary (IL).

The economic inputs can be classified into renewable parts ($F_R + L_R$) and non-renewable parts ($F_N + L_N$) where $F = F_N + F_R$ and $L = L_N + L_R$. The emergy input from source i is defined as Em_i and the available energy of the product j is defined as En_j. In Equations (2.3) –(2.7), different emergy indicators were defined with respect to the four variables; R, N, F and L. The descriptions of each notation were summarized in Table II.6. Also, in this dissertation, the color code has been used to easily identify the categories of the input emergy; green color is for R, yellow color is for N, blue color is for F and turquoise is for L, as depicted in Figure II.3 and Figure II.5.

$$\text{UEV of the product(s), } \tau = \frac{\sum_{i=1}^{n} Em_i}{\sum_{i=1}^{n} En_i} \qquad (2.3)$$

$$\text{Global Renewability, } \%R_{global} = \frac{R+F_R+L_R}{R+N+F+L} \qquad (2.4)$$

$$\text{Environmental Loading Ratio, } ELR = \frac{N+F+L}{R} \qquad (2.5)$$

$$\text{Emergy Yield Ratio, } EYR = \frac{R+N+F+L}{F+L} \qquad (2.6)$$

$$\text{Emergy Sustainability Index, } ESI = \frac{EYR}{ELR} \qquad (2.7)$$

The global renewability in equation (2.4), $\%R_{global}$, is the indicator that is used to identify the fraction of resources used that comes from global renewable resources. While ELR, in Equation (2.5), is the ratio of local non-renewable and economic inputs emergy to local renewable emergy, which implies the ecosystem stress due to the processes within the system boundary. The value reflects the renewable fraction of the system in a different way from $\%R_{global}$. The ELR value indicates only the locally renewable resources that support the system while the $\%R_{global}$ also counts the renewable fraction from economic inputs.

The emergy yield ratio (EYR), in Equation (2.6), is the ratio of the total emergy that drives the system to the economic inputs emergy, and measures the ability of the system to exploit the local resources. The value should be much higher than 1 otherwise the process will act as a consumer rather than a producer. Finally, the ratio between ELR and EYR is presented as ESI in Equation (2.7), the emergy sustainability indicator (ESI). In Equations (2.3) – (2.7), the sustainability in the ESI indicator was defined with respect to the four variables; R, N, F and L. The lowest possible value of ESI is zero. ESI value close to zero indicates the process produces negative yield to the society and creates large burden to environment. In the other hand, those greater than one indicates the process has high contribution to the economy without creating heavily loads to its environment (Brown and Ulgiati, 2004).

By using emergy analysis, it provides us two perspectives for decision making; the economic growth and the environmental burden. For example, Figure II.8 presented the alternative ways to produce electricity from the well-known renewable sources including; solar power, hydro power, geothermal power and wind power. In Figure II.8a, the number on the y-axis represent the UEV, the amount of emergy or natural resource in term of solar energy required to produce 1 J of electricity. Here, we can see that one system can produce the same product, however use different amount of resources. Between these four power plants, wind and hydro power plant consumed minimum natural resources.

Also, in term of ELR, we divided the emergy into the free renewable fraction (R) and the imported and non-renewable fraction (N + F + L), as shown in Figure II.8b. By doing this, we can see that these technologies are not completely renewable. They required some amount of non-renewable inputs in various portions as shown in this figure. What we need for an ideal technology is a lot amount of the renewable input. In the other side, the system with high dependent on external resource (F + L) than local resource (R + N) will be less self-sufficient (Figure II.8c). The ideal system should require only small amount of external resources with regard to the production process. If not, the system would act as a consumer not a producer.

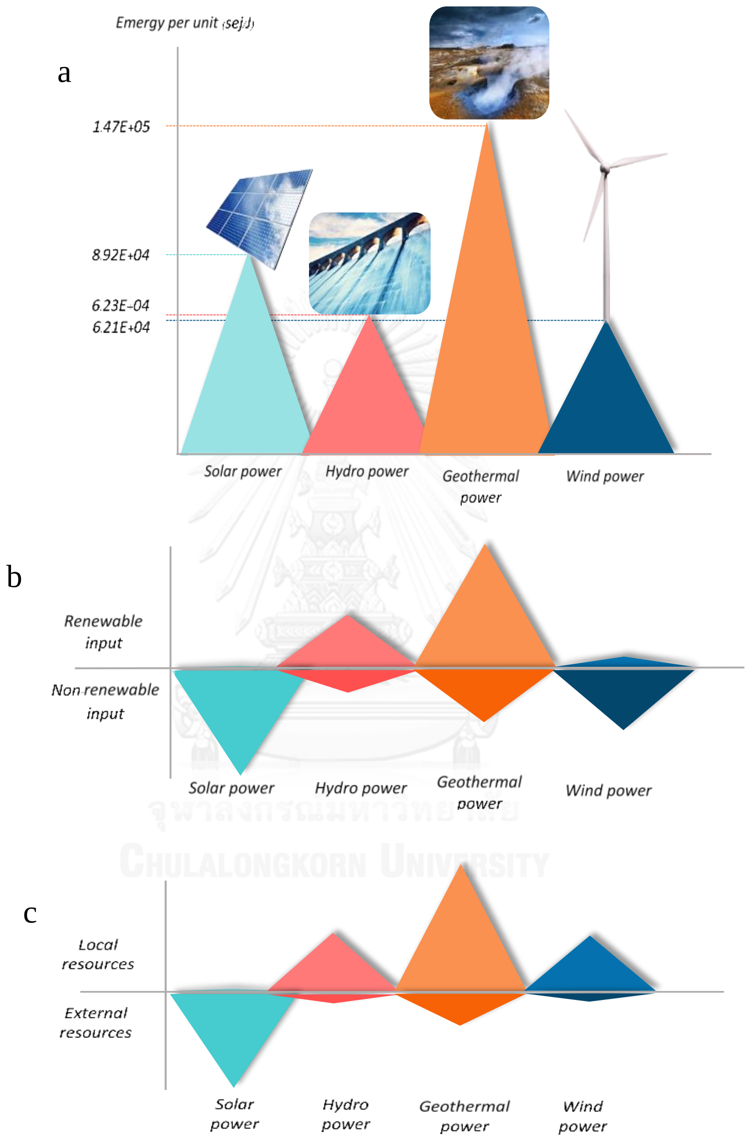

Figure II.8. Three sustainable dimensions of four power production processes from emergy analysis including; (a) emergy per unit of power production (b) environmental burden (c) economic growth

2.3.4. Track-Summing Method

For a general system with only one product and no feedback stream, the emergy can be obtained by transforming all inputs into solar energy flow and summing these up to obtain the emergy of the product. If the input UEVs are known, the given energy inputs can be converted to emergy by multiplying them with the relevant UEVs. Moreover, the UEV of a product stream can be used to express the emergy required along the transformation process. However, the systems with higher complexity require more particular computational methods such as the 'Track Summing Method' (Odum, 1996), which is a well-known method for emergy analysis.

The method was firstly developed by Tennenbaum (Tennenbaum, 1988). The emergy was evaluated by tracing the emergy input flows to every pathway until the path reaches the end of its contribution. The source emergy contributed to the product is calculated by summing the emergy through every possible pathway from that source to the product. Therefore, pathways of the network were required to complete the emergy track-summing.

Before we get into details about the emergy track-summing, I would like to introduce the emergy algebra which was used as a standard principle for emergy accounting. And I will explain about the emergy track-summing procedure in-detail again in Chapter III.

2.3.5. Emergy Algebra

As mentioned, emergy is different from energy or exergy. So, it does not follow the same rules of conservation as other energy-based approaches. The term emergy sometimes is considered as "energy memory" for the solar energy used up during a process and memorized into its output product(s). Thus, when dealt with complex system, the approach for calculating the emergy will relate to the emergy algebra which follows a logic of memorization and not of conservation.

As described in Brown and Herendeen (Brown and Herendeen, 1996) and Odum (Odum, 1996), the rules that applied to the algorithm include:

(R1) For the process with only one product output, the summation of source emergy to a process is assigned to the output stream (Figure II.9a).

(R2) For the process with two or more products (i.e., co-products), the emergy assigned to the main product and *by-products* is *equal to the summation of source emergy* to the process (Figure II.9b).

(R3) For the process with only one product output and the product *splits*, the assigned emergy to each '*leg*' of the split is based on the *fraction of the total energy flow* on the pathway (Figure II.9c).

(R4) Emergy cannot be counted twice within a system:

  (a) Emergy in a feedback stream cannot be double counted (Figure II.9d).

  (b) By-products, when reunited, cannot be summed. Only the emergy of the stream with maximum emergy flow is counted (Figure II.9e).

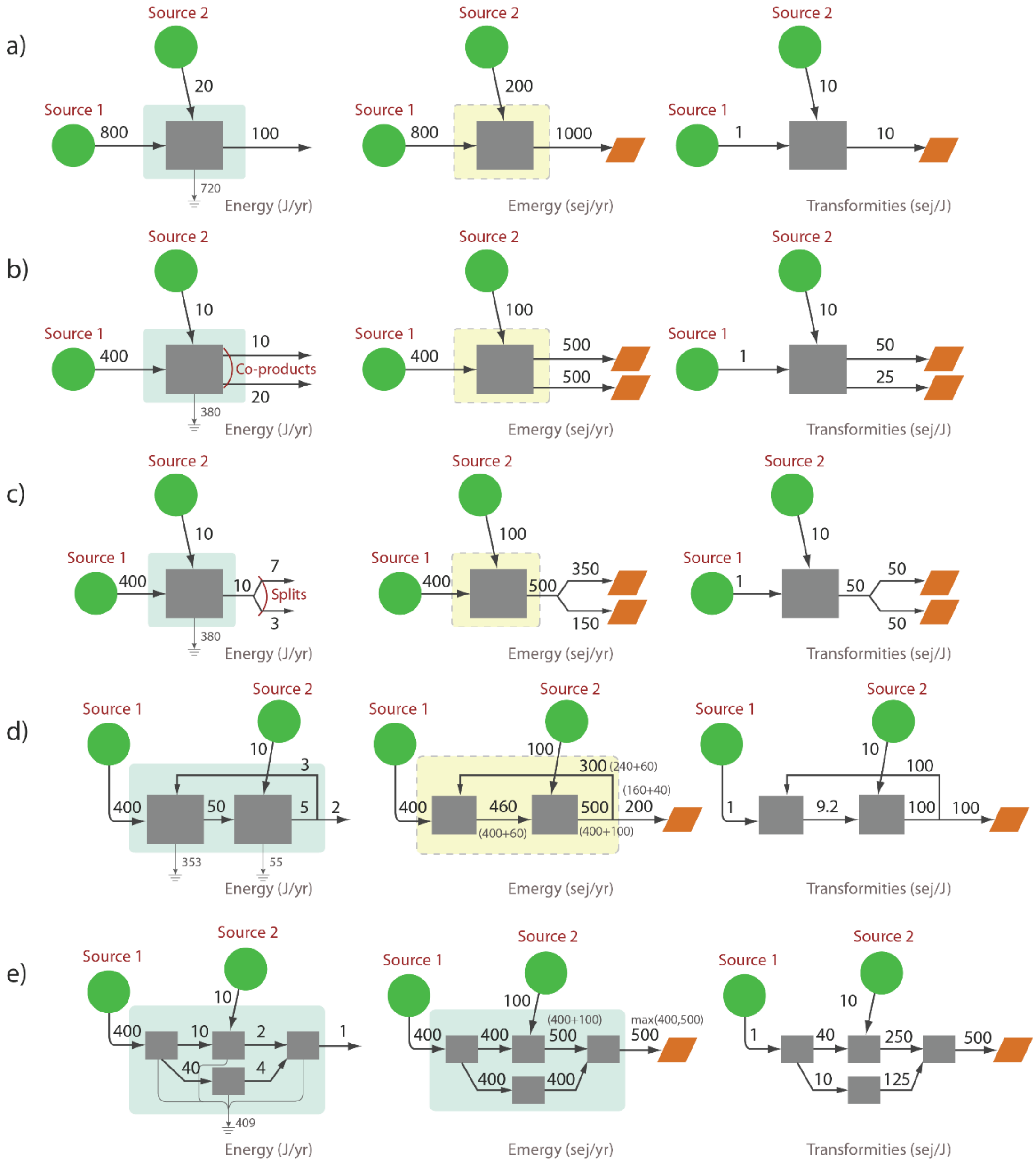

Figure II.9. Diagrams of energy flow, emergy flow and transformities to illustrate emergy rules including; (a) single-output system (b) system with by-products (c) single-output system with splits (d) system with feedback stream (e) system with by-products. (Odum, 1996)

2.4. Novel Emergy Concepts

Besides the general accounting method, there are particular cases for emergy accounting related to this work including; UEV of the unknown feed, UEV of the system with multiple products, UEV of the treated wastes and the emergy of human labor.

2.4.1. UEV of the unknown feed

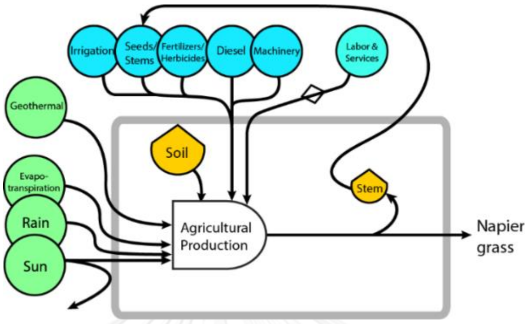

Figure II.10. Diagram of Napier grass cultivation with feedback Napier stem.

Basically, the UEV of the input can be obtained from the previous literatures. However, in this study, the UEV of Napier stem is unknown. Where Napier plantation stage requires initial Napier stem to plant the crop that lasts for 7 years (Section 4.2.1.1). Within this period of time, the UEV of output (Napier grass biomass) and input (initial Napier stem) were assumed to be equal. Iteration is often applied to deal with this issue (Morandi et al., 2016), but the procedure employed in this study was derived from the mathematical formula described below (Equation (2.8)).

Let τ_{Napier} be the UEV of the Napier grass biomass; Em_0, $Em_{Napier,in}$ and $Em_{Napier,out}$ be the emergy flow of all inputs (except initial Napier stem), initial Napier stem and total emergy flow to the Napier grass biomass, respectively; and $M_{Napier,in}$ and $M_{Napier,out}$ be the weight of initial Napier stem and Napier grass biomass, respectively. The emergy accounted to the output will be equal to the summation of all the inputs including the initial Napier stem ($Em_{Napier,out} = Em_0 + Em_{Napier,in} = Em_0 + M_{Napier,in}\tau_{Napier}$), while the total emergy to the output will equal the multiplication between the weight of product ($M_{Napier,out}$) and UEV of the product (τ_{Napier}). Thus, Equation (2.8) was obtained.

$$\mathrm{Em}_{\mathrm{Napier,out}} = \mathrm{Em}_0 + \mathrm{M}_{\mathrm{Napier,in}}\tau_{\mathrm{Napier}} = \mathrm{M}_{\mathrm{Napier,out}}\tau_{\mathrm{Napier}}$$

$$\tau_{\mathrm{Napier}} = \frac{\mathrm{Em}_0}{\mathrm{M}_{\mathrm{Napier,out}} - \mathrm{M}_{\mathrm{Napier,in}}} \qquad (2.8)$$

2.4.2. Co-products Emergy

In emergy analysis, total emergy driving the process allocates to each of the products equally (Brown and Herendeen, 1996). While this rule is applied, it is important to understand that one-product systems and multi-product systems cannot directly compare. When products cannot be produced independently in the process the emergy allocated to each product is equal to the total emergy inputs. According to the procedure, most multi-product systems often rely on higher emergy than one-product system, since they carried the emergy of the whole production process. For example, the combined heat and power process which produces electricity and steam as by-product has UEV of 1.20×10^5 sej/$J_{\text{electricity}}$ (Sha and Hurme, 2012). While solar power generates the electricity with UEV only 8.92×10^4 sej/$J_{\text{electricity}}$ (Paoli et al., 2008). It may lead to misinterpretation if we compare the emergy of these products that were generated from these two processes.

'Joint' and 'Weighted average' indicators were defined to help this comparison (Bastianoni and Marchettini, 2000). The joint production process is the process that produces two or more products simultaneously. From Figure II.11a, the joint UEV (τ_{joint}) was calculated by the ratio of the total emergy needed for the co-production (Em_{xy}) to the total energy of the outputs ($En_x + En_y$) as presented in Equation (2.9).

The weighted average indicators can be evaluated from the weighted emergy fraction by the energy contents of the products that have the same quantity as the joint-production products but produced by two or more independent ways (Figure II.11b). The weighted average UEV (τ_{avg}) was evaluated maintaining the same quantities of the outputs (En_x and En_y) as presented in Equation (2.10).

The same procedure can be applied to other indicators, such as the EYR or ELR.

$$\tau_{\text{jo int}} = \frac{\text{Em}_{\text{xy}}}{\text{En}_{\text{x}} + \text{En}_{\text{y}}} \tag{2.9}$$

$$\tau_{\text{avg}} = \frac{\text{Em}_{\text{x}}}{\text{En}_{\text{x}} + \text{En}_{\text{y}}}\tau_{\text{x}} + \frac{\text{Em}_{\text{y}}}{\text{En}_{\text{x}} + \text{En}_{\text{y}}}\tau_{\text{y}} \tag{2.10}$$

For example, the joint and weighted average UEV of biomass power (subscripts 'e') and steam (subscripts 's') production were presented in Figure II.11a and Figure II.11b, respectively. Applying Equation (2.9), the joint UEV is obtained by

$$\tau_{\text{jo int}} = \frac{\text{Em}_{\text{es}}}{\text{En}_{\text{e}} + \text{En}_{\text{s}}} = \frac{3.91\times10^{19}}{3.91\times10^{14} + 9.73\times10^{14}} = 3.54\times10^{4}\,\text{sej/J}$$

while the weighted average of the UEV is given by

$$\tau_{\text{avg}} = \frac{\text{Em}_{\text{e}}}{\text{En}_{\text{e}} + \text{En}_{\text{s}}}\tau_{\text{e}} + \frac{\text{Em}_{\text{s}}}{\text{En}_{\text{e}} + \text{En}_{\text{s}}}\tau_{\text{s}} = \frac{3.91\times10^{19}}{3.91\times10^{14} + 9.73\times10^{14}} \times 8.17\times10^{4}$$

$$+ \frac{9.73\times10^{14}}{3.91\times10^{14} + 9.73\times10^{14}} \times 3.12\times10^{4} = 4.57\times10^{4}\,\text{sej/J}$$

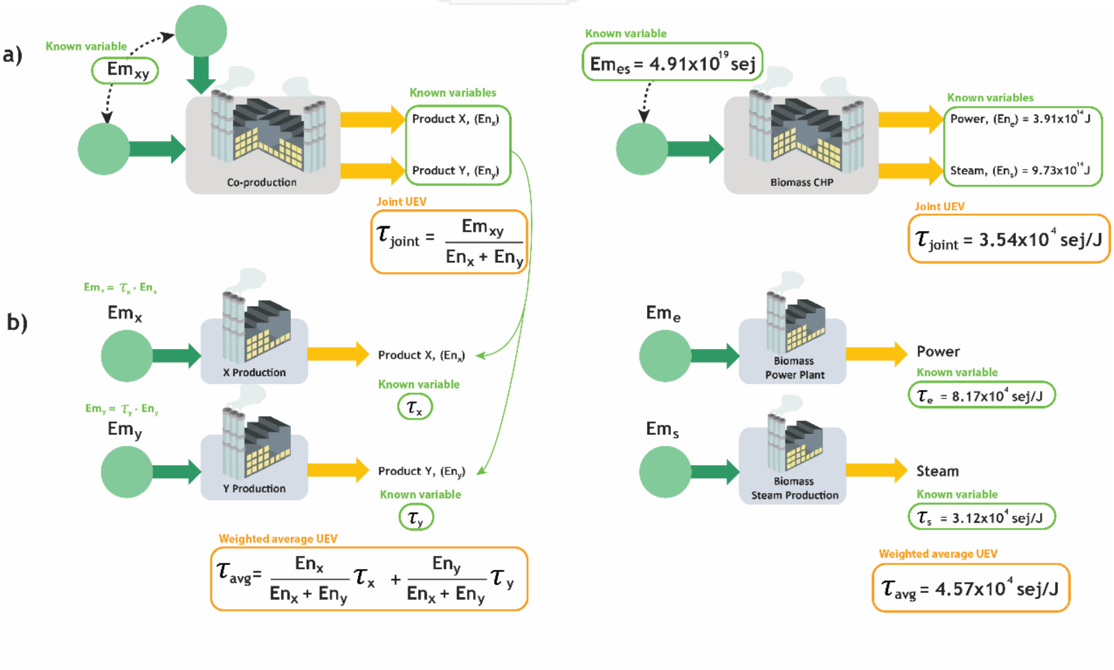

Figure II.11. Diagrams for the definition of (a) joint UEV and (b) weighted average UEV (diagram on the right-hand side is an example of biomass power and steam production).

2.4.3. Emergy of the treated wastes

The emergy analysis of waste treating processes is different from typical emergy studies. Mostly, emergy studies have focused on production systems, such as a biorefinery or power production, whereas in a waste treatment process (CO_2 capture, for example) where the product is the ability of the product (service) to remove a waste (CO_2 from the flue gas) to the same degree with the lowest level of natural investment. Therefore, the UEV reflects the natural investment required to prevent discharging the waste to the environment, and not the natural investment for producing a product. The higher the UEV, the higher the level of natural resources was consumed by the process to treat such amount of wastes. Thus, the UEV can be used for comparing the efficiency of the treating process.

2.4.4. Human labor in emergy accounting

In emergy researches, emergy of human labor has always been a critical issue especially in the biomass agricultural field. Since human labor is the main input to the agricultural system and dominates the sustainability of the downstream processes.

There are different procedures to include human resources into the emergy accounting. One of the conventional procedures is to use the emergy to money ratio (EMR) as the UEV for labor inputs in monetary units, where EMR is an indicator that expresses the quantity of emergy that supports the monetary value of the production or GDP of the country where the production takes place. It is measured in sej/US$ or another relevant currency. For example, the global average EMR can be obtained by dividing the global emergy budget of 1.05×10^{26} sej/y by the global money flow of 6.06×10^{13} US$/y (Kamp et al., 2016) to give an UEV as emergy per monetary value of 1.73×10^{12} sej/US$.

Another approach for human labor accounting is to allocate the emergy budget per hour worked to each category using specific parameters. The refined method has been applied from that of (Kamp et al., 2016) considering the data for three production sectors in Thailand (agricultural, industry and services) for the year 2008 (Aemkulwat, 2010).

The assumption involved is using a money-based distribution to indicate the emergy shared to people working in different levels of the production process. In Thailand, the emergy budget of 3.20×10^{24} sej/y in 2008 was distributed across the labor system based on %GDP distribution as follows; agriculture sector 8.8% (2.82×10^{23} sej/y), industrial sector 48% (1.54×10^{24} sej/y) and services 43.2% (1.38×10^{24} sej/y) (Aemkulwat, 2010).

The hours worked by each production sector were calculated using the average working hours and population of people working in each production sector, where the hours worked by people in the agricultural, industrial and service sectors were 3.11×10^{10} h/y, 1.71×10^{10} h/y and 3.29×10^{10} h/y, respectively. The ratios between the emergy distribution and hours worked by each sector gave UEVs for people working in the agricultural, industrial and service sectors of 9.06×10^{12} sej/h, 8.99×10^{13} sej/h and 4.20×10^{13} sej/h, respectively, as fully described in Appendix B (note 1.11).

Using EMR as human labor UEV or using man-hour UEV has distinct different advantages. The EMR is the expression of the average value of the whole nation, while the man-hour UEV is attempted to be the specific value of a sector sorted by level of income. In this study, both methods are applied. The direct labor input is considered a domestic labor, using man-hour UEV based on Thailand. Only the agricultural and industrial sectors are considered, since the labor involved farmers and industrial operators. For the indirect labor, which corresponded to external labor, the global average EMR is used as the labor UEV. The summary for labor UEV used in this study is shown in Table II.4.

Table II.4. The human labor UEVs used in this study.

	Level	*UEV*	*Unit*	*Appendix B*
Direct labor (DL)	Agricultural sector	9.06×10^{12}	sej/h	Note 1.11
	Industrial sector	8.99×10^{13}	sej/h	
Indirect labor (IL)	Global average	1.73×10^{12}	sej/$	Note 1.12

2.4.5. Emergy Algorithms

In recent years, a number of emergy computational algorithms have been developed, including a computational algorithm for emergy flows and emergy paths by Le Corre and Truffet (Le Corre and Truffet, 2012, 2015), co-emergy analysis by Tennenbaum (Tennenbaum, 2015), and emergy computation of trophic networks by Zarbá (Zarbá and Brown, 2015). Le Corre and Truffet introduced an emergy computational algorithm which applied track-summing method and provided the original emergy algebra accounting (Le Corre and Truffet, 2012, 2015). However, in this paper, the important information for the algorithm such as emergy pathways was assumed to be known. The latter study of Le Corre and Truffet gave explanation about the detail of emergy paths computational algorithm using a recursive rule where the paths represent the sequel of assignations of the emergy source(s) to the intermediate processes within the system. According to Le Corre and Truffet, the problem of emergy computation is the search for an emergy path that requires a complicated mathematical framework that covers all emergy rules (Le Corre and Truffet, 2015). The work of Tennenbaum provides a simple linear algebra approach that requires no emergy path finding (Tennenbaum, 2015). Tennenbaum defined the word co-emergy to represent the emergy from the upstream process(es) required to produce one downstream product. The obtained co-emergy was specific for only one target compartment and the co-emergy of one compartment's product will not be used to calculate the co-emergy of another's. The study was also shown that counting the recycle emergy through processes does not necessarily and lead to double counting of emergy. The computation approach is different from the original emergy algebra that Odum defined and the method is robust under aggregation. But it allows us to explicitly indicate the processes efficiency by using basic linear algebra. Zarbá and Brown pointed out the emergy feedback issue in the emergy algebra (Zarbá and Brown, 2015). The study attempted to estimate the effects of counting emergy feedback which were considered as double counting in the fourth rule in emergy algebra. The argument between including and not including feedback emergy into the calculation stated that the emergy of recycling indicated the emergy required in the past and would not double count with the present emergy. This argument allows us to reconsider the emergy rules. However, counting feedback emergy in case where co-products occurred may lead to the actual double counting.

Table II.5. Researches related to emergy algorithm

Method	Short Description	Drawbacks
Track summing method (Tennenbaum, 1988)	Original emergy accounting algorithm	• Cannot deal with large systems • Only applicable for manual calculation
Exact emergy computational (Le Corre, 2012)	Applied Track summing method algorithm	• Assume all emergy pathways known
Emergy paths computation (Le Corre, 2012)	Emergy pathways computation algorithm	• Complicated and require large data memory • Have not yet applied to any software
Emergy unit value computation (Collins, 2000)	Eigenvectors method	• Require manual pre-analyzed to build appropriate equations

Table II.6. Description of the notations

Notations	Descriptions
Em_i	Emergy of source i (sej/y)
En_j	Energy flow of product j (J/y)
UEV	Unit emergy value (sej/J)
τ	UEV of the product(s)
τ_{joint}	Joint UEV
τ_{avg}	Weighted average UEV
$\%R_{global}$	Global renewability
ELR	Environmental loading ratio
EYR	Emergy yield ratio
ESI	Emergy sustainability index
R	Free natural resources as renewable resources
F_R	Renewable portion of purchased energy and materials (excluded human labor)
L_R	Renewable portion of human labor
N	Free natural resources as non-renewable resources
F	Purchased energy and materials (excluded human labor)
L	Human labor
DL	Direct human labor (farmers, workers)
IL	Indirect human labor (cost of e.g., materials, equipment)

**Remark: note that this dissertation use UEV and τ to represent the unit emergy value of input streams and product, respectively.*

CHAPTER III: SYSTEMATIC TOOL FOR EMERGY ACCOUNTING

This chapter described about an alternative approach for emergy computation base on original emergy algebra that was defined by Brown and Herendeen (Brown and Herendeen, 1996) and Odum (Odum, 1996). The novel of the development is that the developed algorithm can handle both individual products and co-products. The algorithm will (1) find all emergy pathways from the process network and (2) employ these pathways to evaluate and allocate the emergy to each node in the process network. The designed algorithm was developed under MATLAB environment.

3.1. Emergy notions and important abbreviations

All important abbreviations presented in this study applied from the Le Corre and Truffet definitions (Le Corre and Truffet, 2012) as shown below:

$$G_k = (pSource_k, pInte_k, pSink_k, Arcs_k, M_k, S_k, Path_k)$$

Where	$pSource_k$	is the set of sources of graph G_k
	$pInte_k$	is the set of intermediates of graph G_k
	$pSink_k$	is the set of system outputs of graph G_k
	$Arcs_k$	is the set of arcs of graph G_k
	M_k	is the matrix of weights of graph G_k
	S_k	is the vector of assigned emergy sources of graph G_k
	$Path_k$	is the set of all emergy paths of graph G_k
	k	is the index of the system, $k \in 1, \ldots, N$

3.2. Track-summing method

Traditional emergy accounting method introduced by Odum (1996) (Odum, 1996) was track-summing method which was firstly developed by Tennenbaum (Tennenbaum, 1988). In the track-summing method, the emergy was evaluated by tracing the emergy input flows to every pathway until the path reaches the end of its contribution. The source emergy contributed to the product is calculated by summing the emergy through every possible pathway from that source to the product. Therefore, pathways of the network were required to complete the emergy track-summing.

An Energy Systems Language was used as the basis for creating emergy diagram to elaborate the relationship among processes within the system. There are three types of nodes, or elements, to describe the system: sources, intermediates, and outputs. Sources are the external resources supplied to the system. Intermediates represent internal processes in the system. Outputs are the products produced by the system. Each node is represented by an integer. Figure III.1 depicts symbols representing each node type used in construction of an emergy diagram for a system.

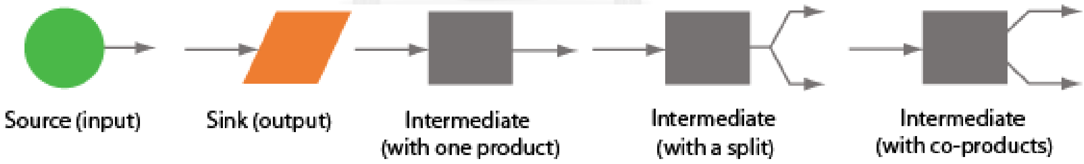

Figure III.1. Symbols used in the diagrams

Referring to Le Corre and Truffet (Le Corre and Truffet, 2012), Figure III.2 is an example of a system called 'G_1' which is consisted of 2 input sources, 4 intermediates, and 1 output. The system contains the network relation with split and co-product branching. The values displayed in emergy pathway diagram in Figure III.2b indicated the portion of emergy contributed to the output stream(s). These values indicate the fraction of emergy allocation in the system. For example, emergy from source 1 (node 1) flows to process 3 (node 3) with the allocation of 1. That is, all emergy from source 1 goes to process 3. Then process 3 (node 3) produces two products as the co-product with an emergy allocation of 1 for each product stream. According to rule R2, the total emergy input to node 3 is assigned to each co-product equally, since they were produced together. While a single product produced from process 6 (node 6) was split into two streams with an emergy allocation of 4/5 and 1/5, respectively, based on its fraction of the total energy flow on each stream.

Several possible emergy pathways from node 1 to output 7 of system G_1 were presented in Figure III.3. Assuming the emergy sources (node 1 and node 2) are 400 sej and 100 sej, respectively, the results of track summing were calculated as follows.

Emergy from source 1 (node 1) to output 7 (node 7):

a) 400 sej from node 1 flows to node 3, node 4, and then splits to 4/5 through node 6 and eventually output 7 with emergy distributed to 400 × 4/5 = 320 sej.
b) 400 sej from node 1 flows to node 3, node 5 and then splits to 4/5 through node 6 and output 7 with emergy distributed to 400 × 4/5 = 320 sej.

To evaluate the emergy flows of path a) and path b) to output 7, all emergy pathways will be evaluated and compared their values. Then, the maximum value among them will be selected (rule R4b). In this case, there are two pathways from node 1 to output 7 and the maximum of their emergies to output 7 is 320 sej.

Emergy from source 2 (node 2) to output 7:

c) 100 sej from node 2 to node 4 and then splits to 4/5 through node 6 and ends at output 7 with emergy distributed to 100 × 4/5 = 80 sej.

Finally, the emergy to output 7 will be equal to 320 sej + 80 sej = 400 sej.

The solar transformities of each stream then can be calculated by dividing the emergy flow by the energy flow of that stream. For example, in this case, the UEV of product to output 7 will be equal to 400 sej/ 4 J = 100 sej/J.

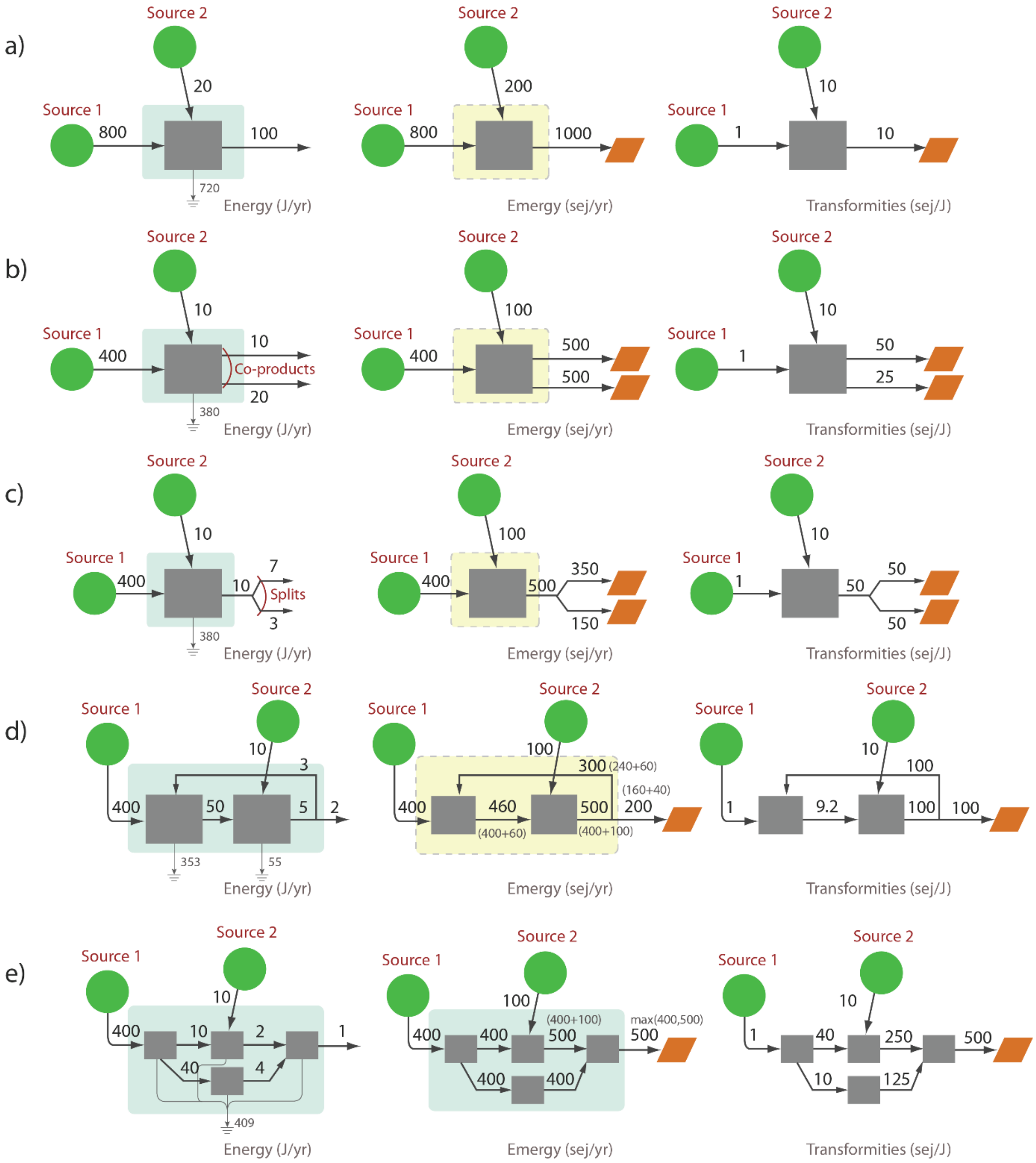

Figure III.2. Diagrams of energy flow, emergy flow and transformities to illustrate emergy rules including; (a) single-output system (b) system with by-products (c) single-output system with splits (d) system with feedback stream (e) system with by-products (illustrate rule 4b).

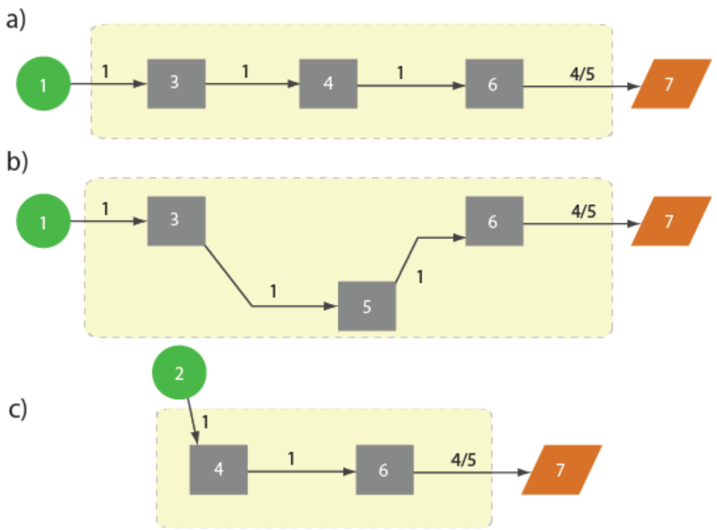

Figure III.3. Possible pathways from node 1 to output 7 of the system G_1

(a) path [1, 3][3, 4][4, 6][6, 7] (b) path [1, 3][3, 5][5, 6][6, 7] (c) path [2, 4][4, 6][6, 7]

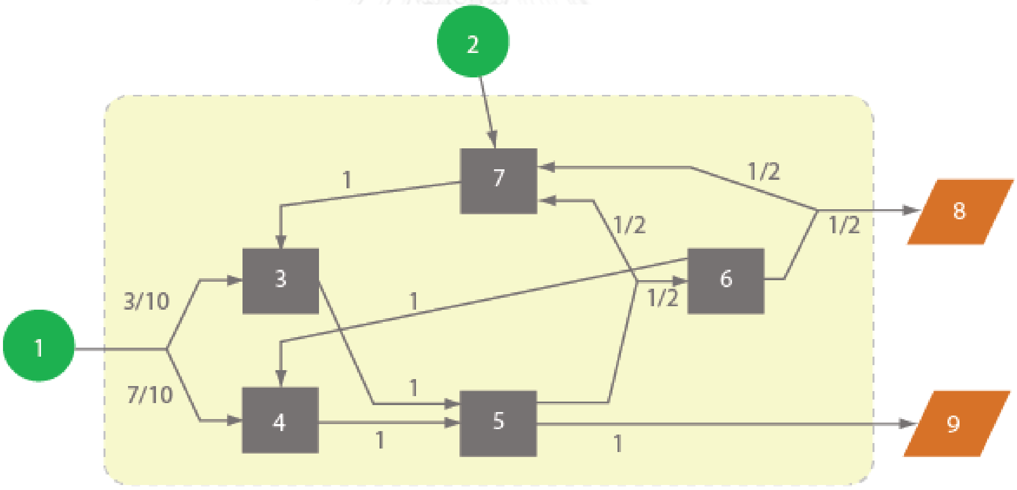

Figure III.4. Emergy flow diagram of a system G_2 with 2 sources 5 intermediates and 2 outputs

3.3. Emergy path-finding algorithm

To illustrate how the emergy path-finding algorithm work, in this dissertation, the algorithm was applied on two case studies. The system in the first case was adopted from Le Corre and Truffet (Le Corre and Truffet, 2012). It is called 'G_1' which is a simple system consisting of 2 input sources, 4 intermediates, and 1 output, as shown in Figure III.2. Then, adopted from Odum (Odum, 1996) is the second system which is more complex. The system was consisting of 2 input sources, 5 intermediates and 2 outputs as shown in Figure III.4. It is called 'G_2'.

According to the emergy pathway graph of the system G_1, Figure III.2, the external energy sources are fed to the system and distributed among the processes (nodes) inside the system that are represented by intermediates. The relationships of each intermediate within the system can be described in a matrix form as shown in Table III.1, which is called matrix 'M_1'. Where 7×7 row and column of the matrix represents an upstream and downstream node of the system, respectively. For example, row no. 6 of the matrix represents node no. 6, or the 6th node in Figure III.2b. In this row, there are numbers shown in the 5th and 7th columns, and the rest are null. This shows that there are energy flows from the 6th node to the 5th and 7th nodes. The number shown in each cell represents the weighting factors or fraction of total energy flow distributed to each downstream node (the column). In this case, the fractions of the energy flow from the 6th node to the 5th and 7th nodes are 1/5 and 4/5, respectively. In addition, the columns and rows with zeros or null elements indicate that there is no connection, i.e., no energy flow, between those pairs.

According to Table III.1, the information in the matrix 'M_1' can also be arranged in terms of sets of the same kind of elements where the relevant nodes are the members in the set. In the system G_1, the set of sources '$pSource_1$' is {1, 2} the set of output '$pSink_1$' is {7}; and the set of intermediates '$pInte_1$' is {3, 4, 5, 6}. Moreover, the summation of each row, which is greater than one, indicates where the co-products occurred. As reported in the matrix 'M_1', the row with a summation greater than one is row no. 3. This implies that the co-products take place at node no. 3, referring to arc [3, 4] and [3, 5]. Finally, the non-zero elements in the matrix 'M_1' will be compiled as the set of arcs '$Arcs_1$' {[1, 3], [2, 4], [3, 4], [3, 5], [4, 6], [5, 6], [6, 5], [6, 7]}.

In this dissertation, the entire emergy pathway network has been created based on the Depth-First Search (DFS) method (Tarjan, 1972). The DFS algorithm will search and explore neighbor nodes along each branch as far as possible until the deepest node is reached. Then the search will track back to the last explored node where it is possible to visit a new branch. This method is depicted in Figure III.5 with different colors used to distinguish the steps and paths of the exploration. The DFS method was coded under a Matlab environment as described in the flow diagram shown in Figure III.6. By using the information of obtained from the matrix *M*, the process starts by selecting each arc in the set and searching for pathways from a source node to an output node of the system. The path obtained from each iteration step is stored as a subset in each cell of a matrix named '*Path*' with the location (i, j), the ith row and jth column, that changes at the end of each loop. Finally, all pathways from individual sources are combined as a matrix called '*Path*{a}', where 'a' indicates the source being used as a starting point.

Table III.1. matrix 'M_1' which represent the relations between intermediate processes within the system G_1

	1	**2**	**3**	**4**	**5**	**6**	**7**
1	0	0	1	0	0	0	0
2	0	0	0	1	0	0	0
3	0	0	0	1	1	0	0
4	0	0	0	0	0	1	0
5	0	0	0	0	0	1	0
6	0	0	0	0	1/5	0	4/5
7	0	0	0	0	0	0	0

For example, in the DFS algorithm of the 1st source in system G_1 shown in Figure III.5, the pathway search will start from node 1 for initial iteration. Node 1 is then marked as a visited node. Then, the search will move to the next neighbor of node 1, node 3. The edge between these nodes is an arc [1, 3], and the arc is then stored in cell row 1 and column 1 (for one arc in the path) in *Path* (1, 1). Nodes 1 and 3 will then be marked as already visited. After this, the 2nd iteration starts searching for unvisited neighbors of node 3, which are node 4 and node 5. The search will choose the lowest order in its branch first, which is node 4. The edge between these nodes will also be an arc [3, 4]. Concatenation can then be performed with the previous arc [1, 3] to get a path [1, 3][3, 4], and this path will be stored in cell row 1, column 2 (for having 2 arcs in the path) in *Path*(1, 2). Next, node 3 and node 4 are marked as already visited. After this, the search continues until node 6 is reached in the 5th iteration and the path [1, 3][3, 4][4, 6][6, 5][5, 6] is obtained. The path can then be stored in cell row 1, column 5 in *Path*(1, 5) after which node 6 can be marked as visited. In the 6th iteration, the code will continue searching for the neighbor of node 6, which is node 5 with an edge [6, 5]. After performing concatenation, the path [1, 3][3, 4][4, 6][**6, 5**][5, 6][**6, 5**] will be obtained, and node 6 will have been used twice as an inlet with the 4th and 6th arcs in this path. This means that double counting has occurred in this path. Therefore, the code will terminate the loop [**6, 5**][5, 6][**6, 5**] and return to the last explored node where it is possible to find a new branch other than the previous node 5.

The unvisited neighbor of node 6 is output 7. The path after concatenation will be [1, 3][3, 4][4, 6][6, 7] and stored in cell row 2, column 4 in *Path*(2, 4) (the row 'i' is expanded when the former path is terminated and the path is stored in the column next to where its parent root is stored. Since the parent root of this pathway [1, 3][3, 4][4, 6], is stored in column 3, the obtained path in this iteration is stored in the next column, column 4. As the output node is reached, the search will track back to the last explored node where it is possible to visit a new branch, which is node 3. The unvisited neighbor of node 3 is node 5. The search can continue until all nodes are marked as visited nodes. The set of paths for the 1st source in the system G_1 is obtained as follows:

With similar approach, one can obtain the set of paths for the 2nd source of the system G_1 as follows:

The algorithm described above was shown in Figure III.6. After introducing the matrix M_1, the Matlab code (in Appendix A) will be used to diagnose the matrix M_1 to obtain the sets of pathways from sources to outputs for each source, 1 and 2, and the result will be stored in Matrices $Path_1\{1\}$ and $Path_1\{2\}$.

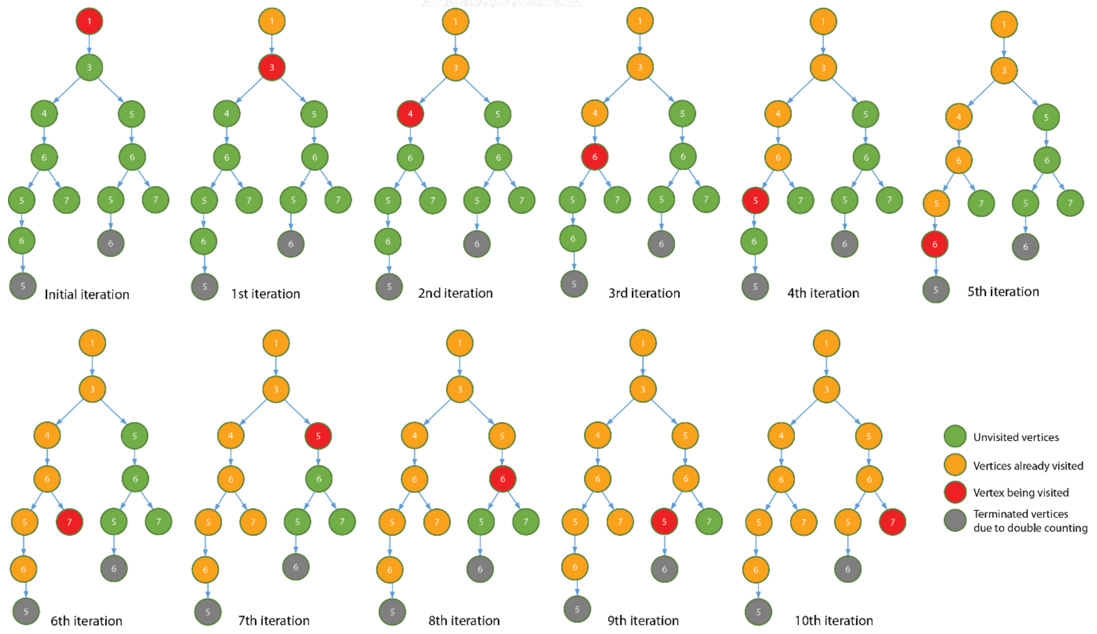

Figure III.5. Depth First Search (DFS) algorithm of the 1st source in system G_1

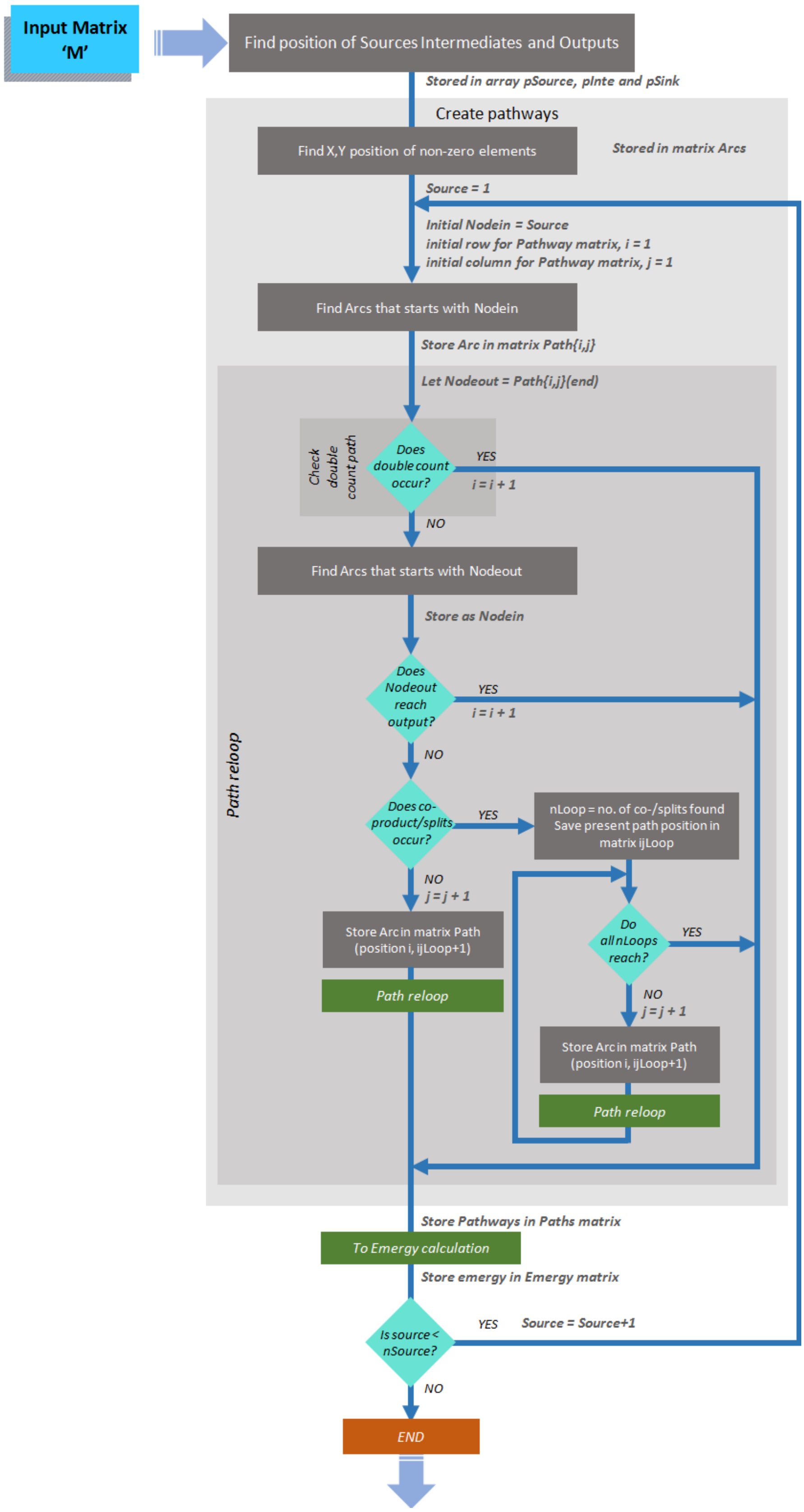

Figure III.6. Block diagram of path computation algorithm by MATLAB

3.4. Emergy accounting algorithm

After obtaining emergy path Matrix $Path_1$, the emergy accounting can be performed. This section will fully describe how to compute the values of emergy flows between the nodes in the system G_1 by tracing back emergy flow from the target node to the sources. The proposed procedure is called track-summing method as introduced by Odum (Odum, 1996) and Tennenbaum (Tennenbaum, 1988). For a complex system with feedback and co-products, the calculation process needs close attention in order to avoid double counting emergy flows, which is a major concern on emergy accounting. In this section, the system G_1 is used as an example to explain computation process within a system that has both feedback and co-products.

Figure III.7 shows the computation process for determining an emergy flow based on the emergy rules developed with the Matlab code. Referring to the previous section, to evaluate the emergy flow to the output 7, as an example, we found that there are 3 pathways that reach output 7 as the terminal node. These pathways are [1, 3][3, 4][4, 6][6, 7], [1, 3][3, 5][5, 6][6, 7] and [2, 4][4, 6][6, 7]. These pathways can be depicted in Figure III.3. As stated in the aforementioned emergy rules, a simple pathway without feedbacks, co-products, and splits can be handled by rule no. 1. For example, in Figure III.3c, the emergy flow to node 6 is equal to total emergy from the input source 2. While the emergy flow from node 6 was split between node 5 and output 7, only 4/5 of total emergy was allocated to output 7 as defined by rule no. 2. Finally, the emergy flow to the output 7 accounts for the amount of emergy input from source 2 multiplied by the weight fraction of 4/5. In conclusion, the weighted fraction of emergy flow based on rules no. 1 and 2 can be rewritten as follows:

(3.13)

When represents the emergy weighted fraction of the path from the upstream arc $[A_j]$ to the downstream arc $[A_k]$, for example, $EmWt([2,\ 4][4,\ 6][6,\ 7])$ is equal to $EmWt([2,\ 4]) \times EmWt([4,\ 6]) \times EmWt([6,\ 7])$.

The total emergy flow to output 7 can be evaluated by the summation of emergy flows from all possible pathways as shown in Figures 3.3a - 3.3c. However, we also found that the co-products occurred at node 3. As mentioned in emergy rule no. 4, each product stream will carry all the emergy input to the process. However, when the co-products recombine with the emergy flow out of the process, only the largest values of these flows will be counted. Thus, the emergy accounting of the total emergy flow to output 7 can be derived as follow:

$$\begin{aligned}\text{Emergy}_1(\text{output } 7) = {} & S_1(1) \times EmWt_1([1,\ 3]) \times \max\{EmWt_1([3,\ 4][4,\ 6][6,\ 7]),\\ & EmWt_1([3,\ 5][5,\ 6][6,\ 7])\} + S_1(2) \times EmWt_1([2,\ 4][4,\ 6][6,\ 7])\end{aligned}$$

where $S_1(1)$ and $S_1(2)$ are the vectors of assigned emergy sources (1) and (2) of graph G_1.

The equation here was created as described in Figure III.8. While this calculation can be evaluated under the Matlab environment expressed in Figure III.8. The sets of paths from source 1 and 2 represented by $Path_1\{1\}$ and $Path_1\{2\}$ was rearranged to produce $P_1\{1\}$ and $P_1\{2\}$, which can be expressed as:

Thus, the sequence of paths can be identified by concatenating the elements in the set P_1, e.g., the concatenation of element $P_1\{1\}(1,\ 1)$ to element $P_1\{1\}(1,\ 5)$ will obtain the path $[1,\ 3][3,\ 4][4,\ 6][6,\ 5][5,\ 6]$, while the concatenation of element $P_1\{1\}(1,\ 1)$ to element

$P_1\{1\}(4, 4)$ obtains the path [1, 3][3, 5][5, 6][6, 7]. The Matlab code was developed to gather information from the furthest element and then move to the next furthest un-visited element and so on. The rule of this code is that it must move from the "highest row", first, and then to the "highest column" until all possible pathways were combined and the source is reached.

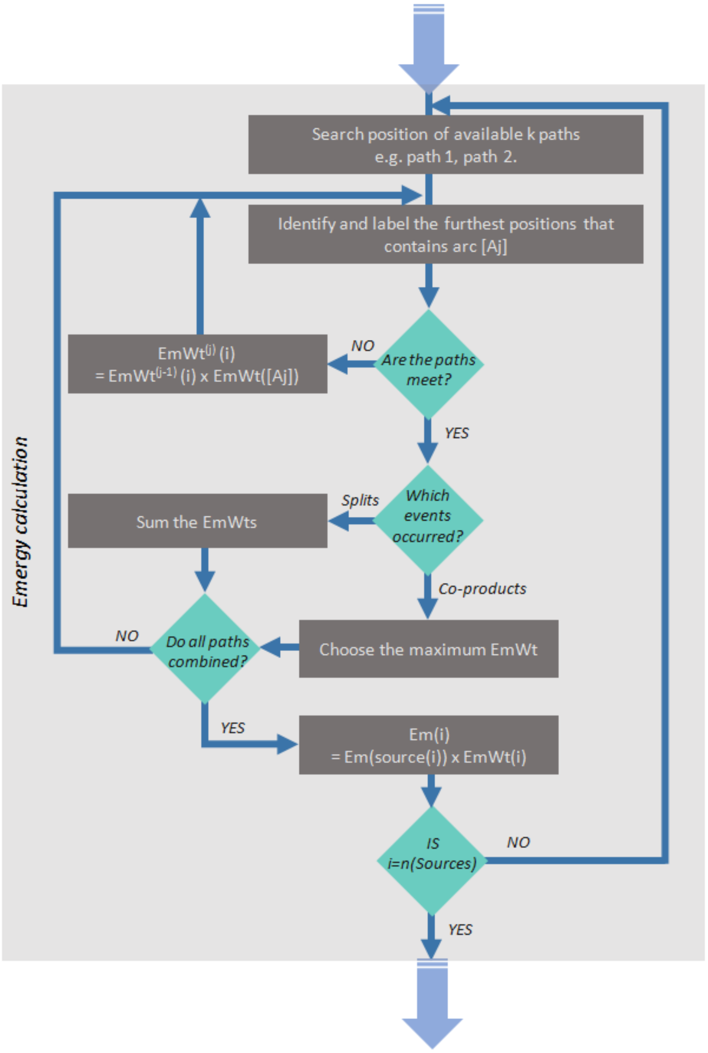

Figure III.7. Block diagram of emergy computation algorithm by MATLAB

Figure III.8. Emergy flowing to output 7 computational diagram

In this case, to work out the emergy flowing to the output 7 the code starts to search for the position of the element in $P_1\{1\}$, where the arcs end with 'output 7'. Thus, in the initial iteration, the code locates arcs [6, 7] in positions (2, 4) and (4, 4). The positions will be labeled as path 1 and path 2, respectively.

Initial iteration:

For 0th iteration, let the $EmWt^{(0)}$ equals to 1 and the positions of the element in the $P_1\{1\}$ matrix where the arcs end with output 7 are marked at (2, 4) and (4, 4).

$EmWt\ \{1\}$ =

iteration	$EmWt^{(0)}$
path 1	1
path 2	1

where $EmWt\{1\}$ is the emergy weight fraction of source 1 to output 7 and path 1 and 2 are [1, 3][3, 4][4, 6][6, 7] and [1, 3][3, 5][5, 6][6, 7], respectively.

The 1st iteration will indicate the furthest position, which is the position (4, 4). The emergy weight fraction will be the product of the emergy weight fraction of previous iteration, (0 iteration), and that of element (4, 4) as follows:

1st iteration:

Current position of elements to output 7 (1st iteration) = (2, 4), <u>(4, 4)</u>

$EmWt\{1\} =$

iteration	$EmWt^{(0)}$	$EmWt^{(1)}$
path 1	1	1
path 2	1	$EmWt^{(0)} \times EmWt(P_1\{1\}(4, 4)) = EmWt([6, 7])$

The 2nd iteration will search for the nearest neighbor element of (4, 4). Since there is no neighbor element in position (4, 3), the search will move to the upper row in the same column, column no.3, and then find the nearest neighbor element at position (3, 3). The emergy weight fraction will be the product of the emergy weight fraction of previous iteration, (1st iteration), and that of element (3, 3).

2nd iteration:

Current position of elements to output 7 (2nd iteration) = (2, 4), (3, 3)

$EmWt\{1\} =$

Iteration	$EmWt^{(2)}$
path 1	1
path 2	$EmWt^{(1)} \times EmWt(P_1\{1\}(3, 3)) = EmWt([6, 7]) \times EmWt([5, 6])$

The 3rd iteration will search for the neighbor element of (3, 3) and then find the nearest element (3, 2). The emergy weight fraction will be the product of the emergy weight fraction of previous iteration, (2nd iteration), and that of element (3, 2).

3rd iteration:

Current position of elements to output 7 (3rd iteration) = (2, 4), <u>(3, 2)</u>

$EmWt\ \{1\}$ =

iteration	$EmWt^{(3)}$
path 1	1
path 2	$EmWt^{(2)} \times EmWt(P_1\{1\}(3, 2)) = EmWt([6, 7]) \times EmWt([5, 6]) \times EmWt([3, 5])$

The 4th iteration will search for the neighbor element of (3, 2). Since there is no neighbor element in position (3, 1), the search moves to the upper row in column no.1 and then finds the nearest neighbor in coordinate (1, 1).

4th iteration:

Current position of elements to output 7 (4th iteration) = (2, 4), <u>(1, 1)</u>

$EmWt\ \{1\}$ =

iteration	$EmWt^{(4)}$
path 1	1
path 2	$EmWt^{(3)} \times EmWt(P_1\{1\}(1, 1)) = EmWt([6, 7]) \times EmWt([5, 6]) \times EmWt([3, 5]) \times EmWt([1, 3])$

In the 5th iteration, it was found that the next furthest coordinate is (2, 4) which belongs to the element of path 1. Thus, the code will move to element (2, 4) and hold the emergy weight fraction data of path 2 in the second column as shown below:

5th iteration:

Current position of elements to output 7 (5th iteration) = <u>(2, 4)</u>, (1, 1)

$EmWt\ \{1\}$ =

iteration	$EmWt^{(5)}$
path 1	$EmWt^{(4)} \times EmWt(P_1\{1\}(2, 4)) = EmWt([6, 7])$
path 2	$EmWt([6, 7]) \times EmWt([5, 6]) \times EmWt([3, 5]) \times EmWt([1, 3])$

The 6th to 8th iteration are used to search for the next nearest elements which are (1, 3), (1, 2) and (1, 1), respectively. The results obtained are as follows:

6th iteration:

Current position of elements to output 7 (6th iteration) = <u>(1, 3)</u>, (1, 1)

$EmWt\ \{1\}$ =

iteration	$EmWt^{(6)}$
path 1	$EmWt^{(5)} \times EmWt(P_1\{1\}(1, 3)) = EmWt([4, 6]) \times EmWt([6, 7])$
path 2	$EmWt([1, 3]) \times EmWt([3, 5]) \times EmWt([5, 6]) \times EmWt([6, 7])$

7th iteration:

Current position of elements to output 7 (7th iteration) = (1, 2), (1, 1)

$EmWt\{1\}$ =

iteration	$EmWt^{(7)}$
path 1	$EmWt^{(6)} \times EmWt(P_1\{1\}(1, 2)) =$ $EmWt([3, 4]) \times EmWt([4, 6]) \times EmWt([6, 7])$
path 2	$EmWt([1, 3]) \times EmWt([3, 5]) \times EmWt([5, 6]) \times EmWt([6, 7])$

8th iteration:

Current position of elements to output 7 (8th iteration) = (1, 1), (1, 1)

$EmWt\{1\}$ =

iteration	$EmWt^{(8)}$
path 1	$EmWt^{(7)} \times EmWt(P_1\{1\}(1, 1)) =$ $EmWt([1, 3]) \times EmWt([3, 4]) \times EmWt([4, 6]) \times EmWt([6, 7])$
path 2	$EmWt([1, 3]) \times EmWt([3, 5]) \times EmWt([5, 6]) \times EmWt([6, 7])$

Finally, in the 8th iteration, it was found that path 1 and path 2 meet at the element (1, 1). Thus, the emergies of both paths have to be combined either by summing or by choosing the one with maximum flow based on events that occurred between split and co-products. As previous mentioned, arc [3, 4] and [3, 5] were the arcs of the co-products flowing out of node 3. The emergy weight fraction of combined paths was equal to the maximum of *EmWt* values among these paths. Since the origin position (1, 1) is reached, the code will terminate and the final emergy weight fraction from source 1 to output 7 will be equal to:

$$EmWt^{(8)}(\text{path 1}) = EmWt\,([1,\ 3]) \times EmWt\,([3,\ 4]) \times EmWt\,([4,\ 6]) \times EmWt\,([6,\ 7])$$

$$= 1 \times 1 \times 1 \times 4/5 = 4/5$$

$$EmWt^{(8)}(\text{path 2}) = EmWt\,([1,\ 3]) \times EmWt\,([3,\ 5]) \times EmWt\,([5,\ 6]) \times EmWt\,([6,\ 7])$$

$$= 1 \times 1 \times 1 \times 4/5 = 4/5$$

$EmWt\ \{1\}$ =

iteration	$EmWt^{\text{final}}$
final	$\max\{EmWt^{(8)}(\text{path 1}), EmWt^{(8)}(\text{path 2})\} = 4/5 = 4/5$

As the vector S_1 is {400 100} in a unit of sej, the emergy from source 1 to output 7 will be equal to:

$$Emergy\{1\}(\text{output 7}) = S_1(1) \times EmWt\ \{1\} = 400 \times 4/5 = 320 \text{ sej}$$

With source 2, there is only one pathway [2, 4][4, 6][6, 7]. With the same approach, the emergy weight fraction for the source 2 can be obtained as follows:

Initial to 3rd iteration:

$EmWt\ \{2\}$ =

iteration	$EmWt^{(0)}$	$EmWt^{(1)}$	$EmWt^{(2)}$
path 1	1	$EmWt^{(0)} \times$ $EmWt(P_1\{2\}(2,\ 3))$ $= EmWt\,([6,\ 7])$	$EmWt^{(1)} \times EmWt(P_1\{2\}(1,\ 2))$ $= EmWt\,([4,\ 6]) \times EmWt\,([6,\ 7])$

$EmWt\{2\}$ =

iteration	$EmWt^{(3)}$
path 1	$EmWt^{(2)} \times EmWt(P_1\{2\}(1, 1))$ $= EmWt([2, 4]) \times EmWt([4, 6]) \times$ $EmWt([6, 7])$

The final emergy weight fraction from source 2 to output 7 will be equal to:

$EmWt\{2\}$ =

iteration	$EmWt^{\text{final}}$
final	$EmWt([2, 4]) \times EmWt([4, 6]) \times EmWt([6, 7]) = 4/5$

The emergy from source 2 to output 7 will be equal to:

$$Emergy\{2\}(\text{output } 7) = S_1(2) \times EmWt\{2\} = 100 \times 4/5 = 80 \text{ sej}$$

Finally, the total emergy flowing from source 1 and source 2 to output 7 will be:

3.5. Emergy accounting of a process with higher complexity

The system G_2 as shown in Figure III.4 consists of 2 sources, 5 intermediates, and 2 outputs with feedbacks, co-products and splits. The emergy flows from source 1 and source 2 act as the vector S_2 {10,000 20,000} in a unit of sej. According to Table III.2, the set of sources is {1, 2}, the set of outputs is {8, 9}, and the set of intermediates is {3, 4, 5, 6, 7}.

Table III.2. Matrix 'M_2' which represent the relations between intermediate processes within the system G_2

	1	**2**	**3**	**4**	**5**	**6**	**7**	**8**	**9**
1	0	0	3/10	7/10	0	0	0	0	0
2	0	0	0	0	0	0	1	0	0
3	0	0	0	0	1	0	0	0	0
4	0	0	0	0	1	0	0	0	0
5	0	0	0	0	0	1/2	1/2	0	1
6	0	0	0	1	0	0	1/2	1/2	0
7	0	0	1	0	0	0	0	0	0
8	0	0	0	0	0	0	0	0	0
9	0	0	0	0	0	0	0	0	0

As reported in matrix M_2, the row with summation greater than one is row no. 3. This implies that the co-products appeared at row no. 5 and row no. 6 elements including arcs [5, 6], [5, 7], [5, 9], [6, 4], [6, 7] and [6, 8]. Matrix $Path_2$ can be rewritten by eliminating the non-terminal arcs in every component of matrix $Path_2$ and store as matrix P_2:

The set of emergy paths ending with output 9 were shown as follow:

$P_2\{1\}([1, ..., 9]) = \{[1, 3][3, 5][5, 9], [1, 4][4, 5][5, 9]\}$

$P_2\{2\}([2, ..., 9]) = \{[2, 7][7, 3][3, 5][5, 9]\}$

Where the position of available paths from source 1 and source 2 to output 9 in matrix $P_2\{1\}$ are (10, 3), (5, 3) and $P_2\{2\}$ is (5, 4), respectively. The emergy weight fraction computation of pathways from source 1 to output 9 was as follows:

Initial iteration:

Current position of elements to node 9 (initial iteration) = (5, 3), (10, 3)

$EmWt\{1\}$ =

iteration	$EmWt^{(0)}$
path 1	1
path 2	1

Where path 1 and path 2 are [1, 3][3, 5][5, 9] and [1, 4][4, 5][5, 9], respectively. The 1st iteration will start the calculation with the furthest element as element at coordinate (10, 3).

1st iteration:

Current position of elements to node 9 (1st iteration) = (5, 3), (10, 3)

$EmWt\{1\}$ =

iteration	$EmWt^{(0)}$	$EmWt^{(1)}$
path 1	1	1
path 2	1	$EmWt^{(0)} \times EmWt(P_2\{1\}(10, 3))$ $= 1 \times 1 = 1$

In the 2nd iteration, since there is no neighbor element in position (10, 2), the search for an element continued in column no.2, and the nearest neighbor was in coordinate (6, 2). Continuing to the 3rd iteration, the neighbor element was in coordinate (6, 1). The emergy weight fraction obtained from the 2nd and 3rd iteration is shown below:

2^{nd} to 3^{rd} iteration:

Current position of elements to node 9 (2^{nd} iteration) = (5, 3), <u>(6, 2)</u>

Current position of elements to node 9 (3^{rd} iteration) = (5, 3), <u>(6, 1)</u>

$EmWt\ \{1\}$ =

iteration	$EmWt^{(1)}$	$EmWt^{(2)}$	$EmWt^{(3)}$
path 1	1	1	1
path 2	1	$EmWt^{(1)} \times$ $EmWt(P_2\{1\}(6, 2))$ $= 1 \times 1 = 1$	$EmWt^{(2)} \times$ $EmWt(P_2\{1\}(6, 1))$ $= 1 \times 7/10 = 7/10$

The 4th iteration searched for the neighbor element of (6, 1), and the nearest element (5, 3) of path 1 was found. Thus, the code moves to element (5, 3) and hold the emergy weight fraction data of path 2 in the second row of matrix $EmWt\ \{1\}$.

4^{th} iteration:

Current position of elements to node 9 (4th iteration) = <u>(5, 3)</u>, (6, 1)

$EmWt\{1\}$ =

iteration	$EmWt^{(2)}$	$EmWt^{(3)}$	$EmWt^{(4)}$
path 1	1	1	$EmWt^{(3)} \times EmWt(P_2\{1\}(5, 3))$ $= 1 \times 1 = 1$
path 2	1	7/10	7/10

In the 5th iteration, as there is no neighbor element in position (5, 2), it searched for an element in column no.2 and found the nearest neighbor in coordinate (1, 2). Then the 6th iteration obtains coordinate (1, 1) as the adjacent element. The emergy weight fraction of 5th and 6th iteration is obtained as shown below.

5th to 6th iteration:

Current position of elements to node 9 (5th iteration) = <u>(1, 2)</u>, (6, 1)

Current position of elements to node 9 (6th iteration) = <u>(1, 1)</u>, (6, 1)

$EmWt\{1\}$ =

iteration	$EmWt^{(4)}$	$EmWt^{(5)}$	$EmWt^{(6)}$
path 1	1	$EmWt^{(4)} \times$ $EmWt(P_2\{1\}(1, 2))$ $= 1 \times 1 = 1$	$EmWt^{(3)} \times$ $EmWt(P_2\{1\}(1, 1))$ $= 1 \times 3/10 = 3/10$
path 2	7/10	7/10	7/10

Finally, the 7th iteration searched for the nearest element and found that both path 1 and path 2 meet the edge of the matrix at column 1. Thus, the emergy of both paths has to be either summed or the one with maximum flow must be chosen on events occurred between split and co-products. As the code indicates that, arcs [1, 3] and [1, 4] are not the arcs of co-products but splits (Section 2.3), the emergy weighted fraction of combined path will be equal to the summation of both *EmWt* values. While the edge positions reached (position (6, 1) and (1, 1)), the code will terminate and the final emergy weight fraction from source 1 to output 9 will be equal to:

7th iteration:

$EmWt\ \{1\}$ =

iteration	$EmWt^{\text{final}}$
final	

Finally, the emergy from source 1 to output 9 will be equal to:

Emergy{1}(output 9) = $S_2(1) \times EmWt\ \{1\}$ = 10,000 × 1 = 10,000 sej

The algorithm is applied to emergy calculation from source 2 to output 9 and the computational data are obtained;

Initial to 4th iteration:

$EmWt\ \{2\}$ =

iteration	$EmWt^{(0)}$	$EmWt^{(1)}$	$EmWt^{(2)}$
path 1	1	$EmWt^{(0)} \times$ $EmWt(P_2\{2\}(5, 4))$ $= 1 \times 1 = 1$	$EmWt^{(1)} \times$ $EmWt(P_2\{2\}(1, 3))$ $= 1 \times 1 = 1$

$EmWt\ \{2\} =$

iteration	$EmWt^{(3)}$	$EmWt^{\text{final}}$
path 1	$EmWt^{(2)} \times$ $EmWt(P_2\{2\}(1, 2))$ $= 1 \times 1 = 1$	$EmWt^{(3)} \times$ $EmWt(P_2\{2\}(1, 1))$ $= 1 \times 1 = 1$

The emergy from source 2 to output 9 will be equal to:

$$Emergy\{2\}(\text{output } 9) = S_2(2) \times EmWt\ \{2\} = 20{,}000 \times 1 = 20{,}000 \text{ sej}$$

In conclusion, the total emergy flowing from source 1 and source 2 to output 9 will be:

$$Emergy\ (\text{output } 9) =$$

$$= 10{,}000 + 20{,}000 = 30{,}000 \text{ sej}$$

After emergy accounting algorithm was applied to all outputs and intermediates pathways in system G_2, the results are shown in Figure III.9. It was found that the results of emergy accounting obtained from MATLAB code can predict emergy flow, in this case, precisely compared to track-summing method by manual calculation from the Odum (Odum, 1996) and Le Corre and Truffet algorithm (Le Corre and Truffet, 2012).

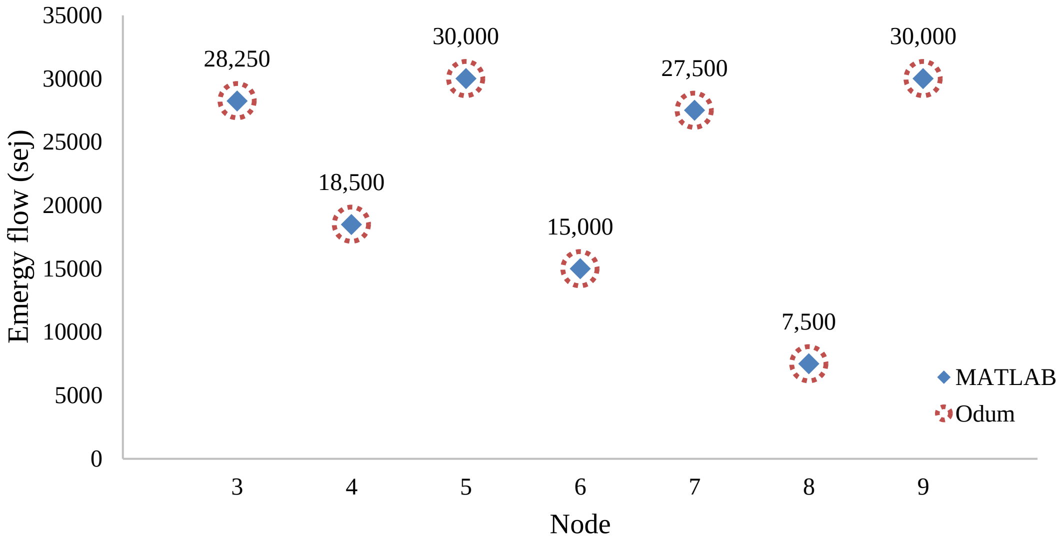

Figure III.9. Emergy flowing to each node in system G_2

3.6. Including feedbacks or stream recycle into emergy algorithm

According to Zarbá and Brown study, the study suggested that the emergy feedback or recycle should be considered in the emergy accounting (Zarbá and Brown, 2015). We would like to point out that we found some issues to be concerned when dealing with the system where co-product occurred. From Figure III.10, consider the emergy of system G_2 (in Chapter 3) when emergy recycle was presented. It was found that when we included the feedback into the calculation, the emergy assigned to product 9 (120,000 sej) was much higher than the total emergy sources (30,000 sej) which turned out unreasonable. It is necessary to understand more about emergy recycling where there is the co-product in the system. Thus, knowing the emergy pathways is still essential to describe the interaction and the possibility of how we can allocate the emergy within the system.

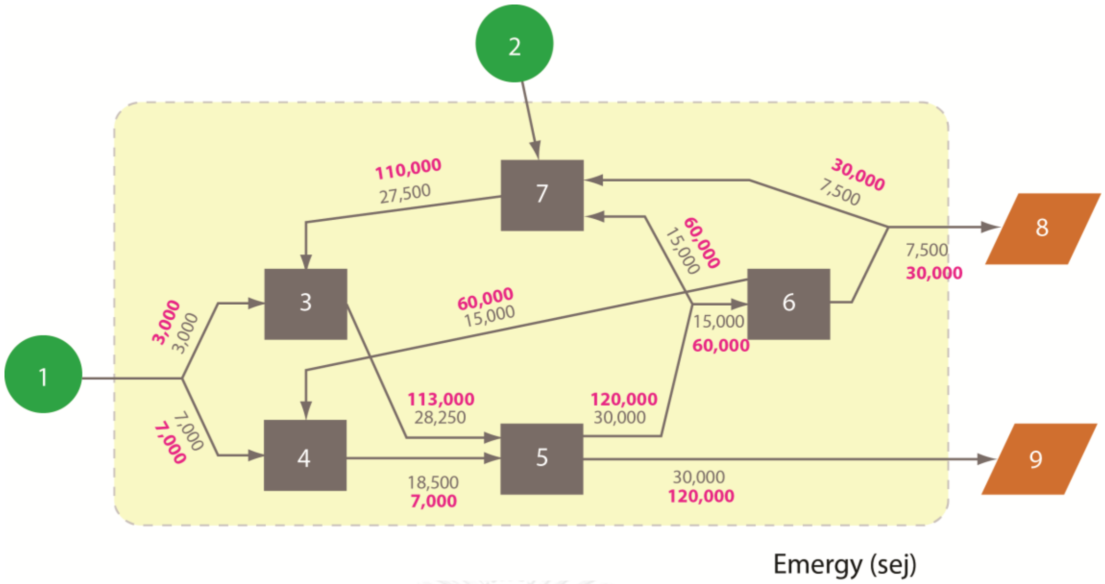

Figure III.10. Amount of emergy source contributing to each process (the emergy in normal text indicate the calculation from emergy algebra and the emergy in bold indicate the calculation concerning feedbacks.

CHAPTER IV: DESIGN AND IMPLEMENTATION OF EMERGY ANALYSIS

In this chapter, the implementation of emergy-based sustainable decision was presented. The main topics includes; the implementation of emergy accounting in the three alternative Carbon-dioxide capture processes (Section 4.1) and the bio-based eco-industrial park (Section 4.2).

4.1. Three Alternative Carbon-dioxide Capture Processes

It is widely acknowledged that fossil fuel levels are non-renewable and are depleting, whilst its use forms the main contribution to global warming. Thus, environmental degradation has become a serious global problem. Renewable energy sources, such as biomass, solar, wind and hydropower, which have been mooted as alternative energy supplies, still require further technical improvement to reduce their investment costs, which are currently higher than conventional fossil-fuel-based technologies (Sims et al., 2003). Over the last few decades there have been a number of studies focused on bio-based technology to reduce fossil fuel dependency by obtaining fuels, power, heat and value-added chemicals from renewable feedstocks. These could lower the environmental impacts and increase the economic development. Nevertheless, the current major energy source remains fossil fuels, and they are the primary source of carbon dioxide (CO_2) emission. Although, the biorefinery can lower the net CO_2 emission through its life cycle, capturing CO_2 emission from co-combustion is still an important issue in alternative energy development. Within the present alternative technologies, CO_2 capture plays an important role in progressing towards a low-CO_2 emission society.

Currently, an abundance of research studies have focused on CO_2 capture techniques, such as the widely used chemical absorption (Hadri et al., 2015; Manzolini et al., 2015; Muhammad and GadelHak, 2015), solid sorbent adsorption (Lee et al., 2015; Plaza et al., 2012; Valverde et al., 2013), membrane separation (Franz et al., 2014; Lu et al., 2014) and other advanced techniques (Campanari et al., 2014; Iloeje et al., 2015; Rekha et al., 2016). Absorption of CO_2 is performed by chemical or physical absorption. Chemical absorption is suitable for dilute CO_2 sources, such as the flue gas from power plants, but it requires a large amount of heat for absorbent (solvent) regeneration and a fair amount of the absorbent is lost due to the acidic contents in the flue gas stream. Physical absorption requires less energy than chemical absorption and the properties of the physical sorbent make it less susceptible to the impurities in the flue gas. However, it requires a high-pressure operation, is subject to corrosion issues and is only suitable for high CO_2 concentration sources. Nevertheless, adsorption is one of the promising technologies for CO_2 capture due to its availability, low cost and high thermal stability. Membrane separation methods are also one of the new upcoming technologies and have the advantage of being space efficient and yield a high CO_2 purity. However, the cost of the membrane is very high.

From an economic viewpoint, the vacuum pressure swing adsorption was considered the best option compared to other techniques (Kuramochi et al., 2011), where increasing the flow rate of the absorbent solution gave a higher CO_2 removal efficiency (Yincheng et al., 2011). However, the large chemical consumption involved in the process may lead to a high level of toxic waste. Moreover, alkyl amine (chemical) absorption requires a large energy consumption for the solvent regeneration (Øi and Kvam, 2014). With respect to the other CO_2 capture techniques, similar queries about the comparative advantages and disadvantages of each technique have also arisen. Thus, a proper assessment is needed to use as a guideline for decision making.

In this study, emergy accounting was applied to quantify the resource utilization and to compare the process performance, in terms of sustainability, of three alternative carbon capture technologies, using representative examples from the literature. Currently these three processes are believed to be promising ways for CO_2 capture. The results were then used to indicate the weak points of each process that could serve as guidelines for further improvement of each CO_2 capture process.

4.1.1. Process Description

Flue gas containing CO_2 is the waste product generated from many systems, such as combustion chambers, power plants, gasification process and other production activities. This study was focused on the post-combustion CO_2 capture and storage of a pulverized coal fired power plant system with a capacity of 400–550 MW. The system boundaries were scoped around the CO_2 capture units, with flue gas as the main or sole input and clean air as the output of the process. Here, we have reviewed that the selected cases shared similar features with the other reported systems. The system boundaries for the MEA-based chemical absorption system, supported amine solid-based physical adsorption and two-stage polymeric membrane separation are depicted in Figure IV.1 where the selected case studies all considered both CO_2 capture and CO_2 compression units. The system information needed for the emergy calculation is briefly explained in the following sections.

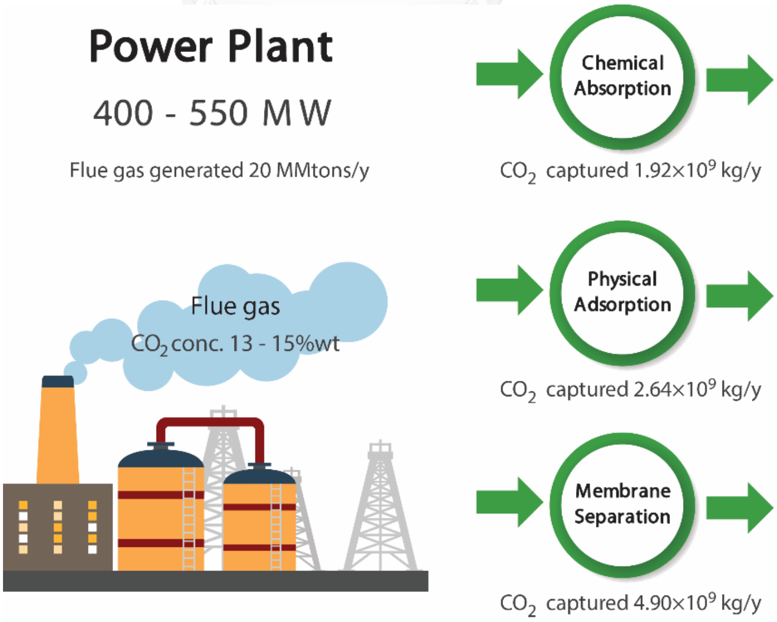

Figure IV.1. System boundary of the CO_2 capture processes

4.1.1.1. Chemical (MEA) Absorption of CO_2

Among various CO_2 capture technologies, chemical absorption methods are the most common processes, since they are suitable for dealing with a large amount of flue gas. In this study, the information of CO_2 capture using MEA as the sorbent was obtained from a previously studied 400 MW pulverized coal fired power plant (Desideri and Antonelli, 2014; Singh et al., 2003b). The MEA-based CO_2 capture process has been modeled in the literature using simulation software Hysys & Aspen Plus. In this process, the inlet flue gas with low CO_2 concentration (13-15% wt) fed into the absorption column where CO_2 absorption by MEA solvent was carried out. Continuously, the lean MEA solvent was then regenerated in a distillation column where its high purity CO_2 was discharged from the solution and the rich MEA solvent was sent back into the absorption column. Additionally, besides absorption and regeneration column in the amine scrubber process, the process also required supplemental power supply system (the chosen technology was gas turbine combined cycles or GTCC) to provide additional power to the absorption process (including flue gas compression and CO_2 compression system), but pump duties were not considered since the units operated at relatively low pressures (1-2 bar). To maintain the power output (400 MW), natural gas was used as a fuel for this power supply and also, required for boilers in the MEA regeneration column. In order to perform the emergy accounting, the data for CO_2 capture and storage was calculated as follows: (i) The annual cost of cooling water was \$2,869,812/y (unit cost \$0.01/m^3; (ii) makeup MEA consumption was 1.6 kg/ton CO_2 produced (CO_2 emissions totaled 2,960,000 tons CO_2 produced/y); (iii) the cost for additional chemical consumption was \$7,000,000/y; (iv) total natural gas demand to auxiliary power supply section for the absorption process was 12,564,747 MMBtu/y; (v) installation and maintenance cost of the CO_2 capture system was \$19,082,053/y; (vi) total operating and maintenance cost of the CO_2 capture system was \$20,463,061/y; and (vii) CO_2 removal capacity was 1,923,685 tons/y.

4.1.1.2.Physical Adsorption of CO_2

Solid sorbent technology is another potential CO_2 capture process, and it has been claimed to have a lower cost and energy consumption. Solid sorbent adsorption can handle a high flue gas capacity and so could be a competitor of the alkyl amine chemical absorption, while it reduces the drawbacks of the alkyl amine absorption system, including equipment corrosion, high energy consumption in the sorbent regeneration stage and the size of the required absorption tower (Kongkitisupchai and Gidaspow, 2013). The feasibility of solid-based CO_2 capture technology was investigated in a temperature swing adsorption system with supported amine as the solid sorbent, based upon treating the flue gas produced by a 400 MW coal-fired power plant, which was simulated from a1 kW pilot scale (Krutka and Sjostrom, 2011). The proposed system consisted of a co-current reactor as the adsorber, where CO_2 in flue gas from a power plant was adsorbed onto the supported amine sorbent, and a fluidized-bed as the regenerator, where the solid sorbent released the adsorbed CO_2 before recycling to the adsorption section. The CO_2 capture required supplemental steam and electricity supply resulting in the net power output to be reduced from 433,778 kW to 343,324 kW due to the parasitic load was from CO_2 capture, which accounted for 90,454 kW (costs $47,281,000/y). This value reflects the amount of steam and electricity required for the CO_2 capture system where most electrical load consumed by the CO_2 compressor (35% of total load). The calculation of the solid-based system (option B in (Krutka and Sjostrom, 2011) without an exchanger network) was as follows: (i) make-up solid sorbent feed rate was 3.74 tons/d and cost $12,780,666/y; (ii) sodium hydroxide consumption for the chemical treatment cost $499.75/ton and totaled $21,707/y; (iii) additional chemical costs of lime and sulfuric acid in the feed were $242.56/ton and $160/ton, respectively, accounting for $67,126/y and $22,834/y, respectively; (iv) makeup water (unit cost $0.000378/gallon) for evaporation and blowdown totalled $81,060/y and $40,530/y, respectively; (v) natural gas consumption was $464,949/y (unit cost $7.41/MMBTU); (vi) leveled makeup power cost was $47,281,000/y (unit cost 7.02 ¢/kWh); (vii) material and equipment cost of the adsorption process was \$7.21 × 10^6 /y (based on a 20 y life-time assumption); (viii) labor for the startup plant was \$9.04 × 10^6 /y; (ix) miscellaneous services cost was \$5,066,228/y; and (x) the CO_2 production rate was approximately 2,635,065 tons/y.

4.1.1.3.CO_2 Removal by Membrane (two-stage polymeric) Separation

In addition to chemical absorption, membrane-based separation is an alternative technology to capture CO_2. Through solution-diffusion, CO_2 in flue gas is diffused through a membrane layer using the pressure difference as the driving force. This system has no need for sorbent regeneration and can operate without a chemical input (Zhai and Rubin, 2012). However, the membrane stability is low under high temperatures and so heat exchangers are required to provide a stable operation. The calculation of the membrane separation, obtained from a feasibility analysis of a 550 MW coal-fired power plant, was as follows: (i) power consumption for CO_2 capture was 31.1% of the gross electrical output (883.2 MW); (ii) additional capital cost of electricity for CO_2 capture and storage was \$57.6/MWh; (iii) process operator cost was \$249,480/y; (iv) CO_2 emission rate from the flue gas before CO_2 capture was 0.812 kg/kWh; (v) the capacity of the membrane separation process was approximately 85%, giving a CO_2 emission rate after CO_2 capture of 0.122 kg/kWh.

4.1.2.Emergy analysis of the three alternative CO_2 capture processes

The results of emergy analysis are summarized in Table IV.1-Table IV.3, where the resources utilized from the upstream process that produced the flue gas were not taken into account. This is because the flue gas was not the product of the upstream process and those processes were not in the boundary system. Rather, the flue gas is the undesirable product generated from the process activities and so unlike in conventional systems, it is not a feedstock. Thus, the emergy value of the flue gas was zero. Also, in the case of the solid adsorption and membrane separation, the referenced data was the up-scaled estimation from the pilot scale, since it was important to compare data from power plants of similar characteristics. By doing this the upstream processes will have no effects on the results.

From Table IV.1, although the CO_2 capture in the MEA absorption process was mainly dependent on the chemical solvents, including MEA and inhibitors, the chemical consumption accounted for only 2% of the total emergy consumption due to the regeneratable properties of the absorbent within the process. Since a large proportion of the MEA and chemicals were regenerated, the highest emergy consumption in the MEA absorption process was the natural gas (91% of total emergy consumption) used to power the steam boiler and heater. In addition, the cooling water, required for controlling the temperature in the regeneration reactor and to remove the heat produced by the two-stage compressor in the CO_2 purification section, accounted for 4% of the total emergy consumption. The installation, maintenance materials and services of the CO_2 capture section had only a small emergy distribution (4% of the total emergy consumption) compared to natural gas and cooling water consumption. The CO_2 capture installation cost was mainly derived from the absorption column. The regeneration column and the rest of the costs were from the piping, heat exchangers, tanks and pumps. Thus, the main variable that dominates the MEA absorption process was the natural gas used to heat the process. While the UEV of CO_2 capture in the process was 1.06 × 10^{12} sej/kg CO_2 as presented in Table IV.1.

For the solid sorbent adsorption, the emergy analysis was carried out and the result is shown in Table IV.2. The major UEV contribution to the process was the electricity consumption, which accounted for 75% of the total emergy consumption in the process. In this case, natural gas was only used to provide supplementary energy, with the main energy supply being electricity. Steam was mainly employed to drive the sorbent regeneration process and support the adsorption reaction, since CO_2 removal by a solid sorbent requires a certain amount of steam to complete the reaction effectively (Seo et al., 2007). The supported amine sorbent in the current process can be regenerated thermally and so the sorbent and chemicals accounted for only 8% of the total emergy. The UEV of the CO_2 capture by this solid sorbent was 1.09 × 10^{11} sej/kg CO_2. In this case study, the thermal regeneration is applied to the supported amine sorbent. Although the solid sorbent can be regenerated by alternative procedures such as reduced pressure method which is easier to handle than thermal regeneration and could lower the heat consumption within the process (Kongkitisupchai and Gidaspow, 2013). However, we cannot conclude that the reduced pressure method is preferable in this case since we require the studies on the compatibility between amine-based solid sorbent and the reduced pressure regeneration procedure to confirm the assumption.

The two-stage polymeric membrane-based CO_2 capture system was operated by a complex reactor with high cost per kg of CO_2 captured, the emergy analysis is shown in Table IV.3. The two main contributors to the UEV of the process were the installation materials used (7.04 × 10^{20} sej, 51% of the total emergy consumption) and the electricity consumption (6.66 × 10^{20} sej, 49% of the total emergy consumption). The electricity was mainly used to pressurize the flue gas for processing through the membrane, with no chemicals required in this separation process since the material and reactor design play significant role to its efficiency. The UEV of CO_2 captured in this membrane separation was 2.79 × 10^{11} sej/kg CO_2. In this study, the UEV derived from electricity was 8.92 × 10^4

sej/J, which was obtained from coal in a combined heat and power plant (conventional coal power plant) (Sha and Hurme, 2012). If the electricity could be obtained from renewable resources, such as solar or wind power, the sustainability of the membrane separation process would be higher. Figure IV.2a, b and c represent the emergy diagram summarizing the inputs and outputs of each process.

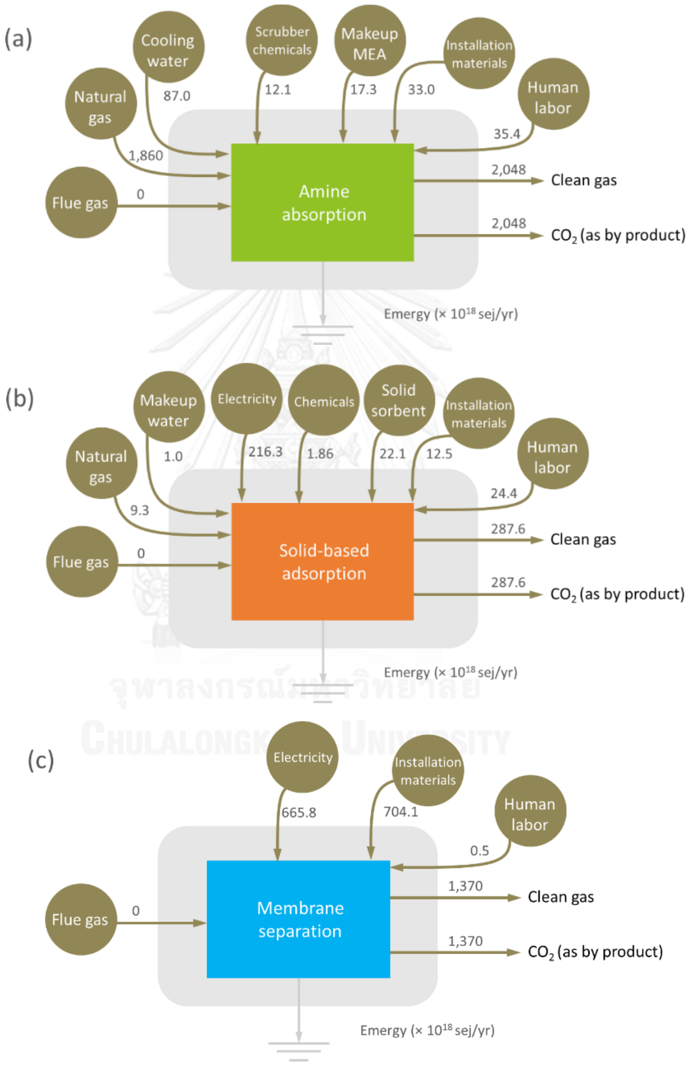

Figure IV.2. Emergy diagram of the (a) MEA chemical absorption, (b) supported amine solid-based physical adsorption and (c) membrane separation processes for CO_2 removal from flue gas

Table IV.1. Emergy analysis of the MEA chemical absorption of CO_2

Note	Item	Amount	Unit	UEV (sej/unit)	Emergy	Unit	% of total emergy used
	Resources from outside (F)						
1	Cooling water	2.87×10^{11}	kg/y	3.03×10^{8}	8.70×10^{19}	sej/y	4%
2	Make up MEA	4.74×10^{6}	kg/y	3.65×10^{12}	1.73×10^{19}	sej/y	1%
3	Scrubber chemicals	7.00×10^{6}	$/y*	1.73×10^{12}*	1.21×10^{19}	sej/y	1%
4	Natural gas	1.33×10^{16}	J/y	1.41×10^{5}	1.86×10^{21}	sej/y	91%
5	Installation material	1.91×10^{7}	$/y*	1.73×10^{12}*	3.30×10^{19}	sej/y	2%
	Labor and services (S)						
6	Miscellaneous services	2.05×10^{7}	$/y*	1.73×10^{12}*	3.54×10^{19}	sej/y	2%
	Products:						
7	CO_2 removed	1.92×10^{9}	kg/y	1.06×10^{12}	2.05×10^{21}	sej/y	

Table IV.2. Emergy analysis of solid-based physical adsorption of CO_2

Note	Item	Amount	Unit	UEVs (sej/unit)	Emergy	Unit	% of total emergy used
	Resources from outside (F)						
1	Solid sorbent	1.28×10^{7}	\$/y	1.73×10^{12}*	2.21×10^{19}	sej/y	8%
2	Sodium hydroxide	4.34×10^{4}	kg/y	8.11×10^{12}	3.52×10^{17}	sej/y	0%
3	Lime	2.77×10^{5}	kg/y	1.27×10^{12}	3.52×10^{17}	sej/y	0%
4	Sulfuric acid	1.43×10^{5}	kg/y	8.11×10^{12}	1.16×10^{18}	sej/y	0%
5	Makeup water	1.22×10^{9}	kg/y	8.71×10^{8}	1.06×10^{18}	sej/y	0%
6	Natural gas	6.62×10^{13}	J/y	1.41×10^{5}	9.30×10^{18}	sej/y	3%
7	Electricity (PP feedback)	2.42×10^{15}	J/y	8.92×10^{4}	2.16×10^{20}	sej/y	75%
8	Material and equipment cost	7.21×10^{6}	\$/y	1.73×10^{12}*	1.25×10^{19}	sej/y	4%
	Labor and services (S)						
9	Labor (for set up plant)	9.04×10^{6}	\$/y	1.73×10^{12}*	1.56×10^{19}	sej/y	5%
10	Miscellaneous services	5.07×10^{6}	\$/y	1.73×10^{12}*	8.76×10^{18}	sej/y	3%
	Products:						
11	CO_2 removed	2.64×10^{9}	kg/y	1.09×10^{11}	$\overline{2.88\times10^{20}}$	sej/y	

Table IV.3. ***Emergy analysis of the membrane separation of CO_2***

Note	Item	Amount	Unit	UEVs (sej/unit)	Emergy	Unit	% of total emergy used
	Resources from outside (F)						
1	Electricity	7.46×10^{15}	J/y	8.92×10^{4}	6.66×10^{20}	sej/y	49%
2	Installation material	4.07×10^{8}	$/y	1.73×10^{12}*	7.04×10^{20}	sej/y	51%
	Labor and services (S)						
3	Miscellaneous services	2.49×10^{5}	$/y	1.73×10^{12}*	4.80×10^{17}	sej/y	0%
	Products:						
4	CO_2 removed	4.90×10^{9}	kg/y	2.79×10^{11}	1.37×10^{21}	sej/y	

4.1.3.Sensitivity analysis of the three alternative CO_2 capture processes

The sensitivity analysis of dominating factors that influenced the UEVs in each case are shown in Figure IV.3: amine absorption, natural gas consumption; solid-sorbent adsorption, power consumption; membrane separation, power consumption and installation material. We have simulated where emergy of these factors varied from 20% decreased to 20% increased (Table IV.4). The sensitivity indicates that when increase 20% of the dominating factors' emergy the higher UEVs were obtained. The highest UEV was amine absorption case which was 18% higher than the base case. While reducing 20% the dominating factors' emergy leading to lower UEV, the lowest possible UEV was the solid-sorbent adsorption case which accounted for 1.1 × 10^{11} sej/CO_2 captured. Therefore, there is no significant changes in the results since amine absorption and solid-sorbent adsorption were still the highest and lowest emergy consumption, respectively, in both modified cases.

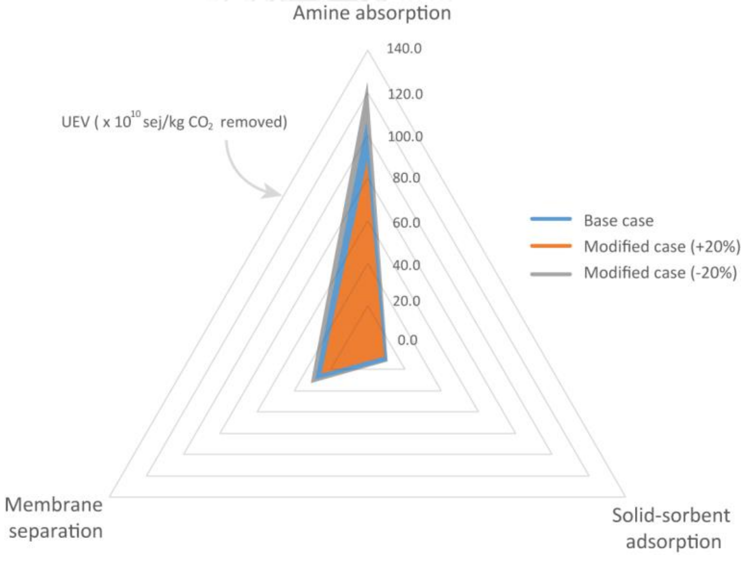

Figure IV.3. Sensitivity analysis of main factors for three carbon capture technologies related to UEV

Table IV.4 Dominant factors in sensitivity analysis

Case	Dominant factors	Annual rate			UEV (× 10^{10} sej/kg CO_2 removed)		
		Base Case	**Reduced (20%)**	**Increased (20%)**	**Base Case**	**Reduced (20%)**	**Increased (20%)**
Amine absorption	NG	1.86E+21	1.49E+21	2.24E+21	106.4	87.1	125.8
Solid-sorbent	Electricity	2.16E+20	1.73E+20	2.60E+20	10.9	9.2	10.9
Membrane	Installation mat.	7.04E+20	5.63E+20	8.45E+20	27.9	25.1	30.8

From the above results, the solid sorbent adsorption was the most efficient among the three-selected CO_2 capture processes for removing CO_2 from the flue gas stream. Moreover, the solid-based physical adsorption process was preferable to the liquid MEA chemical absorption since it required only non-toxic chemicals that were also regeneratable. From an economic viewpoint, the membrane-based separation process had the highest cost of CO_2 capture (Table IV.5), but the emergy analysis indicated that the membrane separation consumed natural resources and it is more efficient than the MEA absorption. The monetary price of input steam, such as when produced by natural gas, underestimates its natural value, but the MEA absorption and membrane separation methods for CO_2 removal can be enhanced to obtain a better result.

Table IV.5. Cost of CO_2 capture for each case study

No.	**Item**	**Annual cost ($/y)**	**$/kg CO_2**	**UEV (sej/kg CO_2)**
	Amine absorption		0.0552	2.05×10^{21}
1	Cooling water	2.87×10^{6}		
2	Make up MEA	6.61×10^{6}		
3	Scrubber chemicals	7.00×10^{6}		
4	Natural gas	5.03×10^{7}		
5	Installation material	1.91×10^{7}		
6	Operating and maintenance	2.05×10^{7}		
	Total	1.07×10^{8}		
	Solid-based adsorption		0.0311	2.88×10^{20}
1	Solid sorbent	1.28×10^{7}		
2	Sodium hydroxide	2.17×10^{4}		
3	Lime	6.71×10^{4}		
4	Sulfuric acid	2.28×10^{4}		
5	Makeup water	1.22×10^{5}		
6	Natural gas	4.65×10^{5}		
7	Electricity (PP feedback)	4.73×10^{7}		
8	Material and equipment cost	7.21×10^{6}		
9	Labor (for set up plant)	9.04×10^{6}		
10	Miscellaneous services	5.07×10^{6}		
	Total	8.21×10^{7}		
	Membrane separation		0.1127	1.37×10^{21}
1	Electricity	1.46×10^{8}		
2	Installation material	4.07×10^{8}		
3	Miscellaneous services	2.77×10^{5}		
	Total	5.53×10^{8}		

4.2. Bio-based eco-industrial park

4.2.1.Process Description

To achieve sustainable bio-based industries, the biorefinery case studies were designed using Aspen Plus software to simulate an industrial symbiosis with the closed loop concept of materials and energy through reuse and recycle. The materials and energy in the process become more optimally used, and the waste generation is minimized. The system boundary were included the feedstock cultivation, where the data were obtained from the literature and published surveys in Thailand, and eight production processes of the biorefinery (Figure IV.4) in total of nine processes: (1) Napier grass crop production (or cultivation), (2) gasification, (3) combined heat and power plant (CHP), (4) syngas cleaning, (5) fuel synthesis, (6) hydroprocessing (HDP), (7) methanol synthesis process, (8) carbon dioxide capture and (9) waste water treatment. In this section, the crop production phase will be presented first, and followed by the biorefinery phase where Napier grasss will be converted into the bio-based products.

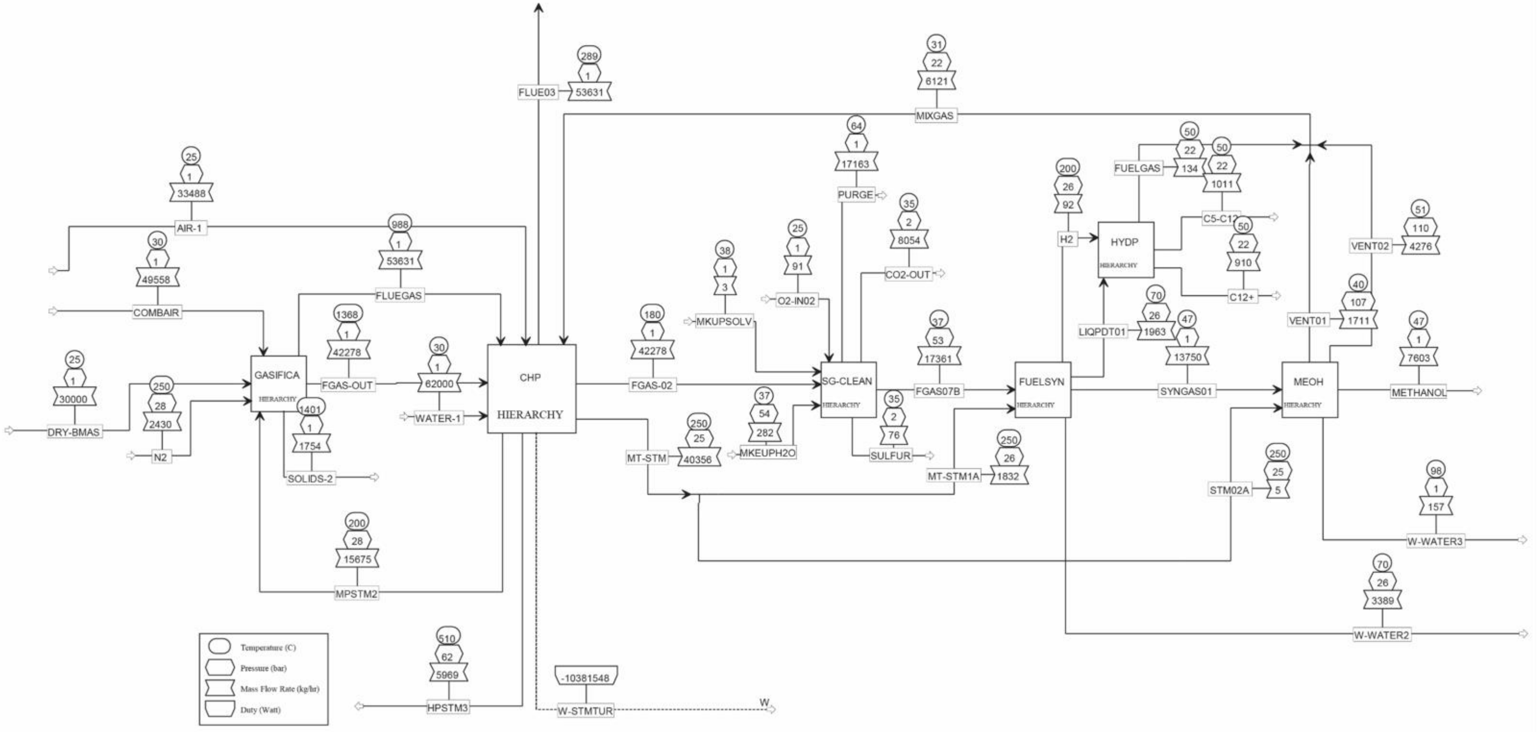

Figure IV.4. Block flow diagram of the biorefinery system.

4.2.1.1.Crop production

Napier grass cultivation data was collected and reported by researchers from Pakchong, Nakhon Ratchasima province in northeastern of Thailand in year 2013 (DEDE, 2013). Napier grass can be harvested 5–6 times per year. The first harvest takes place four months after planting and ratoons are harvested every other month for up to seven years. To maintain the crop yield during the 7 years, soil amendments and harrowing are required after every harvest and weeding are performed twice a year.

Other general assumptions were as follows: (1) local renewable resource information was based on Thailand data including solar radiation, rain and geothermal which were taken from the Thai Meteorological Department (TMD, 2016); (2) evapotranspiration of Napier grass was evaluated using the FAO procedure and the Napier crop coefficient data from Thai Royal Irrigation Department which was equal to 5.70 mm/d or 2.08×10^7 kg/(ha·y); (3) average soil loss from crops in Thailand is 25 t/(ha·y) (Pansak et al., 2008); (4) organic matter in soil is 1.5% (Norsuwan et al., 2014) with the energy content 14.6 GJ/t (Cohen et al., 2006); (5) replanting new crops required initial Napier stems about 3,100 - 3,800 kg/ha; (6) initial Napier stems for cultivation were considered as an external input; (7) diesel fuel consumption rate for Napier grass growing and harvesting was estimated from data referred from (Morandi et al., 2016); (8) for Napier grass transporting the truck capacity and distance from cultivation field to the plant were approximately 3 tons per trip and 56 km per trip, respectively. (9) data for all agricultural machinery was obtained from (Morandi et al., 2016); (10) all machines for Napier grass cultivation were assumed to have 20 years lifetime; (11) the fresh biomass (initial moisture 30%) was sun-dried before transporting to the biorefinery site (after sun-dried moisture 15%); (12) Napier grass annual production rate (fresh Napier grass) is 70–80 t/(ha·y), which was hence assumed to be 75 t/(ha·y) (DEDE, 2013); (13) the energy content of Napier grass is 18 MJ/kg (Flores et al., 2012).

4.2.1.2. Biorefinery

The biofuel production was developed using the Aspen Plus 8.6 simulation software. The main objective of this system is to reduce the dependence of imported inputs. Further, the chosen technologies were (1) potentially applicable and (2) using continuously regenerated raw materials.

The biorefinery model was simulated to provide 3 main purposes; 1) chemical production which were methanol and 2 grades of liquid fuels: the naphtha-range (C_5-C_{12}) and diesel-range (>C_{12}) qualities, 2) a combined heat and power plant to generate utilities within the system and; 3) waste treating unit (syngas cleaning, CO_2 capture and waste water treatment) to capture acid gas, treat and recycle water within the process. Also, the by-product from waste treating units were obtained including concentrated CO_2 and sulfur cake. The details of the whole process were described as follow.

The first process in the biofuel production system was the gasification process, where the biomass is burnt with air and steam to produce syngas (Preciado et al., 2012). The proposed reactor model in this process was the steam blown dual fluidized bed gasifier, since this was claimed to give a higher efficiency than a conventional gasifier (Doherty et al., 2013). The syngas outlet stream composed of steam, H_2, CO, CO_2 and small amount of H_2S. The hot (1,300 °C) gas produced in the gasifier was then sent through the CHP in the third process to extract the heat from the hot syngas stream. Also, the unconverted gas from further processes, such as HDP and methanol synthesis, was recovered back into the CHP where the gas and air combusted to provide more heat to the system. The steam that was generated, which carried a large amount of energy, was sent to the steam turbine to produce electricity. In this process, electricity and heat were produced simultaneously. Besides power, the CHP process produced steam under four conditions to support the whole system. These were medium temperature steam (250 °C, 2.5 MPa), high temperature steam (500 °C, 2.5 MPa), medium pressure steam (200 °C, 2.8 MPa) and high pressure steam (510 °C, 6.2 MPa). The heat and power generated were primarily used within the system, while the remaining were considered as external products including; 7.9 MW electricity and 3.72 × 10^8 MJ high pressure steam/y.

After the CHP process, the cold syngas stream (180 °C) went through the outlet to the gas cleaning process. In this process, the cold syngas was sent to the water scrubber to remove small particulates, such as fly ash, and was then delivered to the sour water-gas shift reactor to adjust the CO: H_2 ratio at 2.1. The sour gas was then sent to the monoethanolamine (MEA) absorber to remove the acid gases (including CO_2 and SO_2). The cleaned syngas was then fed into the fourth stage wherein the refined gas was synthesized to liquid fuels through the Fischer-Tropsch process. The reactor was operated at 200 °C and 2.5 MPa, based on the NREL literature model (Swanson et al., 2010). After the Fischer-Tropsch reaction, to obtain the liquid fuels with a high gasoline portion, the liquid product was treated with H_2 in HDP. Finally, the liquid fuels within the naphtha-range (C_5-C_{12}) and diesel-range (>C_{12}) qualities were obtained. The remaining unconverted syngas from the fuel synthesis was sent to the methanol synthesis process to produce methanol as a by-product. The methanol synthesis was developed using kinetic reaction model referred from De María study (De María et al., 2013).

The assumptions for treatment of the wastes were based on the following literatures: (1) water condensate from the syngas production, which contained soluble volatile matter at less than 0.02% by mass and was treated and recycled to the CHP process for steam production. The emergy calculation data referred from Arbault (Arbault et al., 2013). (2) the flue gas from the CHP process which contained CO_2 at about 980 ppm was sent to the treating unit for carbon capture process where a high CO_2 concentration was obtained as a by-product. The system referred from literature (Desideri and Antonelli, 2014) where the amine absorption was employed. Also some economic information for emergy accounting referred from Singh (Singh et al., 2003a). No detailed simulation was made for the waste treatment processes.

4.2.2.Emergy analysis

Figure IV.5 depicts the process which is under investigation as described earlier. It is mainly composed of biomass cultivation section and biorefinery section. As shown in Figure IV.5, the biomass cultivation stage involved with three main input resources including free natural resources and imported resources from economy while in biorefinery stage required only imported resources from economy. The free natural resources are renewable resources (R) including solar, rain, geothermal heat and evapotranspiration and non-renewable resources (N) including organic matter in soil. The imported resources from economy or the external resources can be classified into two types, i.e., purchased energy and materials (F) and human labor (L). The labor is the main parameters that distinguishes the emergy analysis from other assessments. Since human labor or manpower cannot be measured in energy or exergy Joule. The following emergy results will explain why human labor is the important factor to the agricultural system and how cultivation stage dominates the sustainability of the entire system.

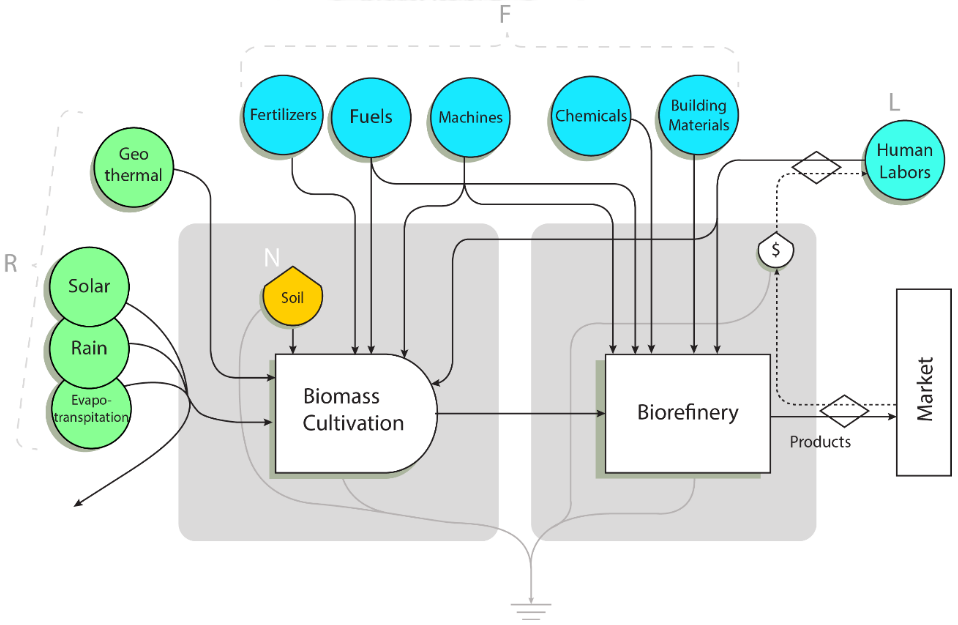

Figure IV.5. Emergy diagram of the system including biomass cultivation and biorefinery.

4.2.2.1.Emergy analysis of biomass cultivation

As presented in Table IV.6 and Figure IV.6, the total emergy consumption of Napier grass cultivation was 6.39×10^{19} sej/yr with 2.21×10^{19} sej/yr or 35% of total emergy dominated by local natural resources (R and N) including evapotranspiration (2.12×10^{19} sej/yr), geothermal heat (9.04×10^{17} sej/yr) and soil loss (3.03×10^{16} sej/yr). The remainders are external resources (F and L) accounts for 4.17×10^{19} sej/yr or 65% of total emergy including irrigation water (1.03×10^{17} sej/yr), napier stems (4.18×10^{17} sej/yr), fertilizers (2.48×10^{18} sej/yr), diesel as a transportation fuel (1.91×10^{19} sej/yr), machinery (4.15×10^{15} sej/yr), direct labor (1.35×10^{19} sej/yr) and indirect labor (6.17×10^{18} sej/yr).

The major sources of emergy inputs to Napier cultivation were evapotranspiration which reflects the amount of water absorbed by Napier grass from natural resources followed by labor at 35% and 31% of the total emergy input, respectively. The direct on-site labor had a high impact on the cultivation processes, due to its being rural farming. Also, the data from NEAD (NEAD, 2010; UND, 2011) reported that the renewability fraction in human resources in Thailand accounted for only 10%, a high direct labor input to the Napier grass cultivation process caused a low renewability to the biomass product.

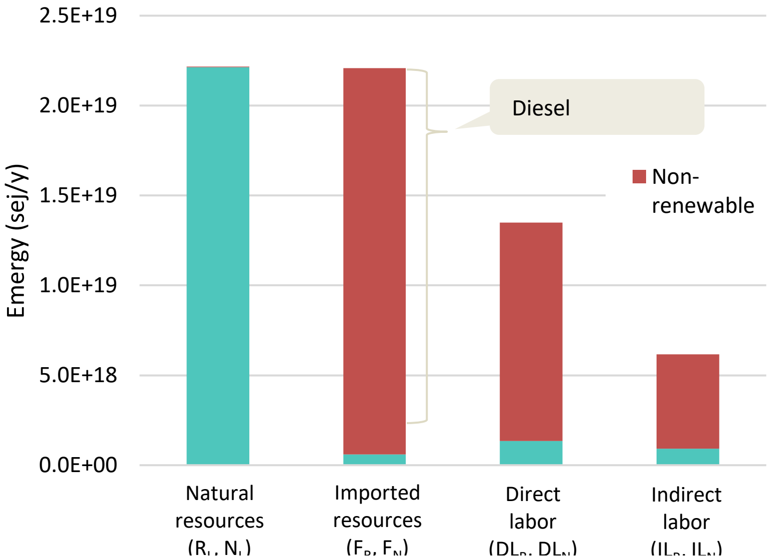

Figure IV.6. Emergy profile of Napier cultivation

** Note: Indirect labor reflects the labor cost occurring upstream in the supply chain associated with the studied system. For example, the Napier plantation required direct labor to plant and operate the machines. While the indirect labor, in this case, represents by the cost of machinery and tools as the upstream labor costs. Calculation detail of indirect labor for each process was shown in the Appendix A.

Moreover, diesel as transportation fuel also played significant role in the cultivation section with the consumption accounted for 30% of total emergy consumption. Figure IV.7 illustrate numerical proportion of diesel consumption in Napier grass cultivation. The highest fuel consumption was biomass transportation. This mainly due to the assumption made on the distance between plantation site and the biorefinery site (which was 56 km). Thus, the significant factor affecting the growth of Napier grass consists of the natural resource, labor and diesel used with 35%, 31% and 30% emergy distribution, respectively.

In Table IV.7, the present result showed that only 39% of emergy are renewable (%R_{global}), causing a high load to the environment, as presented in the ELR. The ELR of Napier cultivation was 1.89, which lies within the moderate impact to the environment range, according to (Brown and Ulgiati, 2004). While in terms of EYR, even the major source of the cultivation is the local resource which is 35% contribute to the system, it is still lower than the external or purchased resources. The ESI of the cultivation is 0.81.

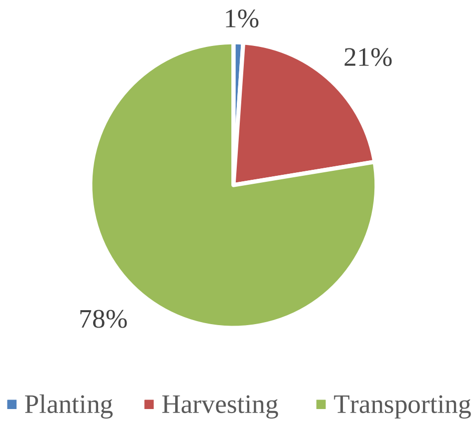

Figure IV.7. Distribution of diesel consumption in Napier cultivation

Table IV.6. Emergy analysis of napier grass cultivation stage.

Note	Item	Amount	Units	UEV (sej/unit)	Emergy (sej/y)	%	Renewable fraction	%R
1	Agricultural phase							
	Local renewable resources (R)							
1.1	Solar insolation**	2.30E+17	J/y	1	2.30E+17	-	-	-
1.2	Rain (Chemical potential)**	2.60E+14	J/y	2.31E+04	6.01E+18	-	-	-
1.3	Geothermal	5.64E+13	J/y	1.60E+04	9.04E+17	1%	9.04E+17	100%
1.4	Evapotranspiration**	3.48E+14	J/y	6.10E+04	2.12E+19	33%	2.12E+19	100%
	Local non-renewable resources (N)							
1.5	Net loss of top soil	1.92E+11	J/y	1.58E+05	3.03E+16	0%	-	0%
	Total local natural resources (sum 1.3-1.5)				2.22E+19	35%		
	Resources from outside (F)							
1.6	Water (irrigation)	1.18E+12	J/y	8.76E+04	1.03E+17	0%	5.16E+16	50%
1.7	Initial napier stem	1.72E+06	kg/y	2.43E+11	4.18E+17	1%	1.63E+17	39%
1.8	Fertilizers	1.47E+06	kg/y	1.68E+12	2.48E+18	4%	3.96E+17	16%
1.9	Diesel consumption	1.35E+14	J/y	1.41E+05	1.91E+19	30%	-	0%
1.1	Machinery	6.01E+04	kg/y	6.90E+10	4.15E+15	0%	-	0%
	Labor and services (L)							
1.11	Direct labor (man-hour UEV)	1.49E+06	h/y	9.06E+12	1.35E+19	21%	1.35E+18	10%
1.12	Indirect labors (global EMR as UEV)	3.56E+06	$/y	1.73E+12	6.17E+18	10%	9.25E+17	15%
	Product:							
1.13	Napier grass	2.63E+08	kg/y	2.43E+11	6.39E+19		2.50E+19	39%
		4.73E+15	J/y	1.35E+04				

*Area required = 3,506 ha, operating time = 8,766 h/y

**Total used emergy is calculated without double counting of flows from the same source, according to the emergy algebra.

Table IV.7. Emergy indicators of Napier grass cultivation in Thailand.

Item		*Unit*
Total Emergy	6.39×10^{19}	sej/y
Local resources (R+N), % from total	35%	
Resources from outside (F), % from total	35%	
Labor (direct & indirect), % from total	31%	
UEV	1.35×10^{4}	sej/J
$\%R_{global}$	39%	
EYR = (R + N + F + L) / (F + L)	1.53	
ELR = (N + F + L) / R	1.89	
ESI = EYR / ELR	0.81	

The obtained emergy analysis of this study for Napier grass cultivation was compared with that previously reported in Table V.8 to indicate the potential of Napier grass from Thailand as a lignocellulosic bioenergy crop. In addition to Napier grass, waste from palm oil production is also a potential bioenergy feedstock in Thailand. As presented in Figure IV.8a, comparison between Napier grass and palm cultivation revealed that the UEV of Napier grass (1.35×10^{4} sej/J) was lower than that for the oil palm (6.94×10^{4} sej/J), also, the lowest one compared to other cultivation scenarios which means that less resources are used in the Napier grass cultivation to produce one joule of Napier grass. Moreover, in Figure IV.8b, the portions of renewable resources of Napier grass cultivation ($39\%R_{global}$) was higher than that of the oil palm ($28\%R_{global}$) which is preferable. In term of ELR, due to the renewability of the processes, Napier grass cultivation (ELR 1.89) generated the lower environmental load than oil palm (ELR 5.64) but higher than that of Miscanthus (ELR 0.05) and sugarcane (ELR 1.83).

Also, Figure IV.8c indicates the portion of external resources and local resources consumed to represent the self-sufficient property of the systems and reflects it in term of EYR. The system with high dependent on external resource than local resource will be less self-sufficient. As presented in the emergy indicator values, the EYR for Napier grass cultivation was 1.53 (higher than 1), which means the process acts as a producer more than a consumer. Nevertheless, the EYR of Napier grass was still lower than those of miscanthus (37.7), switchgrass (1.55) and sugarcane (1.72), since the process required much more imported and human resources as shown in Table IV.9. Finally, the ESI of Napier grass cultivation, which indicated the sustainability of the process from the perspective of EYR and ELR, was one of the suitable candidate compared to the alternative biomasses reported in Table IV.9.

Figure IV.9 represents the emergy ternary diagram which was introduced in Almeida's work (Almeida et al., 2004). The ternary diagram allows clear visualization of the actual contribution of the three parameters including N, R and F + L that govern the sustainability index (ESI). Line ESI equal to one (called equilibrium line) on the diagram locates where the system is balanced in terms of economic and environmental viewpoint. The coordinates below this line represent the systems with the main driving force is non-renewable or external resources. In this figure, the biomass from the previous studies are all below the equilibrium line except miscanthus. Also, the biomass appears to consume high resources from economy leading the deteriorating in self-organization property.

It is important to note that the input of labor may be calculated in different ways and includes more or less indirect labor. For comparison, when evaluated without labor 51% global renewability of Napier grass cultivation can be obtained with a lower ELR (1.00), a higher EYR (2.00) and ESI (2.00). However, comparison of the resource use for the cultivation of biomass by collating UEVs from different studies may be misleading due to the different assumptions and contexts of each study. For example, some literature values did not consider the indirect labor (Coppola et al., 2009; Morandi et al., 2016; Pereira and Ortega, 2010), some did not take into account the renewability of the economic inputs (Lin and Sagisaka, 2012) and some did not describe their assumptions relating to labor accounting, which was the main emergy input into their system (Goh and Lee, 2010; Pereira and Ortega, 2010). For those reasons, recalculation on the same basis is required as attempted in Table V.8.

Table IV.8. Emergy assessment of cultivation of different lignocellulosic biomass as feedstock.

Biomass	**UEV (sej/J)**	**Local resources**		**Imported resources**		**Human labor**				**$\%R_{global}$**	**EYR**	**ELR**	**ESI**	**Ref.**
		R	**N**	**F_R**	**F_N**	**DL_R**	**DL_N**	**IL_R**	**IL_N**					
Energy-crops														
Napier grass (with L)	1.35×10^4	35%	0%	1%	34%	2%	19%	1%	8%	39%	1.53	1.89	0.81	This study
Napier grass (w/o L)	9.35×10^3	50%	0%	1%	49%					51%	2.00	1.00	2.00	
Miscanthus (with L)	1.42×10^4	95%	2%	1%	2%	0%	0%	-	-	96%	37.7	0.05	754	(Morandi et al., 2016)
Miscanthus (w/o L)	1.42×10^4	96%	2%	1%	2%					96%	42.1	0.05	895	
Switchgrass (with L)	2.12×10^4	32%	3%	1%	45%	1%	8%	1%	9%	37%	1.55	2.11	0.73	(Felix and Tilley, 2009)
Switchgrass (w/o L)	1.72×10^4	40%	4%	0%	56%					40%	1.77	1.53	1.16	
Jatropha[a] (with L)	1.95×10^5	6%	3%	0%	6%	8%	70%	1%	6%	23%	1.10	16.56	0.07	(Nimmanterdwong et al., 2015)
Jatropha[a] (w/o L)	3.16×10^4	35%	21%	1%	43%					36%	2.27	1.85	1.23	
Food-crops biomass/														
Wheat straw[b] (with L)	1.16×10^5	19%	1%	14%	65%	0%	1%	-	-	33%	1.26	4.21	0.30	(Coppola et al., 2009)
Wheat straw[b] (w/o L)	1.15×10^5	19%	1%	14%	66%					33%	1.26	4.16	0.30	
Sugarcane (with L)	2.79×10^4	35%	7%	1%	33%	4%	20%	-	-	44%	1.72	1.83	0.94	(Coppola et al., 2009)
Sugarcane (w/o L)	2.12×10^4	47%	9%	2%	43%					48%	2.24	1.15	1.96	
Oil palm[a] (with L)	6.94×10^4	15%	9%	0%	12%	4%	33%	3%	24%	28%	1.32	5.64	0.23	(Nimmanterdwong et al., 2015)
Oil palm[a] (w/o L)	2.54×10^4	41%	25%	0%	34%					41%	2.92	1.43	2.05	
Palm[c] (with L)	3.26×10^4	26%	3%	0%	9%	10%	28%	7%	19%	58%	1.40	2.90	0.48	(Goh and Lee, 2010)
Palm[c] (w/o L)	1.21×10^4	69%	8%	0%	23%					69%	4.32	0.44	9.72	
Rice biomass[d] (with L)	1.45×10^5	8%	0%	-	55%	-	0%	-	37%	8%	1.08	11.91	0.09	(Lin and Sagisaka, 2012)
Rice biomass[d] (w/o L)	9.03×10^4	12%	0%	-	87%					12%	1.14	7.04	0.16	

Remarks: the results have been recalculated based on previous literatures data.

- These missing numbers could not track from the reference literatures.

[a] Jatropha and oil palm production in Thailand, with extracted oil and produced residues as a by-product.

[b] Case LO (organic management in loamy soil) was selected.

[c] Palm production in Malaysia, with extracted oil and produced residues as a by-product.

[d] Rice biomass includes rice grain, rice straw and chaff.

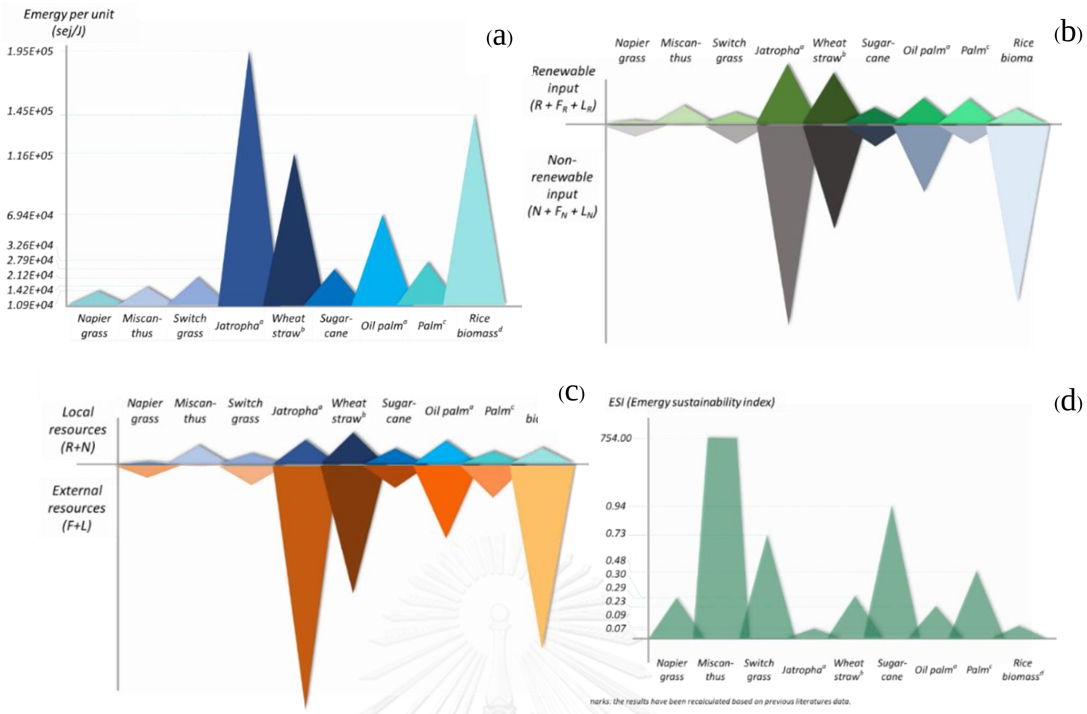

Figure IV.8. Emergy analysis of biomass cultivation (a) UEV of each biomass (b) local and external emergy distributions (c) renewable and non-renewable emergy distributions (d) ESI of each biomass cultivation

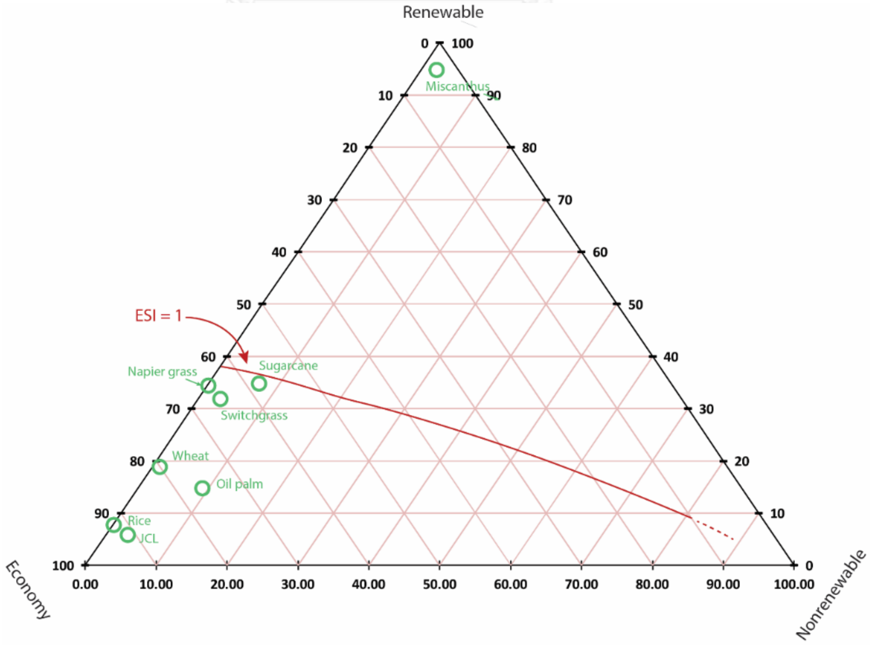

Figure IV.9. Eight biomass cultivations with the aim of emergetic ternary diagrams (Almeida et al., 2004)

4.2.2.2.Emergy analysis of the Napier-based biorefinery

The Napier-based biorefinery system in this study was modeled based on technologies as previously mentioned that operated using material and energy carriers produced within the system as the first priority. In this way, we reduced the dependence of economic inputs and the system acted as partly self-sufficient.

From Figure IV.10, the gasification process requires steam as the gasifying medium to obtain the desirable gas product with suitable H_2 to C ratio as described in Section 4.2.1.2. Also, in case of syngas cleaning process, the solvent regeneration section consumed large amount of steam. Both gasification and syngas cleaning required a large quantity of steam to drive the process. With no heat integration, the system will require large magnitude of steam emergy. However, the proposed biorefinery has the CHP unit which extracts heat and converted them into steam and power to support the entire system. In addition, the wastewater treatment unit provided recycled water to the system that could reduce the otherwise high amount of fresh water input to the system by almost 20 t/h accounting for 1.56×10^{17} sej/y. Therefore, by using the material and energy integration concept, a 27% lower emergy consumption was obtained. Consequently, in emergy viewpoint, the dependence on externally resources was diminished by integrated system.

The products obtained from the biorefinery were including; methanol 7,603 kg/h, electricity, high-pressure steam 5,969 kg/h and liquid fuels 1,921 kg/h (grades C5-C12 and C12+). The other products, such as ash, concentrated CO_2 and sulfur cake, were considered as by-products and not taken into account in the UEV of the system since the references used to compare with our study might also have by-products that could not be directly compared with our case. Also, these by-products accounted for only small amount of the energy among all output products.

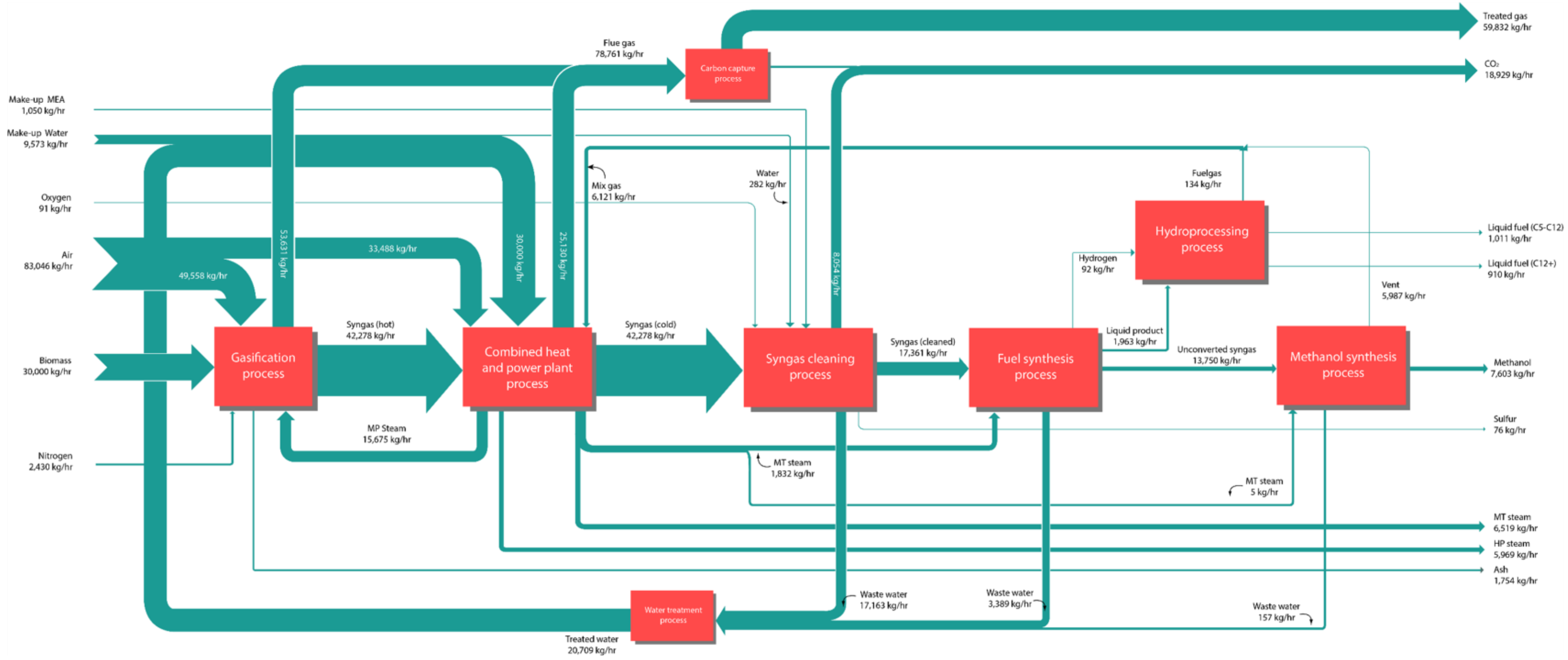

Figure IV.10. Material flow diagram of the biorefinery.

As mentioned in Chapter 2, system boundary is the important issue in emergy analysis, especially when dealing with large and complicated systems such as biorefinery. The biorefinery can be considered as a lumped model as shown in Figure IV.11a or an aggregated model as shown in Figure IV.11b. Each of the scale provides distinct emergy perspective. The lumped model will consider the system as a black box and all emergy inputs will directly allocate to the product output. While in the aggregated model the emergy will consider each intermediate process and interaction flow inside the biorefinery individually via emergy algebra. Therefore, the emergy algorithm developed in Chapter III is necessary for the aggregated model.

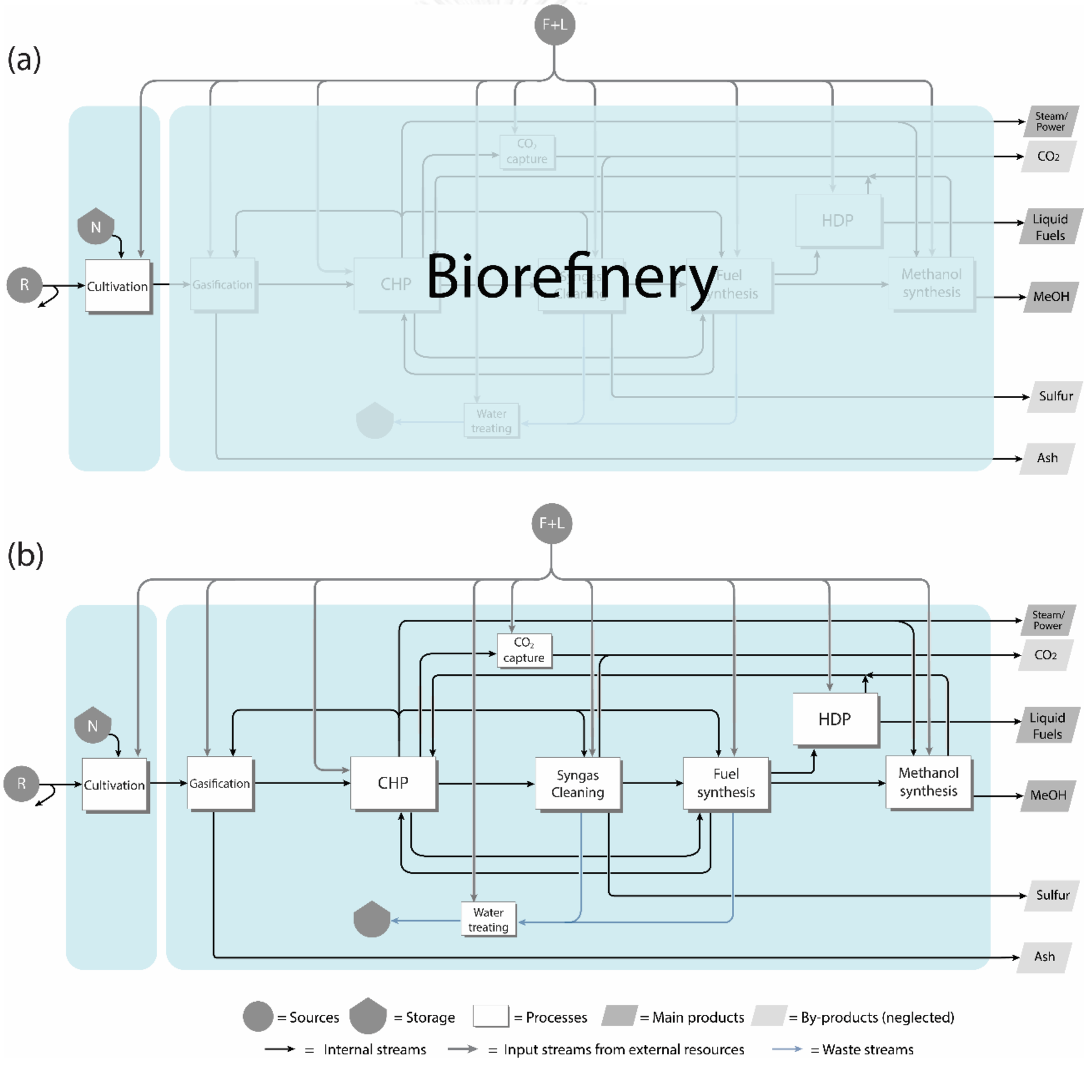

Figure IV.11. System boundary of the biorefinery
(a) lumped model (b) aggregated model

From Table IV.9-Table IV.15, the emergy analysis of the aggregated model was presented including; gasification, combined heat and power (CHP), syngas cleaning, fuel synthesis, hydroprocessing (HDP), methanol synthesis and waste treating processes. The total emergy distributed to each process accounts for 6.95×10^{19} sej/y (37%R), 7.89×10^{19} sej/y (34%R), 8.33×10^{19} sej/y (33%R), 9.94×10^{19} sej/y (28%R), 3.72×10^{19} sej/y (26%R), 7.69×10^{19} sej/y (26%R) and 4.71×10^{18} sej/y (0.7%R).

According to the results, the emergy contributing to these processes are mainly from the upstreams product and feedback streams; 92% of emergy to gasification was from Napier grass and steam fedback from CHP, 88% of emergy to CHP was from hot syngas from gasification process and steam fedback from CHP, 94% of emergy to syngas cleaning was from cold syngas from gasification process and steam fedback from CHP, 83% of emergy to fuel synthesis was cleaned syngas from syngas cleaning and steam fedback from CHP, 89% of emergy to HDP was gas and liquid products from fuel synthesis and 86% of emergy to methanol synthesis was unconverted gas from fuel synthesis and steam fedback from CHP.

It is important to note that each emergy contributed to the processes, was calculated followed the emergy algebra (Section 2.3.5), where the emergy from upstream processes allocates to each downstream process based on its exergy fraction on the pathway. The emergy from Table IV.9-Table IV.15 was summarized to the emergy diagram in Figure IV.12. And all emergy diagrams were combined into one complete emergy diagram for the whole biorefinery as shown in Table IV.16.

Table IV.9. Emergy analysis of biomass gasification process.

Note	Item	Amount	Units	UEV (sej/unit)	Emergy (sej/y)	% of total	Renewable fraction	%R
2	Gasification process							
	Local resources							
	Biomass	2.63E+08	kg/y	-	6.39E+19	92%	2.50E+19	39%
	MP Steam from CHP*	2.42E+14	J/yr	-	2.07E+18	3%	1.91E+17	9%
	MT Steam from CHP (as utility)*	1.27E+11	J/yr	-				
	Air and N_2**	4.56E+08	kg/y					
2.1	Resources from outside (F)							
	Installation material							
	Purchased Equipment	6.56E+04	$/y	1.73E+12	1.14E+17	0%	0	0%
	Piping	4.18E+03	$/y	1.73E+12	7.25E+15	0%	0	0%
	Instrumentation	1.86E+04	$/y	1.73E+12	3.22E+16	0%	0	0%
	Electrical	3.65E+04	$/y	1.73E+12	6.33E+16	0%	0	0%
	Other	5.94E+04	$/y	1.73E+12	1.03E+17	0%	0	0%
	Labor and services (L)							
2.2	Direct labor (man-hour UEV)	3.51E+04	h/y	8.99E+13	3.15E+18	5%	3.15E+17	10%
2.3	Indirect labors (global EMR as UEV)	5.00E+04	$/y	1.73E+12	8.66E+16	0%	1.30E+16	15%
	Products:							
2.4	Syngas	3.71E+08	kg/y	1.88E+11	6.95E+19		2.55E+19	37%
		3.71E+15	J/yr	1.87E+04				

*Feedback streams, emergy allocated via emergy algorithm

** Air and N_2 were assumed as free natural resource with zero emergy input.

Table IV.10. Emergy analysis of CHP process

Note	Item	Amount	Units	UEV (sej/unit)	Emergy (sej/y)	% of total	Renewable fraction	%R
3	CHP process							
	Local resources							
	Syngas from Gasification*	3.71E+15	J/yr	-	6.89E+19	88%	2.55E+19	38.3%
	Fluegas feedback from Gasification*	4.26E+14	J/yr	-				
	Unconverted gas feedback*	5.59E+14	J/yr	-				
	Air**	2.94E+08	kg/y					
	Resources from outside (F)							
3.1	Water (for steam production)	8.39E+07	kg/y	8.71E+08	7.31E+16	0%	3.65E+16	50%
3.2	Installation material							
	Purchased Equipment	1.86E+05	$/y	1.73E+12	3.22E+17	0%	0	0%
	Piping	1.01E+05	$/y	1.73E+12	1.75E+17	0%	0	0%
	Instrumentation	1.78E+04	$/y	1.73E+12	3.08E+16	0%	0	0%
	Electrical	3.64E+04	$/y	1.73E+12	6.30E+16	0%	0	0%
	Insulation	4.43E+03	$/y	1.73E+12	7.66E+15	0%	0	0%
	Other	1.04E+05	$/y	1.73E+12	1.80E+17	0%	0	0%
	Labor and services (L)							
3.3	Direct labor (man-hour UEV)	2.63E+04	h/y	8.99E+13	2.36E+18	3%	2.36E+17	10%
3.4	Indirect labors (global EMR as UEV)	3.58E+06	$/y	1.73E+12	6.19E+18	8%	9.29E+17	15%
	Products:			UEV (sej/J)				
3.5	Syngas (cooled)	3.71E+08	kg/y	2.15E+04	7.83E+19			
		3.04E+15	J/y					
3.6	MP steam (to Gasification)	2.42E+14	J/y					
3.7	MT steam (Net)	0.00E+00	J/y					
3.8	HP steam (Net)	8.38E+13	J/y					
3.9	Electricity (Net)	2.68E+14	J/y					

*Feedback streams, emergy allocated via emergy algorithm

** Air and N_2 were assumed as free natural resource with zero emergy input.

Table IV.11. Emergy analysis of syngas cleaning process.

Note	Item	Amount	Units	UEV (sej/unit)	Emergy (sej/y)	% of total	Renewable fraction	%R
4	Gas cleaning process							
	Local resources							
	Syngas from CHP*	3.04E+15	J/yr	-				
	Electricity from CHP*	7.67E+12	J/yr	-	7.81E+19	94%	2.67E+19	34%
	MT steam from CHP (as utility)*	3.99E+14	J/yr	-				
	Resources from outside (F)							
4.1	Copper-zinc catalyt	2.17E+03	kg/y	6.44E+13	1.40E+17	0%	0	0%
4.2	Makeup MEA	2.63E+04	kg/y	3.65E+12	9.60E+16	0%	0	0%
4.3	Cooling water	2.47E+06	kg/y	3.07E+08	7.59E+14	0%	3.79E+14	50%
4.4	Oxygen**	7.98E+05	kg/y					
4.5	Installation material							
	Purchased Equipment	4.20E+04	$/y	1.73E+12	7.27E+16	0%	0	0%
	Piping	2.90E+04	$/y	1.73E+12	5.02E+16	0%	0	0%
	Steel	3.85E+03	$/y	1.73E+12	6.66E+15	0%	0	0%
	Instrumentation	3.73E+04	$/y	1.73E+12	6.45E+16	0%	0	0%
	Electrical	3.69E+04	$/y	1.73E+12	6.38E+16	0%	0	0%
	Insulation	7.08E+03	$/y	1.73E+12	1.22E+16	0%	0	0%
	Other	1.21E+05	$/y	1.73E+12	2.09E+17	0%	0	0%
	Labor and services (L)							
4.6	Direct labor (man-hour UEV)	4.38E+04	h/y	8.99E+13	3.94E+18	5%	3.94E+17	10%
4.7	Indirect labors (global EMR as UEV)	3.06E+05	$/y	1.73E+12	5.29E+17	1%	7.94E+16	15%
	Products:							
4.8	Syngas (cleaned)	3.71E+08	kg/y	2.25E+11	8.33E+19			
		3.04E+15	J/y	2.74E+04				

*Feedback streams, emergy allocated via emergy algorithm

** Air and N_2 were assumed as free natural resource with zero emergy input.

Table IV.12. Emergy analysis of fuel synthesis process.

Note	Item	Amount	Units	UEV (sej/unit)	Emergy (sej/y)	% of total	Renewable fraction	%R
5	Fuel synthesis process							
	Local resources							
	Syngas from Gas cleaning*	3.04E+15	J/yr	-	8.26E+19	83%	2.71E+19	33%
	Electricity from CHP*	3.10E+12	J/yr	-				
	MT steam from CHP*	1.94E+13	J/yr	-				
	Resources from outside (F)							
5.1	Cobalt catalyt	7.75E+04	kg/y	9.85E+13	7.63E+18	8%	0	0%
5.2	Installation material							
	Purchased Equipment	4.64E+04	$/y	1.73E+12	8.03E+16	0%	0	0%
	Piping	1.41E+04	$/y	1.73E+12	2.44E+16	0%	0	0%
	Steel	1.60E+03	$/y	1.73E+12	2.77E+15	0%	0	0%
	Instrumentation	2.65E+04	$/y	1.73E+12	4.58E+16	0%	0	0%
	Electrical	3.54E+04	$/y	1.73E+12	6.12E+16	0%	0	0%
	Insulation	2.65E+03	$/y	1.73E+12	4.58E+15	0%	0	0%
	Other	9.35E+04	$/y	1.73E+12	1.62E+17	0%	0	0%
	Labor and services (L)							
5.3	Direct labor (man-hour UEV)	4.38E+04	h/y	8.99E+13	3.94E+18	4%	3.94E+17	10%
5.4	Indirect labors (global EMR as UEV)	2.79E+06	$/y	1.73E+12	4.83E+18	5%	7.24E+17	15%
	Products:			UEV (sej/J)				
5.5	Hydrogen (to hydroprocessing)	8.09E+05	kg/y	3.64E+04	9.94E+19			
		9.84E+13	J/y					
5.6	Liquid fuels (to hydroprocessing)	1.72E+07	kg/y					
		8.12E+14	J/y					
5.7	Gas products (to MeOH synthesis)	1.21E+08	kg/y					
		1.82E+15	J/y					

*Feedback streams, emergy allocated via emergy algorithm

Table IV.13. Emergy analysis of hydroprocessing process

Note	Item	Amount	Units	UEV (sej/unit)	Emergy (sej/y)	% of total	Renewable fraction	%R
6	Hydroprocessing process							
	Local resources							
	Liquid fuels from Fuel synthesis	8.12E+14	J/yr	3.64E+04	3.29E+19	89%	9.37E+18	28%
	Hydrogen from Fuel synthesis	9.84E+13	J/yr					
	Resources from outside (F)							
6.2	Installation material							
	Purchased Equipment	3.67E+04	$/y	1.73E+12	6.35E+16	0%	0	0%
	Piping	5.22E+03	$/y	1.73E+12	9.03E+15	0%	0	0%
	Steel	1.81E+03	$/y	1.73E+12	3.13E+15	0%	0	0%
	Instrumentation	1.95E+04	$/y	1.73E+12	3.37E+16	0%	0	0%
	Electrical	2.65E+04	$/y	1.73E+12	4.58E+16	0%	0	0%
	Insulation	2.67E+03	$/y	1.73E+12	4.62E+15	0%	0	0%
	Other	6.53E+04	$/y	1.73E+12	1.13E+17	0%	0	0%
	Labor and services (L)							
6.3	Direct labor (man-hour UEV)	4.38E+04	h/y	8.99E+13	3.94E+18	11%	3.94E+17	10%
6.4	Indirect labors (global EMR as UEV)	1.98E+04	$/y	1.73E+12	3.43E+16	0%	5.14E+15	15%
	Products:			UEV (sej/J)				
6.5	Fuel gas (to CHP process)	1.17E+06	kg/y					
		1.15E+14	J/y					
6.6	Liquid fuels (grade C5-C12)	8.86E+06	kg/y	4.09E+04	3.72E+19			
		4.20E+14	J/y					
6.7	Liquid fuels (grade >C12)	7.97E+06	kg/y					
		3.74E+14	J/y					

*Feedback streams, emergy allocated via emergy algorithm

Table IV.14. Emergy analysis of methanol synthesis process.

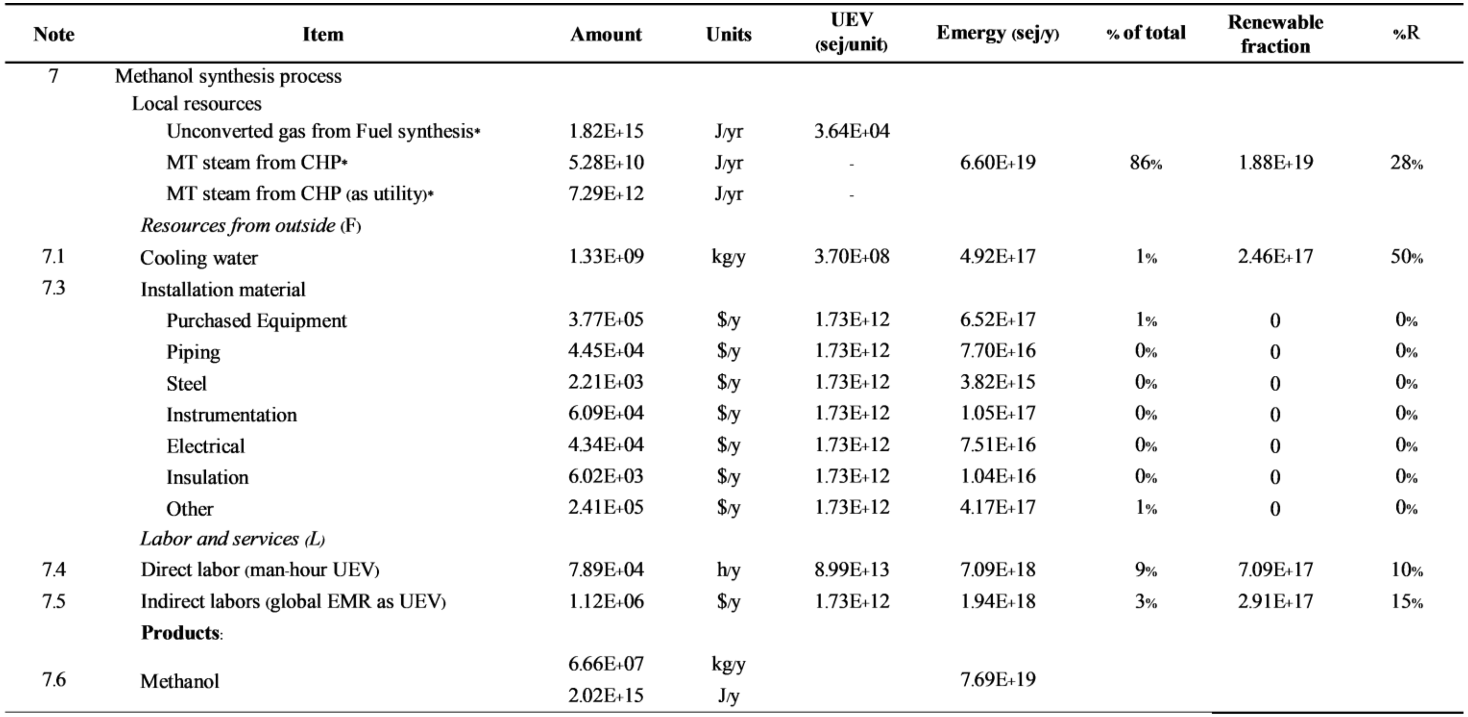

Note	Item	Amount	Units	UEV (sej/unit)	Emergy (sej/y)	% of total	Renewable fraction	%R
7	Methanol synthesis process							
	Local resources							
	Unconverted gas from Fuel synthesis*	1.82E+15	J/yr	3.64E+04	6.60E+19	86%	1.88E+19	28%
	MT steam from CHP*	5.28E+10	J/yr	-				
	MT steam from CHP (as utility)*	7.29E+12	J/yr	-				
	Resources from outside (F)							
7.1	Cooling water	1.33E+09	kg/y	3.70E+08	4.92E+17	1%	2.46E+17	50%
7.3	Installation material							
	Purchased Equipment	3.77E+05	$/y	1.73E+12	6.52E+17	1%	0	0%
	Piping	4.45E+04	$/y	1.73E+12	7.70E+16	0%	0	0%
	Steel	2.21E+03	$/y	1.73E+12	3.82E+15	0%	0	0%
	Instrumentation	6.09E+04	$/y	1.73E+12	1.05E+17	0%	0	0%
	Electrical	4.34E+04	$/y	1.73E+12	7.51E+16	0%	0	0%
	Insulation	6.02E+03	$/y	1.73E+12	1.04E+16	0%	0	0%
	Other	2.41E+05	$/y	1.73E+12	4.17E+17	1%	0	0%
	Labor and services (L)							
7.4	Direct labor (man-hour UEV)	7.89E+04	h/y	8.99E+13	7.09E+18	9%	7.09E+17	10%
7.5	Indirect labors (global EMR as UEV)	1.12E+06	$/y	1.73E+12	1.94E+18	3%	2.91E+17	15%
	Products:							
7.6	Methanol	6.66E+07	kg/y		7.69E+19			
		2.02E+15	J/y					

*Feedback streams, emergy allocated via emergy algorithm

Table IV.15. Emergy analysis of waste treating process.

Note	Item	Amount	Units	UEV (sej/unit)	Emergy (sej/y)	% of total	Renewable fraction	%R
8	Waste water treating process							
	Resources from outside (F)							
	Chemicals							
8.2	Activated carbon	733.3	kg/y	1.56E+13	1.14E+16	25%	0	0%
8.3	Regenerated activated carbon	471.8	kg/y	8.54E+12	4.03E+15	9%	0	0%
8.4	Acrylic acid	29.3	kg/y	3.55E+12	1.04E+14	0%	0	0%
8.5	Al_2SO_4	4,240.60	kg/y	1.18E+12	5.00E+15	11%	0	0%
8.6	Cl_2 gas	236.9	kg/y	6.67E+12	1.58E+15	3%	0	0%
8.7	Lime	1,268.80	kg/y	1.00E+12	1.27E+15	3%	0	0%
8.8	H_3PO_4, 85%	14.8	kg/y	6.20E+12	9.18E+13	0%	0	0%
8.9	Caustic soda	1,973.20	kg/y	1.46E+12	2.88E+15	6%	0	0%
8.1	H_2SO_4	1,172.30	kg/y	4.15E+11	4.87E+14	1%	0	0%
	Labor and services (L)							
8.11	Direct and indirect labor (global EMR as UEV)	1.08E+04	$/y	1.73E+12	1.87E+16	41%	2.80E+15	15%
8.12	Material transport (truck)	25.9	tkm/y	6.61E+11	1.71E+13	0%	0	0%
	Products:							
	Treated water	1.82E+08	kg/y	2.51E+08	4.56E+16			
9	Carbon capture process							
	Resources from outside (F)							
9.1	Cooling water	6.54E+08	kg/yr	3.03E+08	1.98E+17	4%	0	0%
9.2	Make up MEA	1.08E+04	kg/yr	3.65E+12	3.94E+16	1%	1.97E+16	50%
9.3	Scrubber chemicals	1.59E+04	$/yr	1.73E+12	2.76E+16	1%	0	0%
9.4	Natural gas	3.02E+13	J/yr	1.41E+05	4.24E+18	91%	0	0%
9.5	Installation materials	4.35E+04	$/yr	1.73E+12	7.52E+16	2%	0	0%
	Labor and services (L)							
9.6	Direct and indirect labor (global EMR as UEV)	4.66E+04	$/yr	1.73E+12	8.07E+16	2%	1.21E+16	15%

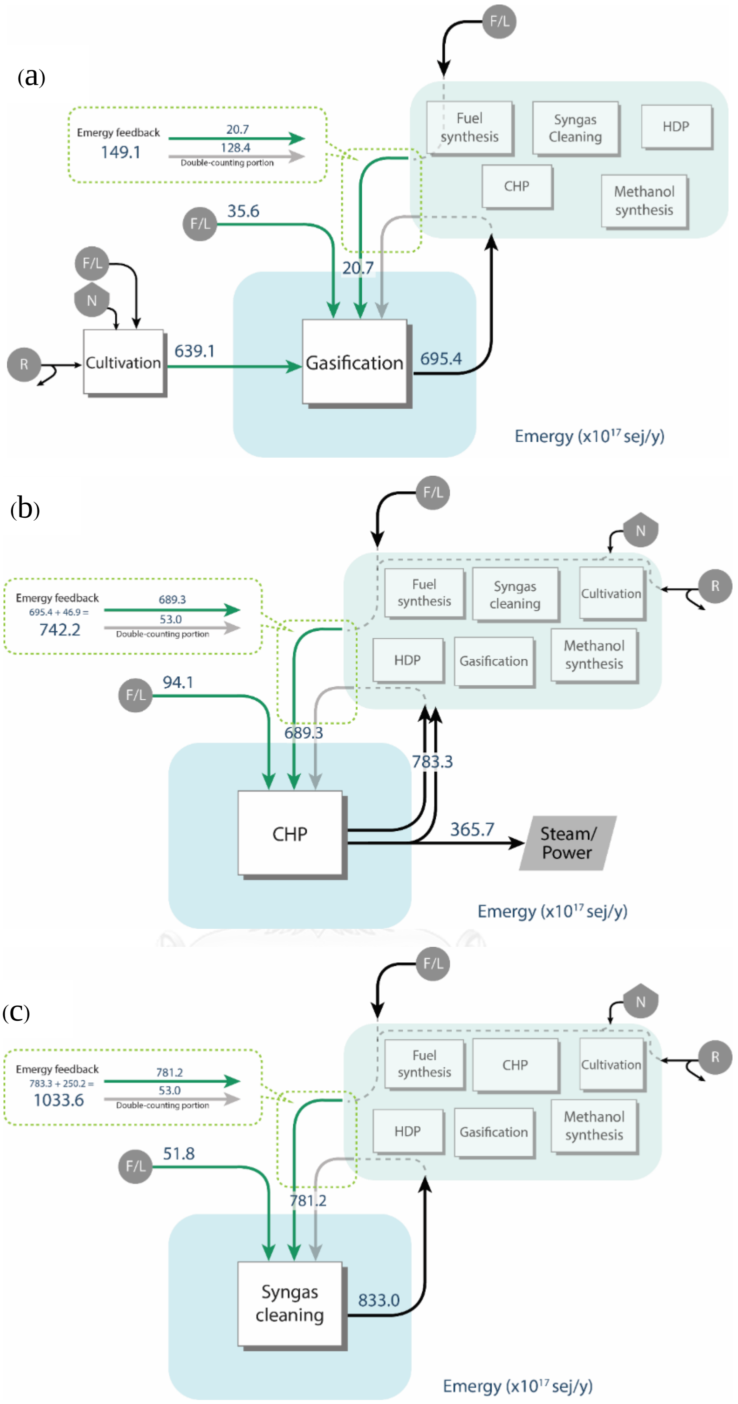

Figure IV.12. Emergy diagram of the aggregated model (a) gasification (b) CHP (c) syngas cleaning (d) fuel synthesis (e) HDP (f) methanol synthesis

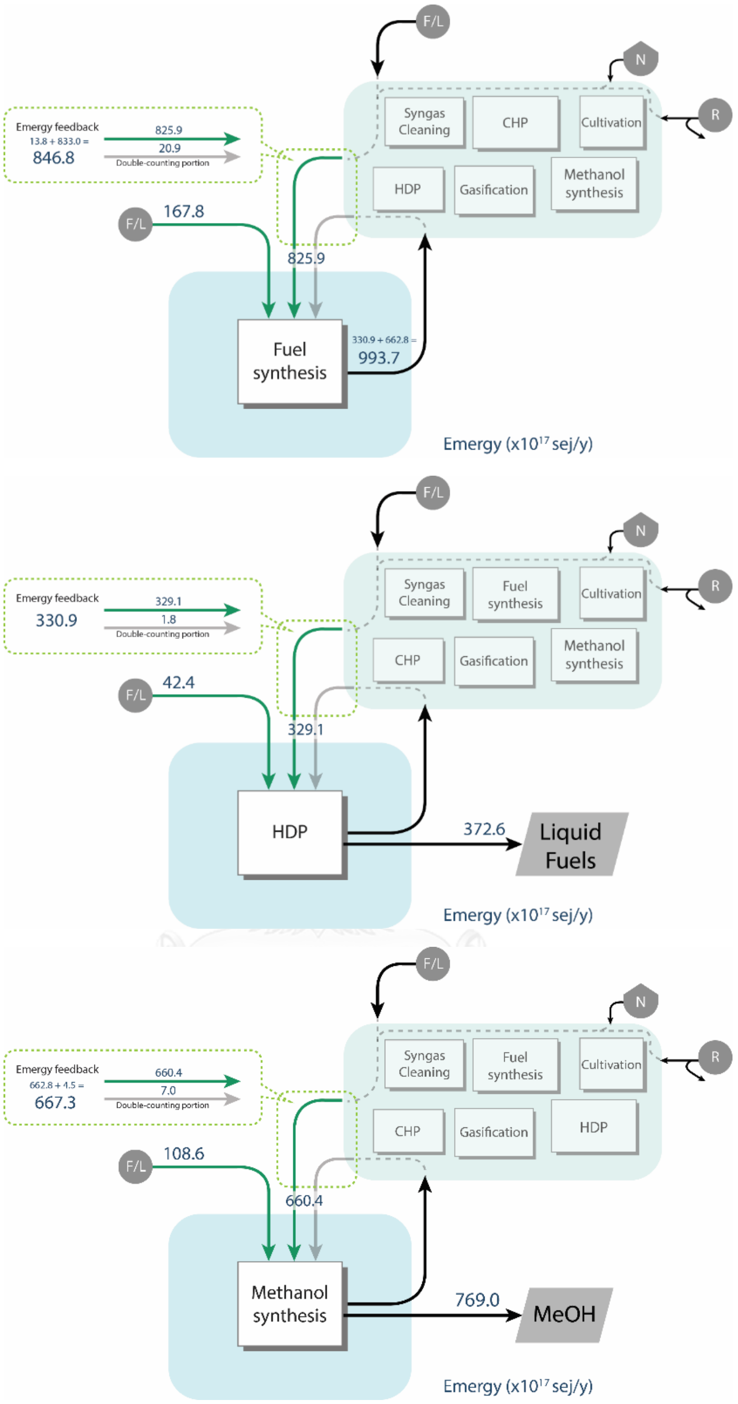

Figure IV.12. (cont.) Emergy diagram of the aggregated model (a) gasification (b) CHP (c) syngas cleaning (d) fuel synthesis (e) HDP (f) methanol synthesis

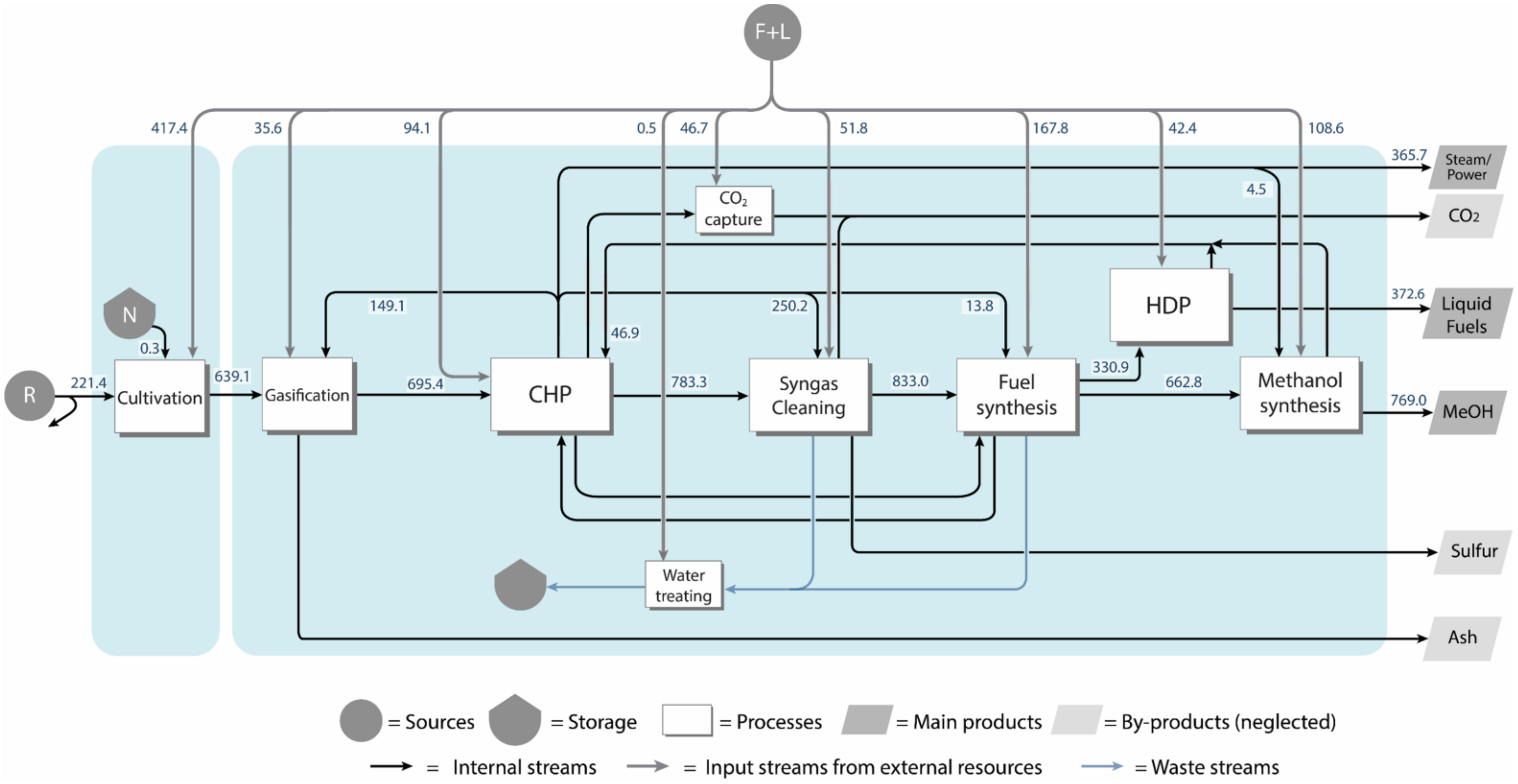

Figure IV.13. Emergy diagram of the biorefinery

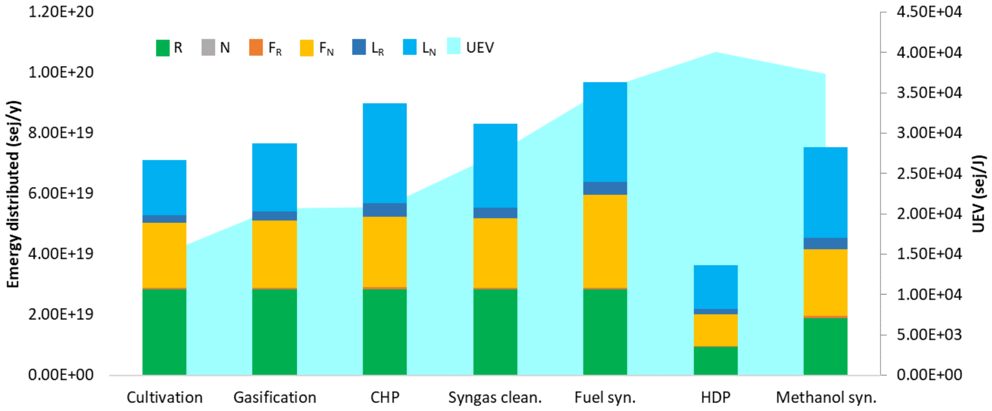

Figure IV.14. Emergy profile for each process from field to biorefinery plant gate.

The emergy profile of the biorefinery, depicted in Figure IV.14, showed that the emergy distributed to each process is equally proportioned. This phenomenon occurs when material and energy within the complex systems interacts with each other. The entire system will share the equal amount of emergy. Except the HDP, which rather seems to be the independent process in the system since only small amount of material and energy of the HDP are shared and circulated within the system.

The UEV of each process output represents the amount of emergy required to the process per one Joule of product output as expressed by the light blue shaded in Figure IV.14. Since the emergy of the upstream and downstream processes are related. For example, the biorefinery processes will receive all emergy from the biomass cultivation. Thus, the UEV of the following processes, such as gasification, tends to be larger when the order of process higher as presented in Figure IV.14. The difference in the height of the cultivation and gasification will be the emergy increment due to the gasification process alone. Therefore, cultivation has the lowest UEV since it is the lowest order of process. While HDP and Methanol Synthesis, the highest order of processes, have the highest UEV as the processes accumulated the upstream emergy into their products.

By considering the biorefinery as the lumped system, the feedback emergy inside the process was neglected and we can focus on only the external resources that dominate the system. As presented in Table IV.16, the total emergy input to the entire system was

1.3×10^{20} sej/y. When considering from the resource point of view, it contains 2.2×10^{19} sej/y (or 17%) of R, 3.0×10^{16} sej/y (or 0.02%) of N, 1.2×10^{18} sej/y (or 1%) of F_R, 5.4×10^{19} sej/y (or 41%) of F_N, 6.1×10^{18} sej/y (or 5%) of L_R and 4.7×10^{19} sej/y (or 36%) of L_N. However, when considering from the process-oriented point of view, the total emergy composed of 6.4×10^{19} sej/y (or 49%) from cultivation, 3.6×10^{18} sej/y (or 3%) from gasification, 3.8×10^{18} sej/y (or 3%) from CHP, 2.2×10^{19} sej/y (or 17%) from syngas cleaning, 1.7×10^{19} sej/y (or 13%) from fuel synthesis, 4.6×10^{18} sej/y (or 3%) from HDP, 1.1×10^{19} sej/y (or 8%) from methanol synthesis, 4.8×10^{18} sej/y (or 4%) from CO_2 capture and 4.6×10^{16} sej/y (or 0.04%) from water treating. Moreover, the heat and power integration inside the biorefinery can reduce the amount of economic inputs by 3.45×10^{10} J/y (steam) and 8.40×10^{9} J/y (electricity), which accounted for 4.25×10^{19} sej/y (in case where steam and electricity were imported from a biomass CHP process refered from Sha's work (Sha and Hurme, 2012)).

The emergy contribution showed that the cultivation stage dominates the emergy consumption of the entire process, followed by the chemical production processes (including gasification, fuel synthesis, HDP and methanol synthesis), waste treatment units and CHP, respectively. While the highest resource consumption in the biorefinery was syngas cleaning and fuel synthesis. Recalling the result from Table IV.12, the main input to fuel synthesis was labor and purchased resources from cobalt catalyst, respectively. While in syngas cleaning, labor and the installation material were the main input to the process.

The emergy contribution of Napier-based biorefinery was compared with that previously reported as shown in Figure IV.15. The emergy profile of the crop-based biodiesel production cases results refered from Ren's work (Ren et al., 2013). From the figure, it was cleary found that the cultivation stage dominates the emergy consumption of the biorefinery in all cases. The result also found that if we utilize the energy more efficient, the trend will shift into lower emergy domination in the biorefinery stage (Figure IV.15d and e).

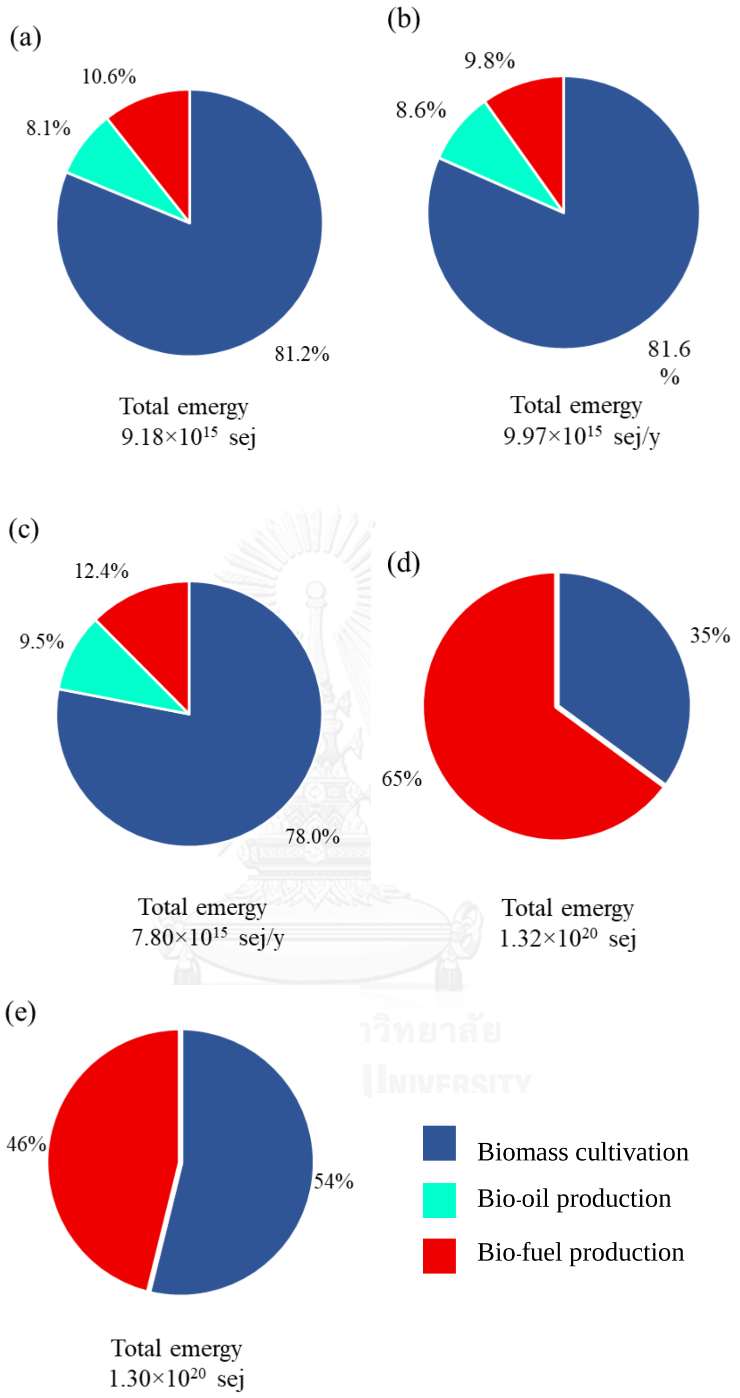

Figure IV.15. The comparison of the biorefinery emergy contribution (a) Rapeseed-based biodiesel production (b) Soybean biodiesel production (c) Sunflower-based biodiesel production (d) Napier-based biorefinery before and (e) after energy integration

The emergy indicators of the biorefinery, including global renewability, EYR, ELR and ESI, were calculated under the simulation information obtained from theoretical assumptions (Table IV.17). Global renewability of the biorefinery system accounted for 23% of the total emergy input, which is quite low due to large fraction of non-renewable materials consumed by the agricultural process and most were consumed by the bio-based production system, such as makeup MEA for syngas cleaning and cobalt catalyst for fuel synthesis. While most resources consumed are external resources leading to lower EYR value (from 1.53 in cultivation phase to 1.21). Due to the low EYR from the upstream production system, an industrial system that always demands import resources as the main input would continuously lower the EYR value and increase the ELR value (accounted for 14%) of the whole system since the import resources are considered as the parameter that caused the principal load to the environment. Finally, the obtained ESI of the Napier-based biorefinery was 0.25. In addition, to achieve higher sustainability, the optimization of chemical consumption is required. From emergy analysis, we found that it is possible to increase ESI up to 10 percent if 50 percent of MEA can be recovered in gas cleaning process.

Table IV.16. Resources distributions to each production process.

Section	*Unit*	R_L	N_L	F_R	F_N	L_R	L_N	*DL(10%R)*	*Total*	
Cultivation (B100)	sej/y	2.21×10^{19}	3.03×10^{16}	6.04×10^{17}	2.15×10^{19}	2.27×10^{18}	1.74×10^{19}	1.35×10^{19}	6.39×10^{19}	*49%*
Gasification (A100)	sej/y			8.72×10^{15}	3.28×10^{17}	3.28×10^{17}	2.91×10^{18}	3.15×10^{18}	3.58×10^{18}	*3%*
CHP (A200)	sej/y			2.07×10^{16}	8.02×10^{17}	3.30×10^{17}	2.66×10^{18}	2.37×10^{18}	3.81×10^{18}	*3%*
Syngas clean. (A300)	sej/y			1.09×10^{15}	1.73×10^{19}	4.74×10^{17}	4.00×10^{18}	3.94×10^{18}	2.18×10^{19}	*17%*
Fuel syn. (A400)	sej/y			4.08×10^{16}	8.06×10^{18}	1.12×10^{18}	7.66×10^{18}	3.94×10^{18}	1.69×10^{19}	*13%*
HDP (A500)	sej/y				2.73×10^{17}	4.46×10^{17}	3.84×10^{18}	3.94×10^{18}	4.56×10^{18}	*3%*
Methanol syn. (A600)	sej/y			2.47×10^{17}	1.59×10^{18}	1.00×10^{18}	8.04×10^{18}	7.10×10^{18}	1.09×10^{19}	*8%*
CO_2 capture (A700)	sej/y			2.87×10^{17}	3.67×10^{18}	1.22×10^{17}	6.92×10^{17}	8.14×10^{17}	4.77×10^{18}	*4%*
Waste water treat. (A800)	sej/y				2.69×10^{16}	2.81×10^{15}	1.59×10^{16}	1.87×10^{16}	4.56×10^{16}	*0%*
Total	sej/y	2.21×10^{19}	3.03×10^{16}	1.21×10^{18}	5.36×10^{19}	6.10×10^{18}	4.72×10^{19}	3.88×10^{19}	1.30×10^{20}	*100%*

From Figure IV.16a, the emergy per unit of product or UEV was considered as a joint production system (Section 2.4.2.) which was calculated by dividing the total emergy input (1.30×10^{20} sej/y) and the total energy of the products (3.96×10^{15} J/y). From Table IV.17, the UEV for the biorefinery, was 3.29×10^4 sej/J and 1.94×10^4 sej/J when including and not including the labor, respectively. The UEV indicates that the system consumed natural resources about 33 thousand solar emergy to produce each joule of products. As the diversity of products created by the system has a different ability to do work, the joint UEV may not be an appropriate value to apply in further studies. On the other hand, it can be used to compare the biorefinery with single process that produces an equal quantity and quality of the same products, as previously suggested (Bastianoni and Marchettini, 2000). These authors defined a weighted average UEV (Equation (2.10), Section 2.4.2), where the UEV of the product is obtained from an independent process (Figure IV.16b).

Table IV.17. Emergy indicators of the system from cultivation to biorefinery.

Item		Unit
Joint UEV of the products with L	3.29×10^4	sej/J
Joint UEV of the products without L	1.94×10^4	sej/J
Global Renewability (%R_{global})	23%	
EYR of the system = (R + N + F + L) / (F + L)	1.21	
ELR of the system = (N + F + L) / R	4.88	
ESI of the system = EYR / ELR	**0.25**	

A number of alternative ways to produce electricity, steam, liquid fuels and alcohol are presented in Table IV.18. Among the given options, the best route to produce the target products (the lowest weighted average UEV) is by producing methanol from willow, heat and power from biomass CHP, additional power from wind power (since the power to heat ratio of biomass CHP is insufficient) and bio-diesel from rapeseed. In the best scenario from Table IV.18, the weighted average UEV (8.74×10^4 sej/J) is 2.7 times higher than the present study (3.29×10^4 sej/J). Meaning that, the biorefinery has utilized, in emergy terms, the resources more efficiently than that of the existing independent production process.

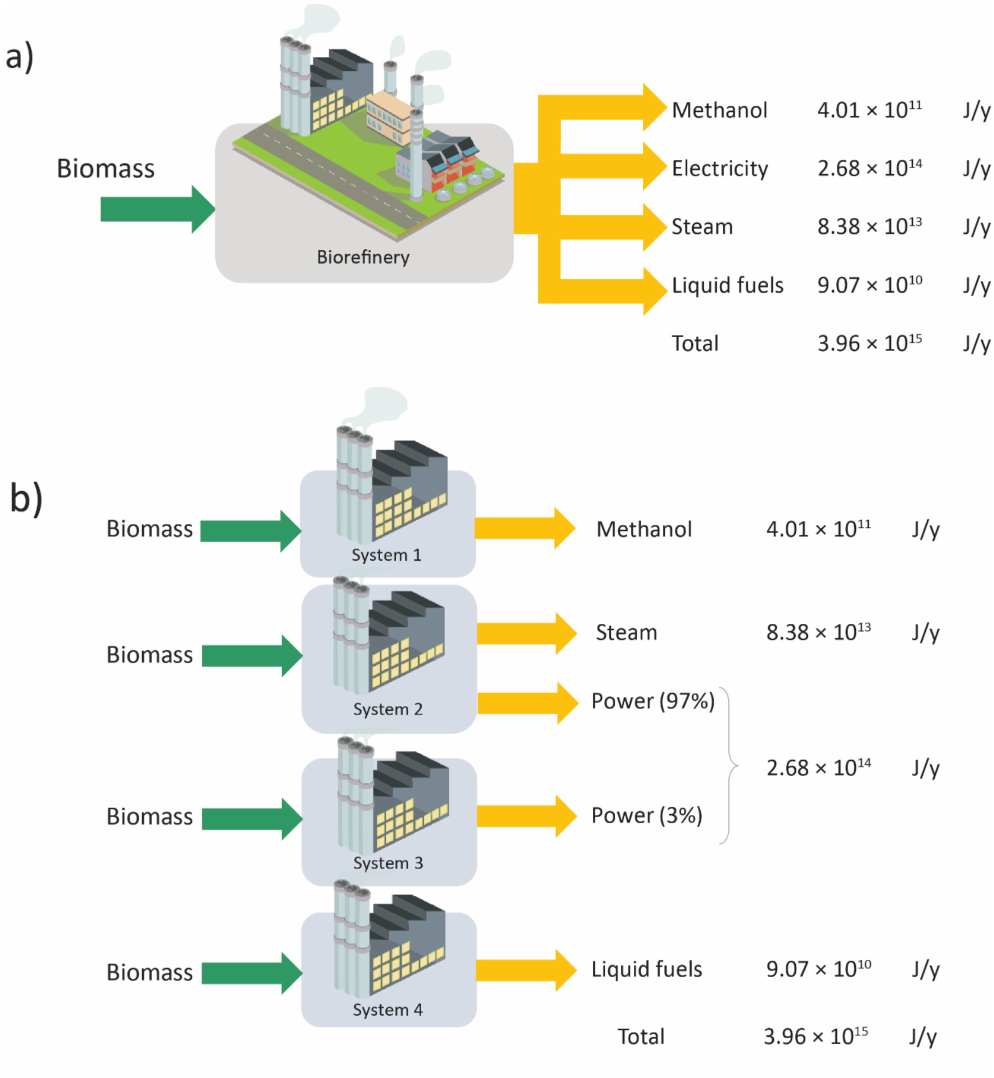

Figure IV.16. Alternative pathways to produce the target products:

(a) the joint production system and (b) the alternative independent production system.

Table IV.18. Alternative pathways to produce the target products.

	Country source	*UEV (sej/J)*	*Ref.*
Bio-alcohol			
Methanol from willow	Sweden	6.06×10^{4}	(Cavalett and Rydberg, 2011)
Methanol from wood	Italy	2.66×10^{5}	(Pimentel and Patzek, 2008)
Steam and power co-production			
Biomass CHP process 1	Finland	1.62×10^{4}	(Sha et al., 2011)
Biomass CHP process 2	Finland	3.44×10^{4}	(Sha and Hurme, 2012)
Biomass CHP process 3	Denmark	2.31×10^{5}	(Kamp and Østergård, 2013)
Power			
Wood power plant	USA	6.72×10^{4}	(Odum, 1996)
CSP powerplant	China	6.39×10^{4}	(Zhang et al., 2012)
Solar power plant	Italy	8.92×10^{4}	(Paoli et al., 2008)
Wind power 1	China	1.74×10^{4}	(Yang et al., 2013)
Wind power 2	Italy	6.21×10^{4}	(Brown and Ulgiati, 2002)
Geothermal power plant	Italy	1.47×10^{5}	(Brown and Ulgiati, 2002)
Hydro power plant 1	Italy	6.23×10^{4}	(Brown and Ulgiati, 2002)
Hydro power plant 2	Tibet	1.56×10^{5}	(Zhang et al., 2016)
Hydro power plant 3	Brazil	8.28×10^{4}	(Tassinari et al., 2016)
Liquid fuels			
Macroalgae oil 1	Italy	2.64×10^{7}	(Bastianoni et al., 2008)
Macroalgae oil 2	Brazil	3.51×10^{5}	(da Cruz and do Nascimento, 2012)
Bio-diesel from soy bean	Brazil	3.90×10^{5}	(Cavalett and Ortega, 2010)
Bio-diesel from palm oil	Thailand	2.14×10^{5}	(Nimmanterdwong et al., 2015)
Weighted average UEV of the best scenario*		8.74×10^{4}	

*Methanol from willow, heat and power from biomass CHP process 1, additional power from Chinese wind power and bio-diesel from palm oil

CSP = concentrating solar power

4.3. Alternative scenario for the eco-industrial park

After the emergy analysis was done, we can see the issues or the factor that driving each process. In this section, the alternative scenario is proposed to provide the example for the implementation of emergy assessment to the industrial production development.

4.3.1.Alternative scenarios for Napier grass crop production

According to the emergy analysis in Section 4.2.2.2, the cultivation stage has critical impact to the emergy of the entire system. To improve the sustainability of Napier grass cultivation, the dependence on economic inputs could be reduced by promoting long term productivity with eco-efficient alternatives such as using biofuel driven machineries, and lower pollution levels on the farm (Maier et al., 2016). This would provide the higher utilization of local resources and lower the dependence on external resources (De Jong et al., 2010). Non-renewable inputs, such as diesel, could be replaced by other fuels, or partially substituted by renewable inputs, to reduce the reliance on fossil fuels. Some might suggest to use machinery instead of human labor to reduce the labor emergy input. However, the use of machinery would need to take into account the indirect labor and fuel consumption. Thus, two scenarios were simulated to predict the possibility of those proposed suggestions; (1) use tractors for weed removal (higher machinery but lower direct labor input) and build the biorefinery plant close to the cultivation site (within 10 km distance); (2) extend scenario (1) by using biodiesel instead of conventional diesel.

The results (Table IV.19) revealed improved processes in many aspects. For the first case, the UEV was reduced 1.45-fold to 9.30 × 10^3 sej/J, %R_{global} increased 1.4-fold to 55%, EYR increased 1.31-fold to 2.01, ELR was reduced 1.91-fold to 0.99 and the ESI was improved 1.95-fold to 2.04. In the second case, using biodiesel instead of conventional diesel fuel did not improve %R_{global}, since the biodiesel production process was highly dependent on external resources and most were non-renewable resources (17%) (Nimmanterdwong et al., 2015). For this reason, the ESI of this scenario in Table

IV.19 also showed that, with current biodiesel production process, the substitution of diesel with biodiesel was not a good alternative (higher UEV but higher $\%R_{global}$). Thus, we propose model (1) over model (2), since it has a higher sustainability indicator and in addition, a lower UEV.

Table IV.19. Two alternative models for improving Napier grass cultivation in Thailand.

	Base case	*Proposed model 1**	*Proposed model 2***
Total Emergy (sej/y)	6.39×10^{19}	4.40×10^{19}	4.81×10^{19}
Local resources (R+N), % from total	35%	50%	46%
Resources from outside (F), % from total	35%	25%	31%
Labor (direct & indirect), % from total	31%	25%	23%
UEV (sej/J)	1.35×10^{4}	9.30×10^{3}	1.02×10^{4}
$\%R_{global}$	39%	55%	55%
EYR = (R + N + F + L) / (F + L)	1.53	2.01	1.86
ELR = (N + F + L) / R	1.89	0.99	1.17
ESI = EYR / ELR	0.81	2.04	1.58

* Using tractors for weed removal, build biorefinery plant close (< 10 km) to the cultivation site

** Using biodiesel instead of diesel, tractors for weed removal, build biorefinery plant close (< 10 km) to the cultivation site

4.3.2. Alternative scenarios for the eco-industrial park

The biorefinery has been designed to maximize the utilization of material and energy as proposed. The two scenarios with and without material and energy integration has already been discussed in Section 4.2.2.2. In this section, we found that the sustainability of the proposed model can be improved after the changed in cultivation stage. The alternative case was designed by the implementation of Napier grass cultivation proposed model 1 and replacing MEA absorption with solid sobent CO_2 capture in Section 4.1.

By applying the solid sorbent method which is the best scenario among the selected CO_2 capture processes, the emergy can be reduced up to 4.19×10^{18} sej/y (3% of total emergy reduced). The renewability was increased from 23% to 27% leading the ELR lower from 4.88 to 3.79. Moreover, the lower external emergy input raise EYR up from 1.21 to 1.26. Consequently, with these improvements, the ESI of this scenario can be fold up to 0.33.

Table IV.20. Emergy indicators of the modified system from cultivation to biorefinery.

Item	**Base Case**	**Alternative Case**	Unit
Joint UEV of the products with L	3.29×10^4	2.70×10^4	sej/J
Joint UEV of the products without L	1.94×10^4	1.58×10^4	sej/J
Global Renewability (%R_{global})	23%	27%	
EYR of the system = (R + N + F + L) / (F + L)	1.21	1.26	
ELR of the system = (N + F + L) / R	4.88	3.79	
ESI of the system = EYR / ELR	**0.25**	**0.33**	

*The alternative case was design with the implement of Napier grass cultivation proposed model 1 and replacing MEA absorption with solid sobent CO_2 capture.

CHAPTER V: EXERGY ANALYSIS OF NAPIER-BASED BIOREFINERY

5.1. Exergy Definition

According to its definition, Exergy was defined to describe the potential energy capable of doing work and being degraded in the process. The availability or exergy refers to the total mechanical physical and chemical exergy potential from environmental state to the operating state. The environmental state, theoretically, is the state where thermodynamic equilibrium occurred where there is no usable energy (exergy) produced. However, in realistic there is no such theoretically thermodynamic equilibrium (fully reversible) since it against the second law of thermodynamics. From those reason, in reality, the exergy of environmental is not null. From those reason, there has been a compromise in the exergy formulation that an ambient environment condition (air at 298.15 K and 1 atm) is acceptable as a reference state. In this Chapter, the subscript 'ref' and subscript 'T, P' indicate the properties of the reference state and operating state, respectively. As depicted in Figure V.1, the changes of exergy from operating state to the environmental state can be divided to physical and chemical exergy.

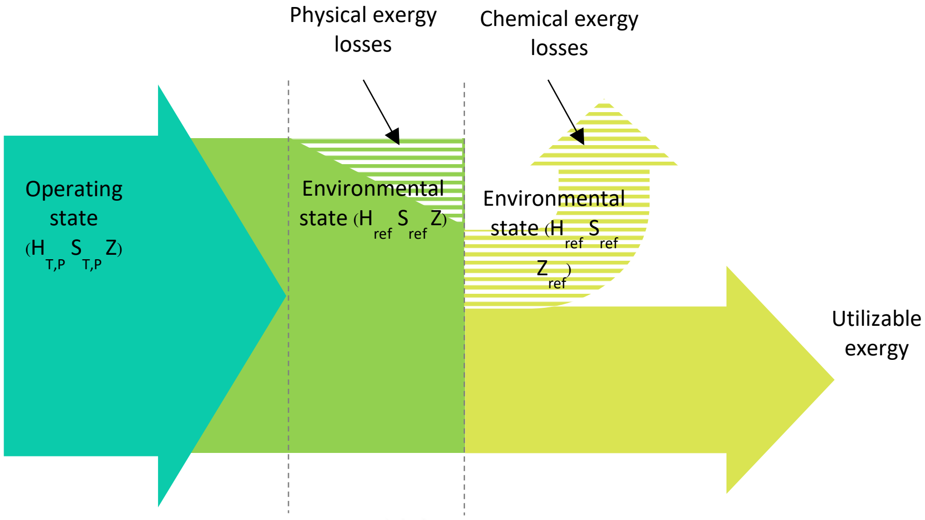

Figure V.1. Graphical presentation of exergy balance

5.2. Physical Exergy

The physical exergy is occurred when there was a difference of the system condition and the reference condition. In the biorefinery system the physical exergy of material streams was calculated using the following equations;

$$Ex_{phy} = \left(H_{H,P} - H_{ref}\right) - T_{ref}\left(S_{H,P} - H_{ref}\right) \qquad (5.1)$$

Where H and S are the enthalpy and entropy, respectively. While subscripts 'T, P' and 'ref' are the operating condition and environmental condition (25°C, 1 atm), respectively. The enthalpy and entropy were obtained from Aspen plus simulation (Table V.1 - Table V.6). For example, the physical exergy of stream SYNGAS (1.01 bar 1,368 °C) from gasification process was calculated from:

$$Ex_{phy} = (-5{,}330{,}000) - (-9{,}270{,}000) - 298.15(4{,}253 - (-2{,}318)) = 1{,}970{,}000 \text{ J/kg}$$

5.3. Chemical Exergy

Once the physical exergy was calculated, the standard chemical exergy of all components was evaluated as follow (de Oliveira Junior, 2012).

$$Ex_{chem}\ (componentA) = \Sigma n_i Ex_i^o (element i) + g_f^o\ (componentA) \qquad (5.2)$$

$$- g_f^o\ (component\ A) = \Sigma n_j H_j^o (element\ j) - Tref\ (\Sigma n_i S_i^o (element\ j)) \qquad (5.3)$$

Where Ex^o, $g^o_{f,}$, H^o and S^o are exergy, gibbs free energy of formation, enthalpy and entropy at standard state. In Equations (2.2) - 3, component A formed by various elements and the exergy of component A can be indirectly evaluated from the exergy balance of the formation reaction. Thus, n_i represents the stoichiometric coefficient of elements stated in formation reaction except component A, in Equation (2.2) while, in Equation 3, n_j represents all elements related to the formation reaction.

For example, the standard chemical exergy of pentane (C_5H_{12}) was calculated as follow:

$$C_5H_{12} + 8\ O_2 \rightarrow 6\ H_2O + 5\ CO_2$$

$$g^o_{f,ref}\ (C_5H_{12}) = H^o_{C5H12} + 8\ H^o_{O2} - 6\ H^o_{H2O} - 5\ H^o_{CO2} - 298.15\ (S^o_{C5H12} + 8\ S^o_{O2} - 6\ S^o_{H2O} - 5\ S^o_{CO2})$$

$$= (-146{,}440\ kJ/kmol) + 8\ (0\ kJ/kmol) - 6\ (-241{,}811\ kJ/kmol) - 5\ (-393{,}486\ kJ/kmol) - 298.15\ K\ (349\ kJ/kmol.K + 8 \times 205\ kJ/kmol.K - 6 \times 189\ kJ/kmol.K - 5 \times 213.7\ kJ/kmol.K)$$

$$= -3{,}334{,}989\ kJ/kmol$$

$$Ex_{chem}\ (C_5H_{12}) = -8\ Ex^o_{O2} + 6\ Ex^o_{H2O} + 5\ Ex^o_{CO2} + g^o_{f,ref}\ (C_5H_{12})$$

$$= -8 \times 3{,}974\ kJ/kmol + 6 \times 9{,}494\ kJ/kmol + 5 \times 19{,}867\ kJ/kmol + 3{,}334{,}989\ kJ/kmol$$

$$= 3{,}459{,}496\ kJ/kmol$$

Finally, the chemical exergy of mixed gas stream SYNGAS from gasification process (composition by mole; 37.0% H_2O, 18.6% CO, 33.4% H_2, 7.0% CO_2, 3.4% N_2, 0.015% CL_2, 0.013% H_2S and 0.5% NH3) was calculated:

$$Ex_{chem} = \Sigma x_k Ex_k^o \text{(componentk)} \qquad (5.4)$$

Where k indicates all relevant mixed components in the gas product.

$Ex_{chem} = 0.37 \times Ex^o_{H2O} + 0.186 \times Ex^o_{CO} + 0.334 \times Ex^o_{H2} + 0.07 \times Ex^o_{CO2} + 0.034 \times$

$Ex^o_{N2} + 0.00015 \times Ex^o_{CL2} + 0.00013 \times Ex^o_{H2S} + 0.00508 \times Ex^o_{NH3}$

$= 0.37 \times 3{,}120$ kJ/kmol $+ 0.186 \times 274{,}710$ kJ/kmol $+ 0.334 \times 236{,}000$ kJ/kmol

$+ 0.07 \times 20{,}140$ kJ/kmol $+ 0.034 \times 720$ kJ/kmol $+ 0.00015 \times 123{,}600$ kJ/kmol

$+ 0.00013 \times 812{,}000$ kJ/kmol $+ 0.00508 \times 341{,}250$ kJ/kmol

$= 134{,}288.4$ kJ/kmol

5.4. Chemical Exergy of Biomass

Chemical exergy of biomass is a particular case where the calculation was based on the composition within the biomass. The study was done on evaluate chemical exergy of biomass (Saidur et al., 2012).

$$Ex_{chem}\,(\text{biomass}) = \beta\,(C + L_W Z_W) + E_{chw} Z_W \qquad (5.5)$$

$$\beta = \frac{1.041 + 0.216(Z_{H_2}/Z_C) - 0.250(Z_{O_2}/Z_C)\left[1 + 0.788(Z_{H_2}/Z_C)\right] + 0.045(Z_{H_2}/Z_C)}{1 - 0.304(Z_{O_2}/Z_C)} \qquad (5.6)$$

Where the enthalpy of phase change for water was shown by L_W which was equal to 2,440 kJ/kg and chemical exergy of water (E_{chw}) was 50 kJ/kg. C represents the net calorific value of the biomass. Z represents the mass fraction of elements H_2, C, O_2 and water in the biomass, respectively. In this study, the net calorific value of the biomass was referred from Boie's equation as shown in the following equation (Sheng and Azevedo, 2005).

$$C\,(\text{Btu/lb}) = 151.2\,Z_c + 499.77\,Z_H + 45.0\,Z_S - 47.7\,Z_O + 27.0\,Z_N \qquad (5.7)$$

From the ultimate analysis of Napier grass, β was equal to 1.138, C was 7,670.6 Btu/lb (or 17,841.8 kJ/kg) and the chemical exergy of Napier grass was 20,683.2 kJ/kg.

5.5. Exergy calculation

The process flow diagram and the stream table of the biorefinery system developed using the Aspen Plus 8.6 simulation software was reported in Appendix C. The proposed biorefinery model includes; (1) gasification, (2) combined heat and power plant (CHP), (3) syngas cleaning, (4) fuel synthesis, (5) hydroprocessing (HDP) and (6) methanol synthesis process. From the simulation results, the exergies of all six processes were evaluated as presented in Table V.1- Table V.6.

For the gasification process, biomass with exergy flow 1.7×10^8 J/y is burnt to produce 1.2×10^8 J/y of syngas product. For the CHP, the hot syngas from gasification is the main exergy input to this process. After the extracting the heat from the hot syngas, the cold syngas left the process with exergy accounted for 9.6×10^7 J/y. Also, the unconverted gas from HDP with exergy of 1.7×10^7 J/y was feed to the gas turbine in the CHP to obtain sufficient amount of steam. In addition, the hot flue gas from gasification also provided heat to the CHP and left with the exergy 7.1×10^6 J/y. These amounts of heat (4.3×10^7 J/y from hot syngas, hot flue gas, unconverted gas) provide sufficient steam and power (total exergy 3.5×10^7 J/y) to support the entire system. For the syngas cleaning, the main exergy input was cold flue gas and steam (1.5×10^7 J/y) from the CHP. After removed the sour gases, the cleaned syngas was sent to the fuel synthesis with the amount of exergy 9.5×10^7 J/y. For the fuel synthesis, the cleaned syngas from syngas cleaning was converted into liquid product (2.5×10^7 J/y) via Fisher-Tropsh process. By-product gases from fuel synthesis including unconverted gas (5.8×10^7 J/y) and H_2 (3.1×10^6 J/y) were sent to the methanol synthesis and HDP, respectively.

Table V.1. Exergy analysis of Gasification process

Mole Fractions	Inlet streams BIOMASS	AIR	N2	STEAM
H_2O		0	0	1
CO		0	0	0
H_2		0	0	0
CO_2		0	0	0
O_2		0.21	0	0
N_2		0.79	1	0
CL_2		0	0	0
H_2S		0	0	0
NH_3		0	0	0
BIOMASS	1	0	0	0
ASH		0	0	0
Temperature (°C)	25	30	250	200
Pressure (bar)	1.01	1.01	28.00	28.00
Mass Flows (kg/h)	30,000	49,558	2,430	15,675
Average MW		28.85	28.01	18.01
$H_{T,P}$ (J/kg)		4,838.60	2.36E+05	-1.50E+07
H_{ref} (J/kg)		-228.2	-216.3	-1.60E+07
$S_{T,P}$ (J/kg.K)		164.2	-399.9	-7,208.40
S_{ref} (J/kg,K)		147.4	-0.8	-9,483.60
Ex_{phy} (J/kg)		42	3.56E+05	1.91E+05
Ex_{phy} (J/s)		578.4	2.40E+05	8.31E+05
Ex_{chem} (kJ/kmol)		1.40E+03	7.20E+02	3.12E+03
Ex_{chem} (J/kg)	2.07E+07	4.86E+04	2.57E+04	1.73E+05
Ex_{chem} (J/s)	1.72E+08	6.69E+05	1.73E+04	7.54E+05
Total exergy (J/kg)	2.07E+07	4.87E+04	3.81E+05	3.64E+05
Total exergy (J/s)	1.72E+08	6.70E+05	2.57E+05	1.58E+06

Mole Fractions	Outlet streams SYNGAS	FLUEGAS	SOLID
H_2O	0.37	0	
CO	0.186	0	
H_2	0.334	0	
CO_2	0.07	0.197	
O_2	0	0.013	
N_2	0.034	0.79	
CL_2	0.00015	0	
H_2S	0.00013	0	
NH_3	0.00508	0	
BIOMASS	0	0	
ASH	0	0	1
Temperature (°C)	1,368	988	1,401
Pressure (bar)	1.01	1.01	1.01
Mass Flows (kg/h)	42,278	53,631	1,754
Average MW	16.71	31.22	
$H_{T,P}$ (J/kg)	-5.33E+06	-1.41E+06	
H_{ref} (J/kg)	-9.27E+06	-2.49E+06	
$S_{T,P}$ (J/kg.K)	4,253	1,740	
S_{ref} (J/kg,K)	-2,318	167	
Ex_{phy} (J/kg)	1.97E+06	6.10E+05	
Ex_{phy} (J/s)	2.32E+07	9.09E+06	
Ex_{chem} (kJ/kmol)	1.34E+05	4.59E+03	
Ex_{chem} (J/kg)	8.04E+06	1.47E+05	
Ex_{chem} (J/s)	9.44E+07	2.19E+06	
Total exergy (J/kg)	1.00E+07	7.57E+05	
Total exergy (J/s)	1.18E+08	1.13E+07	

Table V.2. Exergy analysis of CHP

	Inlet streams				
Mole Fractions	**FGAS**	**AIR**	**MIXGAS**	**WATER**	**FLUEGAS**
H2O	0.37	0	0	1	0
CO	0.19	0	0.11	0	0
H2	0.33	0	0.36	0	0
CO2	0.07	0	0.18	0	0.20
O2	0	0.21	0	0	0.01
N2	0.03	0.79	0.31	0	0.79
NH3	0	0	0	0	0
MEA	0	0	0	0	0
Methanol	0	0	0	0	0
CH4	0.01	0	0	0	0
C2H6	0	0	0	0	0
C2H4	0	0	0.01	0	0
C2H2	0	0	0.01	0	0
C3H8	0	0	0.01	0	0
C4H10	0	0	0	0	0
C5H12	0	0	0	0	0
C6H14	0	0	0.01	0	0
C7H16	0	0	0.01	0	0
	1.00	1.00	1.00	1.00	1.00
Temperature (°C)	1,368	25	31	30	988
Pressure (bar)	1.01	1.01	22.20	1.00	1.01
Mass Flows (kg/h)	42,278	33,488	6,121	62,000	53,631
Average MW	16.71	28.85	22.04	18.02	31.22
$H_{T,P}$ (J/kg)	-5,331,300	-228	-4,024,380	-16,009,953	-1,408,813
H_{ref} (J/kg)	-9,109,400	-228	-4,025,275	-16,034,000	-2,488,355
$S_{T,P}$ (J/kg.K)	4,253	147	-485	-9,403	1,740
S_{ref} (J/kg,K)	-2,162	147	674	-9,484	167
Ex_{phy} (J/kg)	1,864,744	0	346,699	158	610,338
Ex_{phy} (J/s)	21,899,508	0	589,501	2,717	9,092,469
Ex_{chem} (kJ/kmol)	137,162	1,403	222,076	3,120	4,594
Ex_{chem} (J/kg)	8,208,852	48,613	10,076,325	173,186	147,157
Ex_{chem} (J/s)	96,404,570	452,206	17,133,016	2,982,653	2,192,269
Total exergy (J/kg)	10,073,595	48,613	10,423,024	173,344	757,495
Total exergy (J/s)	118,304,078	452,206	17,722,517	2,985,370	11,284,739

	Outlet streams				
Mole Fractions	**FGAS**	**FLUEGAS**	**HPSTM**	**MPSTM**	**MTSTM**
H2O	0.37	0.10	1	1	1
CO	0.19	0	0	0	0
H2	0.33	0	0	0	0
CO2	0.07	0.08	0	0	0
O2	0	0.10	0	0	0
N2	0.03	0.73	0	0	0
NH3	0.01	0	0	0	0
MEA	0	0	0	0	0
Methanol	0	0	0	0	0
CH4	0	0	0	0	0
C2H6	0	0	0	0	0
C2H4	0	0	0	0	0
C2H2	0	0	0	0	0
C3H8	0	0	0	0	0
C4H10	0	0	0	0	0
C5H12	0	0	0	0	0
C6H14	0	0	0	0	0
C7H16	0	0	0	0	0
	1.00	1.00	1.00	1.00	1.00
Temperature (°C)	180	574	510	200	250
Pressure (bar)	1.01	23.00	62.00	28.00	25.00
Mass Flows (kg/h)	42,278	39,609	5,969	15,675	40,356
Average MW	16.70901	28.67676597	18.01528	18.01528	18.01528
$H_{T,P}$ (J/kg)	-7,965,700	-1,243,776	-12,534,000	-15,165,000	-13,056,000
H_{ref} (J/kg)	-9,265,300	-1,981,432	-16,034,000	-16,034,000	-16,034,000
$S_{T,P}$ (J/kg.K)	1,474	364	-2,538	-7,208	-2,954
S_{ref} (J/kg,K)	-2,318	-277	-9,484	-9,484	-9,484
Ex_{phy} (J/kg)	168,619	546,450	1,428,386	190,442	1,030,432
Ex_{phy} (J/s)	1,980,254	6,012,329	2,368,343	829,214	11,551,174
Ex_{chem} (kJ/kmol)	134,288	2,773	3,120	3,120	3,120
Ex_{chem} (J/kg)	8,036,888	96,696	173,185	173,186	173,186
Ex_{chem} (J/s)	94,385,040	1,063,899	287,150	754,082	1,941,423
Total exergy (J/kg)	8,205,507	643,146	1,601,570	363,628	1,203,619
Total exergy (J/s)	96,365,294	7,076,228	2,655,493	1,583,296	13,492,598

Table V.3. Exergy analysis of syngas cleaning process

	Inlet streams			
Mole Fractions	**FGAS**	**SOLVENT**	**O2**	**WATER**
H2O	0.37	0	0	1
CO	0.19	0	0	0
H2	0.33	0	0	0
CO2	0.07	0	0	0
O2	0	0	0.95	0
N2	0.03	0	0	0
AR	0	0	0.05	0
CL2	0	0	0	0
H2S	0	0	0	0
NH3	0	0	0	0
MEA	0	1.00	0	0
	1.00	1.00	1.00	1.00
Temperature (°C)	180	38	25	37
Pressure (bar)	1.01	1.00	1.05	53.50
Mass Flows (kg/h)	42,278	3	91	282
Average MW	16.71	61.08	32.38	18.02
$H_{T,P}$ (J/kg)	-7,965,644	-4,388,274	-258	-15,811,047
H_{ref} (J/kg)	-9,178,976	-4,425,092	-249	-15,857,809
$S_{T,P}$ (J/kg.K)	1,474	-8,009	40	-8,895
S_{ref} (J/kg,K)	-2,082	-8,132	49	-9,031
Ex_{phy} (J/kg)	152,621	210	2,726	6,376
Ex_{phy} (J/s)	1,792,374	0	69	499
Ex_{chem} (kJ/kmol)	134,288	1,536,000	4,354	3,120
Ex_{chem} (J/kg)	8,036,889	25,145,816	134,470	173,186
Ex_{chem} (J/s)	94,385,050	22,846	3,399	13,543
Total exergy (J/kg)	8,189,509	25,146,026	137,197	179,562
Total exergy (J/s)	96,177,423	22,846	3,468	14,042

	Outlet streams			
Mole Fractions	**FGAS**	**CO2**	**PURGE**	**SULFUR**
H2O	0	0.03	0.99	0.90
CO	0.33	0	0	0
H2	0.60	0	0	0
CO2	0	0.95	0	0
O2	0	0.01	0	0
N2	0.06	0	0	0
AR	0	0	0	0
CL2	0	0	0	0
H2S	0	0	0	0
NH3	0	0.01	0.01	0
MEA	0	0	0	0.01
	1.00	1.00	1.00	0.92
Temperature (°C)	37	35	64	35
Pressure (bar)	53.00	1.92	1.00	1.92
Mass Flows (kg/h)	17,361	8,054	17,163	76
Average MW	12.37	42.88	18.00	19.76
$H_{T,P}$ (J/kg)	-2,996,417	-8,864,715	-15,563,742	-12,323,153
H_{ref} (J/kg)	-3,021,037	-8,872,732	-15,724,213	-12,357,937
$S_{T,P}$ (J/kg.K)	394	-34	-8,522	-7,397
S_{ref} (J/kg,K)	2,987	62	-9,023	-7,511
Ex_{phy} (J/kg)	798,025	36,798	10,800	898
Ex_{phy} (J/s)	3,848,504	82,327	51,490	19
Ex_{chem} (kJ/kmol)	234,057	22,612	7,049	74,457
Ex_{chem} (J/kg)	18,927,843	527,342	391,510	3,767,508
Ex_{chem} (J/s)	91,280,234	1,179,823	1,866,497	79,179
Total exergy (J/kg)	19,725,868	564,139	402,311	3,768,407
Total exergy (J/s)	95,128,738	1,262,150	1,917,987	79,198

Table V.4. Exergy analysis of fuel synthesis process

	Inlet streams	
Mole Fractions	**FGAS**	**MTSTM**
H2O	0	1
CO	0.33	0
H2	0.60	0
CO2	0	0
N2	0.06	0
CH4	0	0
C2H6	0	0
C3H8	0	0
C4H10	0	0
C5H12	0	0
C6H14	0	0
C7H16	0	0
C8H18	0	0
C9H20	0	0
C10H22	0	0
C11H24	0	0
C12H26	0	0
C13H28	0	0
C14H30	0	0
C15H32	0	0
C16H34	0	0
C17H36	0	0
C18H38	0	0
C19H40	0	0
C20H42	0	0
	1.00	1.00
Temperature (°C)	37	250
Pressure (bar)	53.00	25.86
Mass Flows (kg/h)	17,361	1,832
Average MW	12.37	18.02
$H_{T,P}$ (J/kg)	-2,994,426	-12,993,049
H_{ref} (J/kg)	-3,020,947	-15,857,809
$S_{T,P}$ (J/kg.K)	414	-2,886
S_{ref} (J/kg,K)	2,987	-9,030
Ex_{phy} (J/kg)	794,012	1,032,227
Ex_{phy} (J/S)	3,829,152	525,321
Ex_{chem} (kJ/kmol)	234,057	3,120
Ex_{chem} (J/kg)	18,927,843	173,186
Ex_{chem} (J/S)	91,280,234	88,138
Total exergy (J/kg)	19,721,855	1,205,414
Total exergy (J/s)	95,109,386	613,459

	Outlet streams			
Mole Fractions	**SYNGAS**	**LIQUIDPDYT**	**H2**	**WASTEWATER**
H2O	0	0	0.00	1.00
CO	0.25	0	0	0
H2	0.57	0	1	0
CO2	0.08	0	0	0
N2	0.09	0	0	0
CH4	0.003	0	0	0
C2H6	0.002	0	0	0
C3H8	0.002	0	0	0
C4H10	0.002	0	0	0
C5H12	0	0.13	0	0
C6H14	0	0.11	0	0
C7H16	0	0.10	0	0
C8H18	0	0.09	0	0
C9H20	0	0.08	0	0
C10H22	0	0.07	0	0
C11H24	0	0.07	0	0
C12H26	0	0.06	0	0
C13H28	0	0.05	0	0
C14H30	0	0.05	0	0
C15H32	0	0.04	0	0
C16H34	0	0.04	0	0
C17H36	0	0.04	0	0
C18H38	0	0.03	0	0
C19H40	0	0.03	0	0
C20H42	0	0.03	0	0
	1.00	1.00	1.00	1.00
Temperature (°C)	47	70	200	70
Pressure (bar)	1.01	26.00	26.00	26.00
Mass Flows (kg/h)	13,750	1,963	92	3,389
Average MW	14.58	147.51	2.02	18.02
$H_{T,P}$ (J/kg)	-4,034,335	-2,001,904	2,528,382	-15,676,920
H_{ref} (J/kg)	-4,079,527	-2,102,349	0	-15,857,805
$S_{T,P}$ (J/kg.K)	2,237	-7,026	-6,716	-8,470
S_{ref} (J/kg,K)	2,090	-7,338	0	-9,030
Ex_{phy} (J/kg)	1,577	7,604	4,531,365	13,628
Ex_{phy} (J/S)	6,022	4,145	116,226	12,828
Ex_{chem} (kJ/kmol)	220,600	6,959,979	236,000	3,120
Ex_{chem} (J/kg)	15,126,145	47,182,966	117,070,461	173,195
Ex_{chem} (J/S)	57,771,907	25,722,891	3,002,763	163,027
Total exergy (J/kg)	15,127,722	47,190,570	121,601,825	186,823
Total exergy (J/s)	57,777,929	25,727,037	3,118,989	175,856

Table V.5. Exergy analysis of HDP

	Inlet streams	
Mole Fractions	**LIQUIDPDYT**	**H2**
H2O	0	0
CO	0	0
H2	0	1
C5H12	0.13	0
C6H14	0.11	0
C7H16	0.10	0
C8H18	0.09	0
C9H20	0.08	0
C10H22	0.07	0
C11H24	0.07	0
C12H26	0.06	0
C13H28	0	0
C14H30	0	0
C15H32	0	0
C16H34	0	0
C17H36	0	0
C18H38	0	0
C19H40	0	0
C20H42	0	0
SULFUR	0	0
	1.00	1.00
Temperature (°C)	70	200
Pressure (bar)	26.00	26.00
Mass Flows (kg/h)	1,963	92
Average MW	147.51	2.02
$H_{T,P}$ (J/kg)	-2,001,904	2,528,382
H_{ref} (J/kg)	-2,102,349	0
$S_{T,P}$ (J/kg.K)	-7,026	-6,716
S_{ref} (J/kg,K)	-7,338	0
Ex_{phy} (J/kg)	7,604	4,531,365
Ex_{phy} (J/s)	4,145	116,226

	Outlet streams		
Mole Fractions	**C5-C12**	**C12+**	**FUELGAS**
H2O	0	0	0
CO	0	0	0
H2	0.03	0	0.988
C5H12	0.14	0	0.008
C6H14	0.15	0	0.003
C7H16	0.14	0	0
C8H18	0.24	0	0
C9H20	0.02	0	0
C10H22	0.10	0	0
C11H24	0.09	0	0
C12H26	0.09	0	0
C13H28	0	0.17	0
C14H30	0	0.15	0
C15H32	0	0.14	0
C16H34	0	0.39	0
C17H36	0	0.11	0
C18H38	0	0.03	0
C19H40	0	0.01	0
C20H42	0	0	0
SULFUR	0	0	0
	1.00	1.00	1.00
Temperature (°C)	50	50	50
Pressure (bar)	22.20	22.20	22.20
Mass Flows (kg/h)	1,011	910	134
Average MW	110.86	216.39	2.94
$H_{T,P}$ (J/kg)	-2,129,484	-1,960,110	-378,611
H_{ref} (J/kg)	-2,186,473	-2,006,664	-634,975
$S_{T,P}$ (J/kg.K)	-7,200	-7,230	-9,779
S_{ref} (J/kg,K)	-7,379	-7,384	-1,862
Ex_{phy} (J/kg)	3,554	792	2,617,685
Ex_{phy} (J/s)	998	200	97,717

Table V.6. Exergy analysis of methanol synthesis

	Inlet streams	
Mole Fractions	**SYNGAS**	**STEAM**
H2O	0	1
CO	0.2532	0
H2	0.5676	0
CO2	0.0779	0
O2	0	0
N2	0.0920	0
AR	0	0
CL2	0.0004	0
H2S	0	0
NH3	0	0
MEA	0	0
Methanol	0	0
CH4	0.0025	0
C2H6	0.0023	0
C2H4	0	0
C2H2	0	0
C3H8	0.0021	0
C4H10	0.0019	0
	1.00	1.00
Temperature (°C)	47	250
Pressure (bar)	1.01	25.00
Mass Flows (kg/h)	13,750	5
Average MW	14.58	18.02
$H_{T,P}$ (J/kg)	-4,034,483	-13,055,892
H_{ref} (J/kg)	-4,079,719	-16,034,032
$S_{T,P}$ (J/kg.K)	2,236	-2,954
S_{ref} (J/kg,K)	2,089	-9,484
Ex_{phy} (J/kg)	1,578	1,030,573
Ex_{phy} (J/s)	6,028	1,431
Ex_{chem} (kJ/kmol)	234	11,242
Ex_{chem} (J/kg)	16,044	624,000
Ex_{chem} (J/s)	61,278	867
Total exergy (J/kg)	17,622	1,654,573
Total exergy (J/s)	67,305	2,298

	Outlet streams			
Mole Fractions	**MEOH**	**VENT1**	**VENT2**	**WASTEWATER**
H2O	0.057	0	0	0.979
CO	0	0.134	0.133	0
H2	0	0.233	0.230	0
CO2	0.003	0.215	0.220	0
O2	0	0	0	0
N2	0	0.376	0.372	0
AR	0	0	0.000	0
CL2	0.001	0.001	0.001	0
H2S	0	0	0	0
NH3	0	0	0	0
MEA	0	0	0	0
Methanol	0.938	0.007	0.009	0.021
CH4	0	0.010	0.010	0
C2H6	0	0.009	0.009	0
C2H4	0	0	0	0
C2H2	0	0	0	0
C3H8	0	0.008	0.008	0
C4H10	0.001	0.006	0.007	0
	1.00	1.00	1.00	1.00
Temperature (°C)	47	40	51	98
Pressure (bar)	1.01	107.30	110.04	1.01
Mass Flows (kg/h)	7,603	1,711	4,276	157
Average MW	31.34	25.67	25.87	18.30
$H_{T,P}$ (J/kg)	-7,745,889	-4,068,922	-4,121,312	-15,379,383
H_{ref} (J/kg)	-7,830,040	-4,053,916	-4,120,414	-15,727,945
$S_{T,P}$ (J/kg.K)	-7,581	-877	-852	-8,339
S_{ref} (J/kg,K)	-7,853	670	646	-9,385
Ex_{phy} (J/kg)	2,967	446,476	446,062	36,571
Ex_{phy} (J/s)	6,267	212,176	529,819	1,599
Ex_{chem} (kJ/kmol)	679,068	159,635	161,682	17,826
Ex_{chem} (J/kg)	21,670,567	6,217,567	6,250,904	973,912
Ex_{chem} (J/s)	45,767,034	2,954,739	7,424,637	42,572
Total exergy (J/kg)	21,673,534	6,664,043	6,696,966	1,010,482
Total exergy (J/s)	45,773,300	3,166,916	7,954,456	44,171

Table V.7. Exergy analysis of methanol synthesis

	Inlet streams	
Mole Fractions	**SYNGAS**	**STEAM**
H2O	0	1
CO	0.2532	0
H2	0.5676	0
CO2	0.0779	0
O2	0	0
N2	0.0920	0
AR	0	0
CL2	0.0004	0
H2S	0	0
NH3	0	0
MEA	0	0
Methanol	0	0
CH4	0.0025	0
C2H6	0.0023	0
C2H4	0	0
C2H2	0	0
C3H8	0.0021	0
C4H10	0.0019	0
	1.00	1.00
Temperature (°C)	47	250
Pressure (bar)	1.01	25.00
Mass Flows (kg/h)	13,750	5
Average MW	14.58	18.02
$H_{T,P}$ (J/kg)	-4,034,483	-13,055,892
H_{ref} (J/kg)	-4,079,719	-16,034,032
$S_{T,P}$ (J/kg.K)	2,236	-2,954
S_{ref} (J/kg,K)	2,089	-9,484
Ex_{phy} (J/kg)	1,578	1,030,573
Ex_{phy} (J/s)	6,028	1,431
Ex_{chem} (kJ/kmol)	234	11,242
Ex_{chem} (J/kg)	16,044	624,000
Ex_{chem} (J/s)	61,278	867
Total exergy (J/kg)	17,622	1,654,573
Total exergy (J/s)	67,305	2,298

	Outlet streams			
Mole Fractions	**MEOH**	**VENT1**	**VENT2**	**WASTEWATER**
H2O	0.057	0	0	0.979
CO	0	0.134	0.133	0
H2	0	0.233	0.230	0
CO2	0.003	0.215	0.220	0
O2	0	0	0	0
N2	0	0.376	0.372	0
AR	0	0	0.000	0
CL2	0.001	0.001	0.001	0
H2S	0	0	0	0
NH3	0	0	0	0
MEA	0	0	0	0
Methanol	0.938	0.007	0.009	0.021
CH4	0	0.010	0.010	0
C2H6	0	0.009	0.009	0
C2H4	0	0	0	0
C2H2	0	0	0	0
C3H8	0	0.008	0.008	0
C4H10	0.001	0.006	0.007	0
	1.00	1.00	1.00	1.00
Temperature (°C)	47	40	51	98
Pressure (bar)	1.01	107.30	110.04	1.01
Mass Flows (kg/h)	7,603	1,711	4,276	157
Average MW	31.34	25.67	25.87	18.30
$H_{T,P}$ (J/kg)	-7,745,889	-4,068,922	-4,121,312	-15,379,383
H_{ref} (J/kg)	-7,830,040	-4,053,916	-4,120,414	-15,727,945
$S_{T,P}$ (J/kg.K)	-7,581	-877	-852	-8,339
S_{ref} (J/kg,K)	-7,853	670	646	-9,385
Ex_{phy} (J/kg)	2,967	446,476	446,062	36,571
Ex_{phy} (J/s)	6,267	212,176	529,819	1,599
Ex_{chem} (kJ/kmol)	679,068	159,635	161,682	17,826
Ex_{chem} (J/kg)	21,670,567	6,217,567	6,250,904	973,912
Ex_{chem} (J/s)	45,767,034	2,954,739	7,424,637	42,572
Total exergy (J/kg)	21,673,534	6,664,043	6,696,966	1,010,482
Total exergy (J/s)	45,773,300	3,166,916	7,954,456	44,171

5.6. Exergy analysis of napier-based biorefinery

The exergy analysis of the napier-based biorefinery was presented in Figure V.2. In the gasification section, about 30% of exergy loss occurred due to the combustion reaction where the gasifier produces syngas from biomass, air and steam. About 6% of exergy output from the gasification section is the flue gas stream, the by-product from syngas production. The exergetic efficiency of the gasification is 64% similar to the related literature (Ptasinski et al., 2007). In the CHP section, the wasted heat from hot flue gas was recovered and used to produce steam supplying the system. Not only the wasted heat that was recovered in the CHP section, but also the heat from hot syngas which has enough exergy to produce 10 MW electricity and almost 50% of total steam supported the entire system. The rest of the heat required for steam consumption came from wasted heat recovery and the combustion of unconverted gas from HDP and methanol synthesis sections. Next section is the syngas cleaning process. This process consumed the largest amount of steam in the regeneration of the absorption solvent. About 60% of steam generated from CHP was consumed in this process. The fuel synthesis and HDP required only small amount of exergy input from electricity and steam since the heat was recovered within the process. The last section, the methanol synthesis, required steam in distillation columns to obtain a high purity of methanol. Also, about 20% of exergy outputs was unconverted gas which was sent to the CHP to produce steam that will be feedback to the processes. Finally, when considered the exergy of biomass as the input and exergies of liquid fuels, methanol and electricity as the outputs, the exergetic efficiency of the proposed biorefinery is equal to 46%. Table V.8 and Figure V.3 show the summary of the exergy analysis of all process in the biorefinery.

Table V.8. Exergy analysis of biorefinery

Section	Σ ***Exergy$_{in}$*** *(J/S)*	Σ ***Exergy$_{out}$*** *(J/S) **	***Exergetic efficiency***	***Dominating factors***
Gasification	183,868,027	117,568,395	64%	Combustion reaction
CHP	160,819,560	120,186,297	75%	Combustion chamber, steam turbines
Syngas cleaning	111,856,395	95,128,738	85%	MEA regeneration column
Fuel synthesis	95,840,289	86,623,954	90%	Fisher-Tropsh reactor
HDP	28,846,026	25,183,723	87%	Hydro-processing reactor
Methanol synthesis	59,971,839	45,773,300	76%	Distillation columns

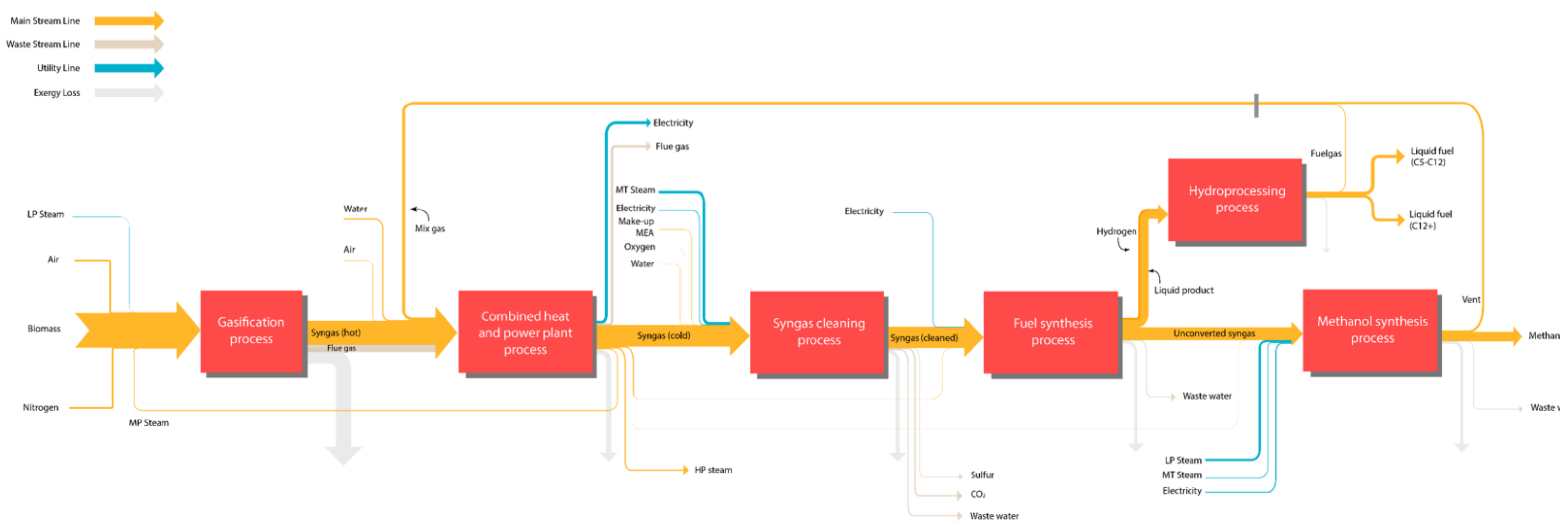

Figure V.2. Exergy of the Napier-based biorefinery

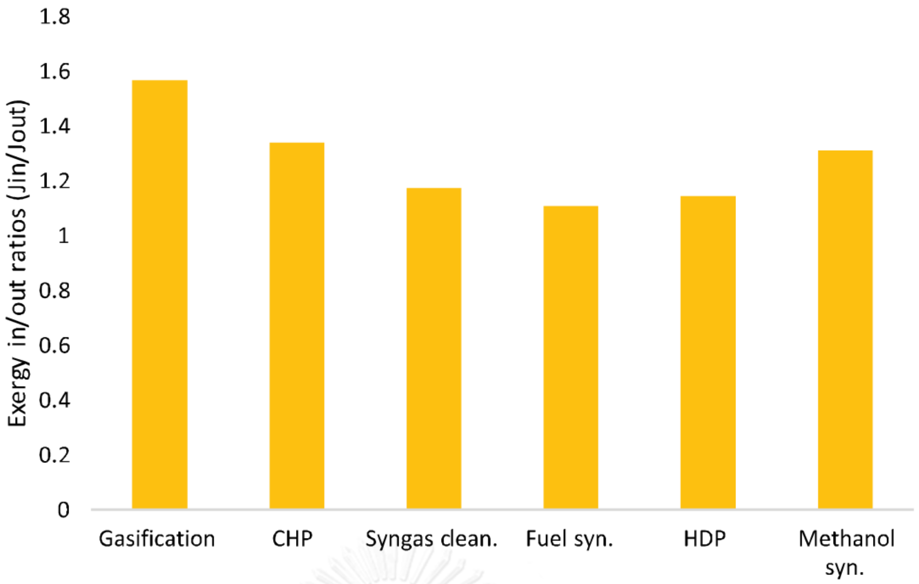

Figure V.3. Exergy input to output ratios of intermediate processes within the biorefinery

5.7. Relation between Emergy and Exergy Analysis

Exergy analysis has its origin from the thermodynamics, whereas emergy analysis origins from the systems ecology. Exergy and emergy analysis related to each other since both method considered that each kind of energy has different ability to do work. When a process produces a single product, the cost of the product can be simply obtained from the ratio between the production costs and the production rate. While in case where a process produces multiple products, for example CHP, heat and power are produced simultaneously. In this case, the cost allocates to each product should be proportionally related to their exergies than energy.

Figure V.3 depicts the exergy input to output ratio which represents the exergetic efficiency of the process. The high value means high exergy loss occurred or the process has low exergetic efficiency. The result indicates that high exergy loss occurred in the gasification process. Meaning that the exergy efficiency was decrease when the process involved with thermal decomposition in the gasification section.

Comparing with emergy, the cumulative exergy input to output was used to represent the exergy used along the transformation process as shown in Figure V.4. From the figure, the cumulative exergy input to output ratio shows in the yellow bar. In each bar, all exergies from upstream processes were allocated to the downstream process.

In emergy aspect, the UEV was presented in the blue shade background. The trends showed that the UEV of the upstream and downstream processes are related in the sequential way. The higher order of process has higher UEV because when the order of process is higher, the larger amount of resources are consumed and lower quantity of the product are generated. Therefore, the fuel synthesis has higher UEV than syngas cleaning, CHP and gasification, respectively. However, the different result was found in the HDP and methanol synthesis. Because they operate in the same sequential as the parallel processes. And the product from fuel synthesis was split into two streams and fed to HDP and methanol synthesis, respectively. According to emergy's rule, the emergy will be assigned to each stream based on their energy fraction. Thus, the reason why UEV of the product from HDP was higher than the one from methanol synthesis is that it required higher emergy input to produce the products than the methanol synthesis. In addition, the gasification is the upstream process, thus the emergy allocated to this section is the lowest. The emergy increment from the upstream-process represents the amount of emergy input top-up to that process. The higher increment reflects the higher emergy input to the process.

We can see that the resource used in term of exergy has the same trend as in emergy analysis. However, it is important to notice that the UEV from emergy analysis has so much more value than the exergy. Because emergy considers more parameters or broader view than exergy, one of those is human labor. The emergy analysis can indicate that the higher order of down-stream processes would require more materials, heat and manpower inputs due to the emergy covered from the up-stream products. Which makes emergy analysis properly accounts for the globality of the energy and resource flows supporting complex systems. For the exergy analysis, it is found to provide the more exact and insightful assessment for thermodynamic features. After all, both exergy and emergy analysis are directly related to each other. The high efficient system in term of exergy will reflect the lower emergy consumption leading to high self-sufficient and, finally, high sustainability.

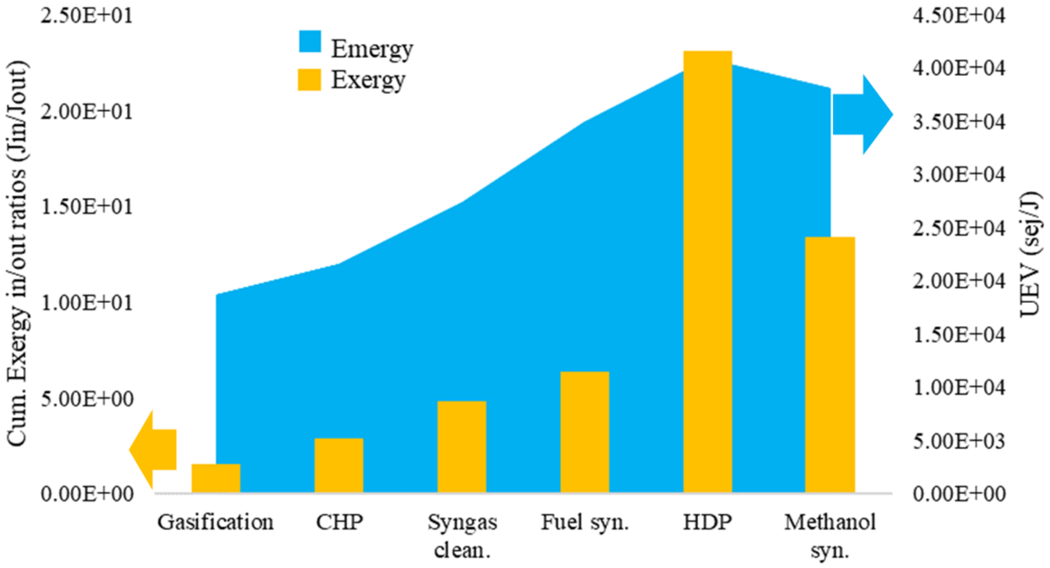

Figure V.4. Cumulative Exergy/Emergy input to output ratios of intermediate processes within the biorefinery

CHAPTER VI: CONCLUSION AND RECOMMENDATIONS

In this study, emergy assessment was used as a tool for evaluating biorefinery based on biomass resources. According to the objectives, the works done here consist of 3 categories; First is the emergy algorithm development, second is the implementation of emergy into 2 industrial systems. One is the existing waste treating processes that is CO2 capture and second is the proposed model of bio-based eco-industrial park. Finally, the result from emergy analysis will be compared with the conventional exergy analysis to indicate the different aspects from those two procedures. The result provided insight into the evaluated system in terms of efficiency and environmental impacts. The values indicated whether the evaluated system is optimally employed.

In Chapter III, the computational algorithm to find the emergy distributed to each intermediate process inside the complex system was designed by using a simple algorithm, like in "Snakes and Ladders" board game. The rule is to search for the furthest position of possible paths stored in matrix *Path*; then trace back until the source is reached. While the paths unite, the rule no. 2 and no. 4.2 will be applied, respectively, to identify paths, i.e., whether splits or co-product occur. As shown by the comparison between emergy calculation data from the MATLAB program and Odum (Odum, 1996), it was found that the developed code can perform the emergy balance precisely even in a complex system with feedbacks, co-products and splits.

In Chapter IV, the implementation of emergy-based sustainable decision was presented. The overall results revealed that the bio-based products are not a completely renewable. They depend mostly on non-renewable resources in both biomass cultivation and biorefinery stages. In the Napier grass cultivation process, the dominating emergy input is evapotranspiration, diesel consumption and human labor, respectively. Even though there was no agreement for human labor accounting methods, different assumptions among present emergy literatures have been made. Therefore, it is important to perform emergy evaluation either with or without human labor input to clarify the range of product UEV for the further studies.

The diesel fuel for biomass cultivation and transportation also dominated the ESI. Additionally, replacing this fossil fuel with alternative fuels cannot directly solve the problem. It would put the situation into a dilemma regarding the high indirect fossil fuel consumption behind the production process.

In most industrial production processes, all emergy inputs other than biomass were considered as external resources (except for some cases for example; geothermal power plant, wind power plant, etc.). Those are often produced from non-renewable resources, which made the system to have a low EYR and to create a high burden to the environment. Our proposed biorefinery model, that attempts to promote the sustainability of the existing system, can achieve a higher efficiency in terms of resources utilization than the conventional production systems currently in existence. Nonetheless, the ESI of the whole system is still too low and requires further improvement. As suggested in the green engineering concept (Allenby and Richards, 1994), besides maximizing resource efficiency, renewable resources should replace non-renewable ones as much as possible.

In Chapter V, the exergy analysis of the proposed biorefinery was presented. The results showed that the highest exergy loss occurred in the gasification section. The exergy input to output ratio was used to compare with the UEV from emergy analysis. The comparison indicated that the exergy and emergy analysis give the different tendency due to their differences in concepts. The exergy analysis provides an insight view in thermal efficiency of the processes while the emergy analysis gives the globality of the resource flows supporting the systems.

Promises and Problems in emergy analysis

The emergy methodology for sustainability assessment has advantages in that it can reveal the importance of free environmental services and resources. However, the limitations of emergy analysis were found.

Due to globalization, societies utilize resources globally. For example, electricity might be imported from neighboring countries that is produced by wind or hydropower.

According to the conventional definition of ESI, only the local renewable emergy is counted in the renewable fraction for calculating the sustainable index. Thus, to be more accurate, the global renewable resources should be recognized in the ESI. This would provide broader perspective to the sustainability of the processes which required a large portion of external inputs but were partially renewable.

However, as emergy analysis related to the behavior of self-organized systems, valuing ecological goods and services, using a mathematical approach to deal with such system is a huge challenge. Many issues have not been settled such as argued in Section 3.6 in this dissertation. Besides the main objectives, the author attempts to clarify many of the common misconceptions about emergy and inform the community of emergy practitioners about the aspects that need to be communicated better or improved.

Suggestions and recommendations for the future work

As the last chapter reached, there are numerous challenges that still need to be improved. To suggest for the future work, the ideas have been listed as follows.

1) The improvement of the proposed biorefinery:

   The proposed model in this dissertation was simulated based on the conventional systems that are currently in existence. In stead of the proposed model, there are recent technologies that would improve the sustainability of the system, however, required tools to measure their feasibility in term of economic and environmental. Also, creating the pathways of biomass utilization and analyzing the sustainability of those options would be valuable for the sustainable development.

2) The issues on emergy analysis:

   As we discussed a lot about the issues on emergy analysis, there is no objection about the importance of improving emergy analysis. The sustainability indicator or ESI should relate more to global renewability. And more important, the guidelines for emergy analysis should be corrected and clarified the actual meaning of emergy evaluation.

REFERENCES

Aemkulwat, C., 2010. Labor force structure change and Thai labor market, 1990-2008, Proceedings of the Second Annual Conference of the Academic Network for Development in Asia (ANDA), pp. 1-19.

Allenby, B.R., Richards, D.J., 1994. The greening of industrial ecosystems. National Academies Press.

Almeida, C., Barrella, F., Giannetti, F., 2004. Graphical tool for emergy analysis: concepts and an example of application. São Paulo: Universidade Paulista.

Arbault, D., Rugani, B., Tiruta-Barna, L., Benetto, E., 2013. Emergy evaluation of water treatment processes. Ecological engineering 60, 172-182.

Bastianoni, S., Coppola, F., Tiezzi, E., Colacevich, A., Borghini, F., Focardi, S., 2008. Biofuel potential production from the Orbetello lagoon macroalgae: A comparison with sunflower feedstock. Biomass and Bioenergy 32, 619-628.

Bastianoni, S., Marchettini, N., 2000. The problem of co-production in environmental accounting by emergy analysis. Ecological Modelling 129, 187-193.

Berndes, G., Hansson, J., 2007. Bioenergy expansion in the EU: cost-effective climate change mitigation, employment creation and reduced dependency on imported fuels. Energy Policy 35, 5965-5979.

Brown, M., Ulgiati, S., 2002. Emergy evaluations and environmental loading of electricity production systems. Journal of cleaner production 10, 321-334.

Brown, M.T., Herendeen, R.A., 1996. Embodied energy analysis and EMERGY analysis: a comparative view. Ecological Economics 19, 219-235.

Brown, M.T., Ulgiati, S., 2004. Emergy analysis and environmental accounting. Encyclopedia of energy 2, 329-354.

Brown, M.T., Ulgiati, S., 2016. Emergy assessment of global renewable sources. Ecological Modelling 339, 148-156.

Brundtland, G., 1987. World Commission on Environment and Development (1987) Our Common Future: Report of the World Commission On Environment and Development. Oxford University.

Campanari, S., Chiesa, P., Manzolini, G., Bedogni, S., 2014. Economic analysis of CO 2 capture from natural gas combined cycles using molten carbonate fuel cells. Applied Energy 130, 562-573.

Campbell, J.E., Lobell, D.B., Genova, R.C., Field, C.B., 2008. The global potential of bioenergy on abandoned agriculture lands. Environmental science & technology 42, 5791-5794.

Cavalett, O., Ortega, E., 2010. Integrated environmental assessment of biodiesel production from soybean in Brazil. Journal of Cleaner Production 18, 55-70.

Cavalett, O., Rydberg, T., 2011. Critical analysis of the Swedish biofuels policy using emergy synthesis, Proceedings of the 6th emergy conference. Gainesville, Florida: Center for Environmental Policy, University of Florida.

Chang, F.-C., Lin, L.-D., Ko, C.-H., Hsieh, H.-C., Yang, B.-Y., Chen, W.-H., Hwang, W.-S., 2017. Life cycle assessment of bioethanol production from three feedstocks and two fermentation waste reutilization schemes. Journal of Cleaner Production 143, 973-979.

Cohen, M.J., Brown, M.T., Shepherd, K.D., 2006. Estimating the environmental costs of soil erosion at multiple scales in Kenya using emergy synthesis. Agriculture, ecosystems & environment 114, 249-269.

Coppola, F., Bastianoni, S., Østergård, H., 2009. Sustainability of bioethanol production from wheat with recycled residues as evaluated by Emergy assessment. Biomass and Bioenergy 33, 1626-1642.

da Cruz, R.V.A., do Nascimento, C.A.O., 2012. Emergy analysis of oil production from microalgae. biomass and bioenergy 47, 418-425.

De Jong, E., Van Ree, R., Sanders, J., Langeveld, J., 2010. Biorefineries: giving value to sustainable biomass use. The Biobased Economy: Biofuels, Materials and Chemicals in the Post-oil Era, 111-130.

De María, R., Díaz, I., Rodríguez, M., Sáiz, A., 2013. Industrial methanol from syngas: kinetic study and process simulation. Int J Chem React Eng 11, 469-477.

de Oliveira Junior, S., 2012. Exergy: production, cost and renewability. Springer Science & Business Media.

Desideri, U., Antonelli, M., 2014. A simplified method for the evaluation of the performance of coal fired power plant with carbon capture. Applied Thermal Engineering 64, 263-272.

Dincer, I., Rosen, M.A., 2012. Exergy: energy, environment and sustainable development. Newnes.

Doherty, W., Reynolds, A., Kennedy, D., 2013. Aspen plus simulation of biomass gasification in a steam blown dual fluidised bed.

Felix, E., Tilley, D.R., 2009. Integrated energy, environmental and financial analysis of ethanol production from cellulosic switchgrass. Energy 34, 410-436.

Flores, R.A., Urquiaga, S., Alves, B.J., Collier, L.S., Boddey, R.M., 2012. Yield and quality of elephant grass biomass produced in the cerrados region for bioenergy. Engenharia Agrícola 32, 831-839.

Fontoura, C.F., Brandão, L.E., Gomes, L.L., 2015. Elephant grass biorefineries: towards a cleaner Brazilian energy matrix? Journal of Cleaner Production 96, 85-93.

Franz, J., Maas, P., Scherer, V., 2014. Economic evaluation of pre-combustion CO 2-capture in IGCC power plants by porous ceramic membranes. Applied Energy 130, 532-542.

Giampietro, M., Ulgiati, S., Pimentel, D., 1997. Feasibility of large-scale biofuel production. BioScience 47, 587-600.

Goh, C.S., Lee, K.T., 2010. Palm-based biofuel refinery (PBR) to substitute petroleum refinery: an energy and emergy assessment. Renewable and Sustainable Energy Reviews 14, 2986-2995.

Hadri, N.E., Quang, D.V., Abu-Zahra, M.R., 2015. Study of Novel Solvent for CO2 Post-combustion Capture. Energy Procedia 75, 2268-2286.

Iloeje, C., Field, R., Ghoniem, A.F., 2015. Modeling and parametric analysis of nitrogen and sulfur oxide removal from oxy-combustion flue gas using a single column absorber. Fuel 160, 178-188.

Kamp, A., Morandi, F., Østergård, H., 2016. Development of concepts for human labour accounting in emergy assessment and other environmental sustainability assessment methods. Ecological Indicators 60, 884-892.

Kamp, A., Østergård, H., 2013. How to manage co-product inputs in emergy accounting exemplified by willow production for bioenergy. Ecological modelling 253, 70-78.

Kongkitisupchai, S., Gidaspow, D., 2013. Carbon dioxide capture using solid sorbents in a fluidized bed with reduced pressure regeneration in a downer. Aiche Journal 59, 4519-4537.

Krutka, H., Sjostrom, S., 2011. Evaluation of solid sorbents as a retrofit technology for CO2 capture from coal-fired power plants final technical report.

Kuramochi, T., Ramírez, A., Turkenburg, W., Faaij, A., 2011. Techno-economic assessment and comparison of CO 2 capture technologies for industrial processes: Preliminary results for the iron and steel sector. Energy Procedia 4, 1981-1988.

Le Corre, O., Truffet, L., 2012. Exact computation of emergy based on a mathematical reinterpretation of the rules of emergy algebra. Ecological Modelling 230, 101-113.

Le Corre, O., Truffet, L., 2015. Emergy paths computation from interconnected energy system diagram. Ecological Modelling 313, 181-200.

Lee, M.S., Goswami, D.Y., Kothurkar, N., Stefanakos, E.K., 2015. Development and evaluation of calcium oxide absorbent immobilized on fibrous ceramic fabrics for high temperature carbon dioxide capture. Powder Technology 274, 313-318.

Lin, B.-L., Sagisaka, M., 2012. Sustainability assessment of bioethanol and petroleum fuel production in Japan based on emergy analysis. Energy policy 44, 23-33.

Londoño, N.A.C., Suárez, D.G., Velásquez, H.I., Ruiz-Mercado, G.J., 2017. Emergy analysis for the sustainable utilization of biosolids generated in a municipal wastewater treatment plant. Journal of Cleaner Production 141, 182-193.

Lu, J.-G., Lu, C.-T., Chen, Y., Gao, L., Zhao, X., Zhang, H., Xu, Z.-W., 2014. CO 2 capture by membrane absorption coupling process: application of ionic liquids. Applied Energy 115, 573-581.

Maier, S., Szerencsits, M., Narodoslawsky, M., Ismail, I.M.I., Shahzad, K., 2016. Current potential of more sustainable biomass production using eco-efficient farming practices in Austria. Journal of Cleaner Production.

Manzolini, G., Fernandez, E.S., Rezvani, S., Macchi, E., Goetheer, E., Vlugt, T., 2015. Economic assessment of novel amine based CO 2 capture technologies integrated in power plants based on European Benchmarking Task Force methodology. Applied Energy 138, 546-558.

Morandi, F., Perrin, A., Østergård, H., 2016. Miscanthus as energy crop: Environmental assessment of a miscanthus biomass production case study in France. Journal of Cleaner Production 137, 313-321.

Muhammad, A., GadelHak, Y., 2015. Simulation based improvement techniques for acid gases sweetening by chemical absorption: A review. International Journal of Greenhouse Gas Control 37, 481-491.

Neff, T.L., 1997. Improving energy security in Pacific Asia: diversification and risk reduction for fossil and nuclear fuels. Project Commissioned by the Pacific Asia Regional Energy Security (PARES) Massachusetts Institute of Technology, Center for International Studies.

Nimmanterdwong, P., Chalermsinsuwan, B., Piumsomboon, P., 2015. Emergy evaluation of biofuels production in Thailand from different feedstocks. Ecological Engineering 74, 423-437.

Norsuwan, T., Marohn, C., Jintrawet, A., 2014. Effects of irrigation treatments and nitrogen applications on Napier grass planted in dry season as energy crop at Chiang Mai province.

Odum, H., Brown, M., Brandt-Williams, S., 2000. Folio# 1: Introduction and global budget. Handbook of Emergy Evaluation: A compendium of data for emergy computation issued in a series of folios. Center for Environmental Policy, Univ. of Florida, Gainesville.

Odum, H.T., 1996. Environmental accounting. Wiley.

Øi, L.E., Kvam, S.H.P., 2014. Comparison of Energy Consumption for Different CO 2 Absorption Configurations Using Different Simulation Tools. Energy Procedia 63, 1186-1195.

Owens, J., 1997. Life□cycle assessment: Constraints on moving from inventory to impact assessment. Journal of industrial ecology 1, 37-49.

Pandey, A., 2011. Biofuels: alternative feedstocks and conversion processes. Academic Press.

Pansak, W., Hilger, T., Dercon, G., Kongkaew, T., Cadisch, G., 2008. Changes in the relationship between soil erosion and N loss pathways after establishing soil conservation systems in uplands of Northeast Thailand. Agriculture, Ecosystems & Environment 128, 167-176.

Paoli, C., Vassallo, P., Fabiano, M., 2008. Solar power: an approach to transformity evaluation. Ecological engineering 34, 191-206.

Patrizi, N., Pulselli, F.M., Morandi, F., Bastianoni, S., 2015. Evaluation of the emergy investment needed for bioethanol production in a biorefinery using residual resources and energy. Journal of Cleaner Production 96, 549-556.

Pereira, C.L., Ortega, E., 2010. Sustainability assessment of large-scale ethanol production from sugarcane. Journal of Cleaner Production 18, 77-82.

Pimentel, D., Patzek, T.W., 2008. Biofuels, solar and wind as renewable energy systems. Benefits and risks. New York: Springer.

Plaza, M., González, A., Pevida, C., Pis, J., Rubiera, F., 2012. Valorisation of spent coffee grounds as CO 2 adsorbents for postcombustion capture applications. Applied energy 99, 272-279.

Preciado, J.E., Ortiz-Martinez, J.J., Gonzalez-Rivera, J.C., Sierra-Ramirez, R., Gordillo, G., 2012. Simulation of Synthesis Gas Production from Steam Oxygen Gasification of Colombian Coal Using Aspen Plus®. Energies 5, 4924-4940.

Ptasinski, K.J., Prins, M.J., Pierik, A., 2007. Exergetic evaluation of biomass gasification. Energy 32, 568-574.

Rekha, P., Sharma, V., Mohanty, P., 2016. Synthesis of cyclophosphazene bridged mesoporous organosilicas for CO 2 capture and Cr (VI) removal. Microporous and Mesoporous Materials 219, 93-102.

Ren, J., Manzardo, A., Mazzi, A., Fedele, A., Scipioni, A., 2013. Emergy analysis and sustainability efficiency analysis of different crop-based biodiesel in life cycle perspective. The Scientific World Journal 2013.

Saidur, R., BoroumandJazi, G., Mekhilef, S., Mohammed, H., 2012. A review on exergy analysis of biomass based fuels. Renewable and Sustainable Energy Reviews 16, 1217-1222.

Sclater, J., Jaupart, C., Galson, D., 1980. The heat flow through oceanic and continental crust and the heat loss of the Earth. Reviews of Geophysics 18, 269-311.

Seo, Y., Jo, S.-H., Ryu, H.-J., Dal Bae, H., Ryu, C.K., Yi, C.-K., 2007. Effect of water pretreatment on CO2 capture using a potassium-based solid sorbent in a bubbling fluidized bed reactor. Korean Journal of Chemical Engineering 24, 457-460.

Sha, S., Hurme, M., 2012. Emergy evaluation of combined heat and power plant processes. Applied Thermal Engineering 43, 67-74.

Sha, S., Losowska, M., Hurme, M., 2011. Renewable Energy Based Environmental Accounting of Heat, Power and Steel Production. Chem. Eng 25, 995.

Sheng, C., Azevedo, J., 2005. Estimating the higher heating value of biomass fuels from basic analysis data. Biomass and Bioenergy 28, 499-507.

Sims, R.E., Rogner, H.-H., Gregory, K., 2003. Carbon emission and mitigation cost comparisons between fossil fuel, nuclear and renewable energy resources for electricity generation. Energy policy 31, 1315-1326.

Singh, D., Croiset, E., Douglas, P.L., Douglas, M.A., 2003a. Techno-economic study of CO2 capture from an existing coal-fired power plant: MEA scrubbing vs. O2/CO2 recycle combustion. Energy conversion and Management 44, 3073-3091.

Singh, D., Croiset, E., Douglas, P.L., Douglas, M.A., 2003b. Techno-economic study of CO 2 capture from an existing coal-fired power plant: MEA scrubbing vs. O 2/CO 2 recycle combustion. Energy conversion and Management 44, 3073-3091.

Swanson, R.M., Platon, A., Satrio, J.A., Brown, R.C., 2010. Techno-economic analysis of biomass-to-liquids production based on gasification. Fuel 89, S11-S19.

Tarjan, R., 1972. Depth-first search and linear graph algorithms. SIAM journal on computing 1, 146-160.

Tassinari, C., Bonilla, S., Agostinho, F., Almeida, C., Giannetti, B., 2016. Evaluation of two hydropower plants in Brazil: using emergy for exploring regional possibilities. Journal of Cleaner Production 122, 78-86.

Tennenbaum, S.E., 1988. Network energy expenditures for subsystem production.

Tennenbaum, S.E., 2015. Emergy and co-emergy. Ecological Modelling 315, 116-134.

Tilman, D., Socolow, R., Foley, J.A., Hill, J., Larson, E., Lynd, L., Pacala, S., Reilly, J., Searchinger, T., Somerville, C., 2009. Beneficial biofuels—the food, energy, and environment trilemma. Science 325, 270-271.

Valverde, J., Raganati, F., Quintanilla, M., Ebri, J., Ammendola, P., Chirone, R., 2013. Enhancement of CO 2 capture at Ca-looping conditions by high-intensity acoustic fields. Applied energy 111, 538-549.

Yang, Q., Chen, G., Liao, S., Zhao, Y., Peng, H., Chen, H., 2013. Environmental sustainability of wind power: an emergy analysis of a Chinese wind farm. Renewable and Sustainable Energy Reviews 25, 229-239.

Yincheng, G., Zhenqi, N., Wenyi, L., 2011. Comparison of removal efficiencies of carbon dioxide between aqueous ammonia and NaOH solution in a fine spray column. Energy Procedia 4, 512-518.

Zarbá, L., Brown, M.T., 2015. Cycling emergy: computing emergy in trophic networks. Ecological Modelling 315, 37-45.

Zhai, H., Rubin, E., 2012. Membrane-based CO2 Capture Systems for Coal-fired Power Plants. NETL-DOE Report.

Zhang, L., Pang, M., Wang, C., Ulgiati, S., 2016. Environmental sustainability of small hydropower schemes in Tibet: An emergy-based comparative analysis. Journal of Cleaner Production 135, 97-104.

Zhang, M., Wang, Z., Xu, C., Jiang, H., 2012. Embodied energy and emergy analyses of a concentrating solar power (CSP) system. Energy Policy 42, 232-238.

APPENDIX

Appendix A
EMERGY ALGEBRA MATLAB CODE

MAIN MFILE:

```
filename1 ='SumM.xlsx';
send=500; %itelation no.
SourceP=find(sum(M,1)==0);
pSource =setdiff(SourceP,SubsPosition);
nSource =numel(pSource);
S=1*ones(1,nSource);
for hh=1:nSource
    Sou=S(hh); %emergy of source hh
    Cs=pSource(hh); %source hh
    cosplitposition
    pathfinder
    Pathz{hh}=Path;
    RRz{hh}=RR;
    TFz{hh}=tf;
    WFz{hh}=wf;
    Rz{hh}=R;
    Itel=0;
 for kk=1:nPathG
        Arc=Pa{kk};
        EmCal1
        EmWt(Arc(1),Arc(2))=EmWtX;
        EmWtY=EmWt;
  if sx<send
            Itel2=1;
  else
            Itel2=0;
  end
        Itel=Itel+Itel2;
 end

 if Itel==kk
        IsItelationDone='yes'
 else
     IsItelationDone='No'
 end
  if ISMn==1
        EmWt(Dsou,:)=EmWt(end,:);
        EmWt(end,:)=[];
        EmWt(:,end)=[];
 end

    EmergyS{hh}=S(hh)*EmWt;

end
for t=1:numel(EmergyS)
 if t==1
        EmergyFinal=EmergyS{t};
```

```
 else
        EmergyFinal=EmergyFinal+EmergyS{t};
 end
end
```

SUB-MFILE 1:

cosplitposition.m

```
Sz=size(M);
zSqu=zeros(Sz(1)+1);
zCol=zeros(Sz(1),1);
zRow=zeros(1,Sz(1)+1);
Dsou=Cs;
nC=numel(find(M(Cs,:)>0));
if nC==1
    ISMn=0; %indicates if source send to >1 sink for further Em
flow calculations
    Mn=M;
else%if source send to >1 sink insert additional block to 'M'
    ISMn=1; %indicates if source send to >1 sink for further Em
flow calculations
    zSqu(1:end-1,1:end-1)=M;
  Mn =zSqu;
    Mn(end,:)=Mn(Dsou,:);
    Mn(Dsou,:)=0;
    Mn(Dsou,end)=1;
end
P=sum(Mn,2); %sum of each row
PP=find(sum(Mn~=0,2)>1); %find x-axis position of non-zero elements
(split/co-prod.)
PN=find(sum(Mn~=0,2)<1); %find x-axis position of non-zero elements (one
product/sinks)
CoPx=find(P>1.01); %find x-axis position of co-products
SpPx=setdiff(PP,CoPx); %find x-axis position of splits
 CoPy=find(Mn(CoPx,:)>0); %find y-axis position of co-products
 co=1;
for cp0=1:numel(CoPx)
    CoPy=find(Mn(CoPx(cp0),:)>0);
 for cp1=1:numel(CoPy)
        copro(co,1)=CoPx(cp0);
        copro(co,2)=CoPy(cp1);
        co=co+1;
 end
end
   SpPy=find(Mn(SpPx,:)>0); %find y-axis position of splits
 sp=1;
for cp0=1:numel(SpPx)
    SpPy=find(Mn(SpPx(cp0),:)>0);
```

```
 for cp1=1:numel(SpPy)
        split(sp,1)=SpPx(cp0);
        split(sp,2)=SpPy(cp1);
        sp=sp+1;
 end
end
Sz=size(Mn);
Em=zeros(Sz(1));
EmWt=zeros(Sz(1));
W1=zeros(Sz(1));
W2=zeros(Sz(1));
PCopro=copro; %3
PSplit=split; %10
Py=sum(Mn,1); %sum.of each col
SiPx=find(P==0);
SiPy=find(Py~=0);
PSink=intersect(SiPx,SiPy);
nSink=numel(PSink);
```

SUB-MFILE 2:

Pathfinder.m

```
RR=[];
R=[];
T=[];
Path=[];
nPRRz=0;
PRRz=[];

[X,Y,v]=find(Mn>0); %find X,Y position of non-zero elements
PathG=[X Y];
nPathG=numel(X);
for ii=1:nPathG
    Pa{ii}=[X(ii) Y(ii)]; %Pa =Arcs
end
%Cnew
C=find(X==pSource(hh));
f=1;
g=1;
h=1;
aa=0;
Q=Pa{C};
RR{g,h}=Q;
h=h+1;
path1
nRR=numel(RR);
[nRRx nRRy]=size(RR);
tf=zeros(nRRx,nRRy);
wf=zeros(nRRx,nRRy);
R=zeros(nRRx,nRRy);
```

```
u=1;
for tt=1:nRR
    T=isempty(RR{tt});
 if T==0
        Path{u,1}=RR{tt};
        u=u+1;
        tf(tt)=1;
        wf(tt)=Mn(RR{tt}(end-1),RR{tt}(end));
        Rco=ismember([RR{tt}(end-1) RR{tt}(end)],PCopro,'rows');
        Rsp=ismember([RR{tt}(end-1) RR{tt}(end)],PSplit,'rows');
        R(tt)=3*Rco+10*Rsp;
 else
        tf(tt)=0;
        wf(tt)=0;
        R(tt)=0;
 end
end
```

SUB-MFILE 3:

Path1.m

```
Cs=Q(end);
Re=frepcheck(RR{g,h-1},Cs); %check repeat path
%position of paths to sinks
if numel(intersect(PSink,Cs))>0
    nPRRz=nPRRz+1;
 PRRz{nPRRz}=[g,h-1];
end
if Re>0
    g=g+1;
else
    C=find(X==Cs);
    nC=numel(C);
 if nC==0
        g=g+1;
 elseif nC==1
        Q=Pa{C};
        RR{g,h}=vertcat(RR{g,h-1},Q);
        h=h+1;
        path1
 else%nC>1; co-or split
```

```
       aa=aa+1;
       Qs{aa}=[g h-1];
       nCx(aa)=nC;
  for jj=1:nC
           QQ{aa,jj}=Pa{C(jj)};
  end
  for kk=1:nC+1
   if kk>nC
               aa=aa-1;
   else
               Q=QQ{aa,kk};
               Qss=RR{Qs{aa}(1),Qs{aa}(2)};
               h=Qs{aa}(2)+1;
               RR{g,h}=vertcat(Qss,Q);
               h=h+1;
               path1
               nC=nCx(aa);
   end
  end
 end
end
```

SUB-MFILE 4:

frepcheck.m

```
function Re=frepcheck(mat,Cs)
nmat=numel(mat(:,1));
for ii=1:nmat
    X(ii)=mat(ii,1);
end
Re=intersect(X,Cs);
```

SUB-MFILE 4:

EmCal1.m

```
RRz1=RRz{hh};
TFz1=TFz{hh};
WFz1=WFz{hh};
Rz1=Rz{hh};
[nRRx nRRy]=size(RRz1); %{1}
ttf=zeros(nRRx,nRRy);
B=find(TFz1==1); %{1}
[Bx By]=find(TFz1==1); %{1}
nB=numel(B);

for ll=1:nB
    RRend{ll}=RRz1{B(ll)}(end,:); %{1}
```

```
     ttf(B(ll))=isequal(Arc,RRend{ll});
end
[BBx BBy]=find(ttf==1);
BB=[BBx BBy];
nBB=numel(BBx);
if nBB~=0
%%%%%%
s=1;
st=[BBx BBy];
stx=BBx;
sty=BBy;
wfe=ones(nBB,1);
for w=1:nBB
    wfe(w,1)=WFz1(st(w,1),st(w,2));
end
s=s+1;
ss=1;
ssend=send;
while ss<ssend
    ss=ss+1;
m=find(stx==max(stx));
mm=[stx(m) sty(m)];
m=m(find(sty(m)==max(sty(m))));
mm=[stx(m) sty(m)];

if numel(m)>1
 [ml,~,mn]=unique(mm,'rows');
 if max(mn)>1
        sty(m,:)=sty(m,:)-1;
        sA=Bx(find(By==sty(m,:)));
        sB=stx(m,:);
        stx(m,:)=max(sA(sB>=sA));
        st(m,:)=[stx(m,:) sty(m)];
        wfe(:,s)=wfe(:,s-1);
        wfe(m,s)=wfe(m,s)*WFz1(st(m,1),st(m,2));
        s=s+1;
 elseif max(mn)==1
  if Rz1(ml(1),ml(2)+1)==10
            wfe(:,s)=wfe(:,s-1);
            wfe(m(1),s)=wfe(m(1),s)+wfe(m(2),s);
   for mo=1:numel(m)-1
                om=numel(m)-mo+1;
                stx(m(om))=[];
                sty(m(om))=[];
                st(m(om),:)=[];
                wfe(m(om),:)=[];
   end
            s=s+1;
  elseif Rz1(ml(1),ml(2)+1)==3 %'{1}'
```

```
            wfe(:,s)=wfe(:,s-1);
            wfe(m(1),s)=max(wfe(m(1),s),wfe(m(2),s));
            wfe(m(1),s-1)=wfe(m(1),s);
   for mo=1:numel(m)-1
                om=numel(m)-mo+1;
                stx(m(om))=[];
                sty(m(om))=[];
                st(m(om),:)=[];
                wfe(m(om),:)=[];
   end
  end

 end

else
 if stx+sty==2
        sx=ss;
        ss=ssend;
 else
    sty(m,:)=sty(m,:)-1;
    sA=Bx(find(By==sty(m,:)));
    sB=stx(m,:);
    stx(m,:)=max(sA(sB>=sA));
    st(m,:)=[stx(m,:) sty(m)];
    wfe(:,s)=wfe(:,s-1);
    wfe(m,s)=wfe(m,s)*WFz1(st(m,1),st(m,2));
    s=s+1;
 end
end


end

EmWtX=wfe(end);

else
    EmWtX=0;
    sx=0;
end
```

Appendix B

DETAILS OF EMERGY ACCOUNTING

Note from Table IV.1.

1. Cooling water consumption = (annual cost of cooling water) × (1/cost per m^3) × (density, kg/m^3) = (\$2,869,812/y) × (1/\$0.01/m^3) × (1000 kg/m^3)
   = 2.87×10^{11} kg/y
2. Make up MEA = (MEA consumption per ton CO_2 produced) × (annual tons CO_2 produced) = (1.6 kg MEA/ton CO_2 produced) × (2,960,000 tons CO_2 produced/y) = 4.74×10^{6} kg MEA/y
3. Additional chemicals = \$7,000,000/y
4. Natural gas = 12,564,747 MMBtu/y = 1.33×10^{16} J/y
5. Installation materials
   Fraction of machinery, assets section from total capital cost = (\$202,155,548) / (\$294,249,975) = 69%
   Amortised machinery, assets = (amortised capital cost) × (fraction of machinery, assets section) = (\$27,775,116/y) × 69% = \$19,082,054/y
6. Labor and Services
   1) L&S cost for plant startup: Fraction of L&S from total capital cost = (\$17,757,351 + \$26,291,636 + \$8,544,782 + \$5,152,430 + \$34,348,228) / (\$294,249,975) = 31%
   Amortised L&S = (amortised capital cost) × (fraction of L&S section) = (\$27,775,116/y) × (31%) = \$8,693,062/y
   2) Annual operating and maintenance cost = 4% of capital investment = \$11,769,999/y
   Total labor and services = \$20,463,061/y
7. CO_2 removal capacity = 1,923,685 tons CO_2 removed/y
   *Global EMR = (Global emergy budget / Global GDP) = (1.05×10^{26} sej/y) / (6.06×10^{13} \$/y) = 1.73×10^{12} sej/\$

Note from Table IV.2.

1. Solid sorbent cost per year= 12,780,666 $/y
2. Sodium hydroxide = (annual cost, $/y) / (unit cost, $/ton NaOH) = ($21,707/y) / ($499.75/ton NaOH) = 43.4 tons/y
3. Lime = (annual cost, $/y) / (unit cost, $/ton Lime) = ($67,126/y) / ($242.56/ton Lime) = 276.7 tons/y
4. Sulfuric acid = (annual cost, $/y) / (unit cost, $/ton H_2SO_4) = ($22,834/y) / ($160/ton H_2SO_4) = 142.7 tons/y
5. Makeup water = (annual cost, $/y) / (unit cost, $/kg water) = ($81,060/y + $40,530/y) / [($0.000378/gallon) × (264.17 gallon/m^3) × (1 m^3 water/1000 kg water)] = 1.22 × 10^9 kg/y
6. Natural gas = (annual cost, $/y) / (unit cost, $/J) = ($464,949/y) / [($7.41/MMBTU) × (1 MMBTU/ 1.055 × 10^9J) = 1.22 × 10^9 J/y
7. Power consumption = (annual cost, $/y) / (unit cost, $/J) = ($47,281,000/y) / [(0.72 ¢/kWh) × (1$/100¢) × (1 kWh/3,600,000 J)] = 2.42 × 10^{15} J/y
8. Material and equipment cost = (material and equipment cost of adsorption process) / (plant lifetime) = ($144,277,565) / (20 y) = 7.21×10^6 $/y
9. Labor (for set up plant) = (direct and indirect labor cost) / (plant lifetime) = ($180,827,924) / (20 y) = 9.04×10^6 $/y
10. Process operator labor = (22 full-time employee) × (annual full cost per full-time employee) = 22 × $135,000 = $2,970,000/y
    Maintenance labor = 1.5% of Initial material and equipment cost = 1.5% × (29,154,000 + 110,594,550) = $2,096,228/y
    Total labor cost = 2,970,000 + 2,096,228 = $5,066,228/y
11. CO_2 removal capacity = 2,635,065 tons CO_2 removed/y
    *Global EMR = (Global emergy budget / Global GDP) = (1.05×10^{26} sej/y) / (6.06×10^{13} $/y) = 1.73×$10^{12}$ sej/$

Note from Table IV.3.

1. Power consumption = (%Power use of gross power output) × (Gross power output) = 31.1% × (883.2×10^{6} J/s) × (8,000 h/y) × (3600 s/h) = 7.46×10^{15} J/y
2. Installation cost = (Cost of equipment per Gross power output, $/MWh) × (Gross power output, MWh/y) = ($57.6/MWh) × [(883.2 MW) × (8,000 hrs/y)] = $4.07×$10^{8}$/y
3. Process operator labor = (wage rate per hour, $/h) × (working hours per year, h/y) = ($34.65/h) × (8,000 h/y) = $277,200/y
4. CO_2 removal capacity = (CO_2 emission rate without CO_2 capture - CO_2 emission rate with CO_2 capture) = (0.816 – 0.122) × (883.2 MW) × (8,000 hrs/y) = 4.90×10^{9} kg/y

*Global EMR = (Global emergy budget / Global GDP) = (1.05×10^{26} sej/y) / (6.06×10^{13} $/y) = 1.73×10^{12} sej/$

Note from Table IV.4.

1 Biomass plantation stage

1.1 Solar energy = (average annual solar exposure) × (cross section area)

= (18 MJ/m^2/d × 365 d/y × 10^6 J/MJ) × (10^4 m^2/ha) = 6.57×10^{13} J/ha/y

average daily solar exposure in Thailand = 18 MJ/m^2/d (Chimres and Wongwises, 2016)

1.2 Energy of rain = (average rainfall) × (area) × (density) × (Gibbs free energy)

= 1.5 m/y × 10,000 m^2/ha × 1000 kg/m3 × 4940 J/kg = 7.41×10^{10} J/ha/y

Average annual rainfall in Thailand = 1,500 mm/yr (Thai Meteorological Department, 2016)

1.3 Geothermal energy = Total inland area (m^2) × Average heat flow (W/m^2) × (3.15×10^7 s/y) = (510 W/ha) × (3.15×10^7 s/y) = 1.61×10^{10} J/ha/y

Average heat flow per area in Nakhon Ratchasima, Thailand = 51 milliW/m^2 = 510 W/ha (Thai Meteorological Department, 2016)

1.4 Evapotranspiration of Napier grass = 8.82×10^9 g/ha/y (calculated in this study using FAO method)

Energy = (Evapotranspiration of Napier grass) × (Gibbs free energy of water) = (8.82×10^6 kg/ha/y) × (4770 J/kg) = 4.21×10^{10} J/ha/y

1.5 Energy of top soil loss = (soil loss) × (organic matter content in soil) × (energy content) = 2.5 t/ha/y × 0.0015 × 1.46×10^{10} J/t = 5.48×10^7 J/ha/y

Average soil loss from crops in Thailand = 2.5 t/ha/y (Pansak et al., 2008), organic matter in soil = 1.5% (Norsuwan et al., 2014),

Energy content = 14.6 GJ/t (Cohen et al., 2006).

1.6 Water, irrigation = (68 m^3/ha/y) × (1,000 kg/m^3) × (4,940 J/kg) = 3.36×10^8 J/ha/y

Average water supplied for irrigation = 68 m^3/ha/y (on-site data)

1.7 Napier rhizomes for planting = 550 kg/rai/7 y × (1 rai/0.16 ha) = 491.07 kg/ha/y

Initially, the crop planted can last for 7 y, prior to replanting with new crops, which require napier stem 500–600 kg/rai (on-site data)

The UEV calculation

Emergy flow of all inputs (except initial napier stem), Em$_0$ = 8.00×10^{19} sej/y

Total amount of napier grass as a product, M$_{\text{Napier,out}}$ = 2.63×10^8 kg/y

Total amount of napier grass as an input, M$_{\text{Napier,in}}$ = 1.72×10^6 kg/y

The UEVs of napier stem as a product and an input calculated by Eq. (8) = 3.06×10^{11} sej/kg

1.8 Fertilizers for growing (on-site data)

1) initial, 2nd week, 2nd month, fertilizer N/P/K 60 kg/rai/7 y= 53.57 kg/ha/y
2) after harvesting, nourishing with manure 10 kg/rai/time = 410 kg/rai/7 y= 366.07 kg/ha/y

			fraction	UEV (sej/kg)	%R
distributions: fertilizer NH_3	17.86	kg/ha/y	4%	3.65×10^{12}	0%
fertilizer P_2O_5	17.86	kg/ha/y	4%	8.33×10^{12}	0%
fertilizer K_2O_5	17.86	kg/ha/y	4%	2.35×10^{12}	0.01%
manure	366.07	kg/ha/y	87%	1.17×10^{13}	18%
Total fertilizers	419.64	kg/ha/y	average UEV	1.08×10^{13}, average %R	16%

1.9 Diesel consumption (diesel consumption rate for each machinery reffered from (Morandi et al., 2016))

1) for growing	Diesel cons. rate (L/h)	Efficiency (ha/h)	Frequency (times per 7 years)	Operating hs (h/ha/y)	Diesel consumption (kg/ha/y)	
Flattening: tractor 100 hp + roller packer	8.7	3	1	0.05	0.41	
Ploughing: tractor 130 hp + plough	22.86	0.9	1	0.16	3.63	
Harrowing: tractor 120 hp + rotary harrow	21.08	1.7	1	0.08	1.77	
Planting: tractor 110 hp + adapted potatoes planter	2.42	0.2	1	0.71	1.73	
Chiseling: tractor 120 hp + chisel	21.12	1.2	1	0.12	2.51	
					10.06	kg/ha/y

2) for harvesting	Diesel cons. rate (L/h)	Efficiency (ha/h)	Frequency (times per 7 years)	Operating hs (h/ha/y)	Diesel consumption (kg/ha/y)	
Cultivating: tractor 100 hp + cultivator	17.55	1.5	41	3.90	68.53	
Tractor 200 hp + trailer	17	1.8	41	3.25	55.32	
Harrowing: tractor 120 hp + rotary harrow	21.08	1.7	41	3.45	72.63	
					196.47	kg/ha/y

3) Diesel used (for transporting) = (biomass production rate per ha per year/t biomass per round) × (distance per round) × (diesel fuel economy) × (diesel density) = (75 t/ha/y / 3 t/round) × (56 km/round / 1.628 km/L) × (0.832 kg/L) = 715.48 kg/ha/y

Total diesel consumption (diesel energy content = 41.84 MJ/kg) = 3.86×10^{10} J/ha/y

1.10 Machinery data (Machinery data reffered from (Morandi et al., 2016))

Machinery for growing	Operators	Weight (kg)	Efficiency (ha/h)	Life span (hs)	Frequency (times per 7 years)	Operating h/ha/y	Diesel cons. (L/h)	Material d from total (kg/
Flattening: tractor 100 hp + roller packer	1	8,064	3	7,000	1	0.05	8.7	0.
Ploughing: tractor 130 hp + plough	1	9,220	0.9	7,000	1	0.16	22.86	0.
Harrowing: tractor 120 hp + rotary harrow	1	7,944	1.7	7,000	1	0.08	21.08	0.
Planting: tractor 110 hp + adapted potatoes planter	2	7,875	0.2	7,000	1	0.71	2.42	0.
Chiseling: tractor 120 hp + chisel	1	8,000	1.2	7,000	1	0.12	21.12	0.
Total	6							1.

Machinery for harvesting	Operators	Weight (kg)	Efficiency (ha/h)	Life span (hs)	Frequency (times per 7 years)	Operating h/ha/y	Diesel cons. (L/h)	Material d from total (kg/
Cultivating: tractor 100 hp + cultivator	1	8,064	1.5	7,000	41	3.90	17.55	4.
tractor 200 hp + trailer	1	17,900	1.8	7,000	41	3.25	17	8.
Harrowing: tractor 120 hp + rotary harrow	1	6,136	1.7	7,000	41	3.45	21.08	3.
Total	4							15.
							Total machinery	17.

UEV calculation of machine (Morandi et al., 2016)

Materials	**UEV (sej/kg)**	**%distributed to 1 kg tractor**	
Aluminum (kg)	5.78×10^{9}	3%	
Brass (kg)	2.17×10^{10}	0%	
Copper (kg)	1.95×10^{11}	1%	
Glass (kg)	7.03×10^{10}	1%	
Lead (kg)	4.81×10^{11}	2%	
Lubricant (kg)	2.55×10^{10}	13%	
Paint (kg)	7.88×10^{9}	1%	
Plastic (kg)	5.28×10^{9}	2%	
Rubber (kg)	7.22×10^{9}	19%	
Steel (kg)	8.60×10^{10}	57%	
Zinc (kg)	4.51×10^{9}	1%	
Weighted average UEV		6.90×10^{10}	sej/kg

1.11 Direct labor man-hours (approximation data)

Working hours = 5 h/d, price of labor = 350 baht/d = 70 baht/h = $10/d

Plantation = (6 person per hectare) × (5 d/7y) × (5 hours per person per day) = 21.4 h/ha/y

Weed removal by hand = (5 person per hectare) × (16 times per 7 years) × (5 hours per person per time) × (5 d/time) = 285.7 h/ha/y

Harvesting = (4 person per hectare per time) × (41 times per 7 years) × (5 hours per person per time) = 117.1 h/ha/y

Total <u>424.3</u> h/ha/y

The UEV calculation in term of man-hour; procedure referred from Kamp's study, based on Thailand agricultural system

Data report year 2008

Thailand emergy budget, α = 3.20×10^{24} sej/y (NEAD, 2010)

Total employed population = 3.83×10^{7} person

Total man-hour, γ = 5.31×10^{10} man-h/y

GDP distributed to people working in agricultural sector, β_1 = 8.8%*

GDP distributed to people working in industrial sector, β_1 = 48.0%*

GDP distributed to people working in service and other sector, β_1 = 43.2%*

Fraction of people working in agricultural sector, β_2 = 42.5%*

Fraction of people working in industrial sector, β_2 = 19.5%*

Fraction of people working in service and other sector, β_2 = 38.0%*

Average weekly working hours in agricultural sector, γ = 41.5 h/person/week**

Average weekly working hours in industrial sector, γ = 49.6 h/person/week**

Average weekly working hours in service and other sector, γ = 49.0 h/person/week**

*data reffered from (Aemkulwat, 2010)

**assumed that average working 46 weeks/y

Fraction of emergy to people working in agricultural sector, $\alpha\beta_1$ = 2.82×10^{23} sej/y

Fraction of emergy to people working in industrial sector, $\alpha\beta_1$ = 1.54×10^{24} sej/y

Fraction of emergy to people working in service and other sector, $\alpha\beta_1$ = 1.38×10^{24} sej/y

Fraction of works done by people in agricultural sector, $\gamma\beta_2$ = 3.11×10^{10} h/y

Fraction of works done by people in industrial sector, $\gamma\beta_2$ = 1.71×10^{10} h/y

Fraction of works done by people in service and other sector, $\gamma\beta_2$ = 3.29×10^{10} h/y

UEV of man-h (farmers), $\alpha\beta_1/\gamma\beta_2$ = 9.06×10^{12} sej/h

1.12	Indirect labor	consumption					
	Fertilizers (only N/P/K fertilizers)	53.57	kg/ha/y	0.46	\$/kg	24.5	\$/ha/y
	Diesel used (for transportation)	4.61×10^{10}	J/ha/y	2.46×10^{-8}	\$/J	1,134.3	\$/ha/y
	Machinery					34.9	\$/ha/y
					total	1,193.7	\$/ha/y

*Diesel price in Thailand 30 Baht/L /(0.832 kg/L) / (41.84 MJ/kg) / (1,000,000 J/MJ) = 2.46×10^{-8} \$/J

Machinery (for 5 ha basis); includings	Depreciation (\$/ha/yr)
(1) 1 2-wheels tractor 48,000 Baht*	13.71
(2) 3 selfpropelled machineries 69,000 Baht*	19.71
(3) buildings 25,000 Baht*	7.14

*data referred from (Liese et al., 2014)

The UEV calculation in term of EMR (referred from (Brown et al., 2011)).

Global emergy budget = 1.05×10^{26} sej/y

Global GDP = 6.06×10^{13} \$/y

Global EMR = (Global emergy budget / Global GDP) = 1.73×10^{12} sej/\$

Global %Renewable = 15%

1.13 Napier grass annual production rate = 70-80 t napier/ha/y □ 75 t/ha/y = 75,000 kg/ha/y

*ref : Energy Research and Development Institute Nakornping, Chiang Mai University

Napier grass energy content = 18 MJ/kg

Capacity = 30,000 kg/h = 262,980 kg/y

Area required = capacity (kg/h) × operating hours (hs/y) / production rate per area (kg/ha/y)

= (30,000 kg/h × 8,766 h/y) / (75,000 kg/ha/y) = 3,506 ha

Note from Table IV.5.

**Data from Note 2 to 7 were from ASPEN PLUS simulation.*

2 Gasification process (A100)

2.1 Reactants

1) Biomass	30,000	kg/h
2) Air	51,988	kg/h

Utilities

1) LP and MT steam from CHP	2.76×10^{10}	J/h

2.2 Installation materials (data from ASPEN ECONOMICS)

			Cost per y	
Purchased Equipment	1,312,100	$/20 y	65,605	$/y
Piping	83,699.4	$/20 y	4,185	$/y
Instrumentation	371,221	$/20 y	18,561	$/y
Electrical	730,095	$/20 y	36,505	$/y
Other	1,187,745	$/20 y	59,387	$/y
Total	3,684,861	$/20 y	184,243	$/y

2.3 Labor cost (data from ASPEN ECONOMICS)

Direct labor man-hour basis

Operator LV1		
Operators per shift	2	person
Operating Hours per Period	8,766	
LV1 man-hours	17,532	hrs/yr
Operator LV2	8,766	hrs/yr
Operator LV3		
Operators per shift	1	
Operating Hours per Period	8,766	
LV3 man-hours	8,766	hrs/yr
Total	35,064	hrs/yr

2.4 Indirect labor

Project indirect costs	1,000,104	$
Project lifetime	20	y
	50,005	$/y

2.5 Product(s)

1) Syngas	42,278	kg/h

Note from Table IV.6.

3 CHP process

3.1 Reactants

1) Syngas	42,278	kg/h
2) Air	33,488	kg/h

Utilities

1) Water (for steam production)	28,970	kg/h
water treated from water treating unit	19,397	kg/h
Makeup water (for steam production)	9,573	kg/h

3.2 Installation materials (data from ASPEN ECONOMICS) Cost per y

Purchased Equipment	3,731,400	$/20 y	186,570	$/y
Piping	2,026,440	$/20 y	101,322	$/y
Instrumentation	356,389	$/20 y	17,819	$/y
Electrical	728,779	$/20 y	36,438	$/y
Insulation	88567.1	$/20 y	4,428	$/y
Other	2,084,013	$/20 y	104,201	$/y
Total	<u>9,015,589</u>	$/20 y	<u>450,779</u>	$/y

3.3 Labor cost (data from ASPEN ECONOMICS)

Direct labor man-hour basis

Operator LV1		
Operators per shift	1	person
Operating Hours per Period	8,766	
LV1 man-hours	8,766	hrs/yr
Operator LV2	8,766	hrs/yr
Operator LV3		
Operators per shift	1	
Operating Hours per Period	8,766	
LV3 man-hours	8,766	hrs/yr
Total	<u>26,298</u>	hrs/yr

3.4 Indirect labor

Project indirect costs	7,162,090	$
Project lifetime	20	y
	<u>358,104</u>	$/y

3.5 Product(s)

1) Electricity (total) 10,806 kW = 3.89×10^{10} J/h

Consumed by

Syngas cleaning process	7.86×10^{8}	J/h
Fuel synthesis process	3.53×10^{9}	J/h
Methanol synthesis	7.06×10^{9}	J/h
Total electricity consumption	8.29×10^{9}	J/h
Electricity (Net)	3.06×10^{10}	J/h

2) Steam (HP steam 510 oC; 62bar) 2.65×10^{6} J/s

3) Steam (MP steam 200 oC; 28bar) 7.67×10^{6} J/s

4) Steam (MT steam 250 oC; 25bar) 1.35×10^{7} J/s (all used up)

<u>Note from Table IV.7.</u>

4 Gas cleaning process

4.1 Reactants

1) Copper-zinc catalyt 8 $/lb

Applied on first operation year and then every thee years115,000$ for 3-y replacement

Cost of catalyst each year = 38,333 $/y*considered as indirect labor

Amount of catalyst each year = 4,792 lb/y or 2,173 kg/y

The UEV calculation

UEV of Copper = 7.43×10^{13} sej/kg

UEV of Zinc = 5.46×10^{13} sej/kg

Assume that copper-zinc catalyt UEV equal to the avg. between copper and zinc UEVs

UEV of Copper-zinc catalyst =	6.44×10^{13}	sej/kg
2) Syngas (Cooled)	42,278	kg/h
3) Oxygen	91	kg/h
4) Makeup MEA	3	kg/h
5) MT steam from CHP	4.55×10^{10}	J/h
Utilities		
1) Cooling water	282	kg/h
2) Electricity from A200	8.76×10^{8}	J/h

4.2 Installation materials (data from ASPEN ECONOMICS)

			Cost per y	
Purchased equipment	839,900	$/20 y	41,995	$/y
Piping	579,431	$/20 y	28,972	$/y
Steel	77,049	$/20 y	3,852	$/y
Instrumentation	746,770	$/20 y	37,338	$/y
Electrical	737,995	$/20 y	36,900	$/y
Insulation	141,706	$/20 y	7,085	$/y
Other	2,424,059	$/20 y	121,203	$/y
Total cost	5,546,910	$/20 y	277,345	$/y

4.3 Labor cost (data from ASPEN ECONOMICS)

Direct labor man-hour basis

Operator LV1		
Operators per shift	2	person
Operating Hours per Period	8,766	
LV1 man-hours	17,532	hrs/yr
Operator LV2	8,766	hrs/yr
Operator LV3		
Operators per shift	2	
Operating Hours per Period	8,766	
LV3 man-hours	17,532	hrs/yr
Total	43,830	hrs/yr

4.4 Indirect labor

Project indirect costs	5,348,170	$
Project lifetime	20	y
Accounted for	267,408	$/y
Total indirect labor	305,742	$/y

Note from Table IV.8.

5 Fuel synthesis process

5.1 Reactants

1) Cobalt catalyst	15	$/lb

Applied on first operation year and then every thee years

$7,687,000 for 3-y replacement

Cost of catalyst each year = 2,562,333 $/y *considered as indirect labor

Amount of catalyst each year = 170,822lb/y or 77,484 kg/y

1) Syngas (Cleaned)	42,278	kg/h
2) MT steam from CHP	2.21×10^9	J/h

Utilities

1) Electricity from A200	3.53×10^8	J/h

5.2 Installation materials (data from ASPEN ECONOMICS)

			Cost per y	
Purchased equipment	928,500	$/20 y	46,425	$/y
Piping	282,709	$/20 y	14,135	$/y
Steel	32,098	$/20 y	1,605	$/y
Instrumentation	529,939	$/20 y	26,497	$/y
Electrical	707,055	$/20 y	35,353	$/y
Insulation	53,083	$/20 y	2,654	$/y
Other	1,869,179	$/20 y	93,459	$/y
Total cost	4,402,564	$/20 y	220,128	$/y

5.3 Labor cost (data from ASPEN ECONOMICS)

Direct labor man-hour basis

Operator LV1		
Operators per shift	2	person
Operating Hours per Period	8,766	
LV1 man-hours	17,532	hrs/yr
Operator LV2	8,766	hrs/yr
Operator LV3		
Operators per shift	2	
Operating Hours per Period	8,766	
LV3 man-hours	17,532	hrs/yr
Total	43,830	hrs/yr

5.4 Indirect labor

Project indirect costs	4,527,360	$
Project lifetime	20	y
Accounted for	226,368	$/y
Total indirect labor	2,788,701	$/y

5.5 Product(s)

1) Hydrogen (to HDP)	92	kg/h
2) Liquid fuel (to HDP)	1,962	kg/h
3) Gas products (to methanol synthesis)	13,749	kg/h

Note from Table IV.9.

6 Hydroprocessing process (HDP)

6.1 Reactants

1) Hydrogen	92	kg/h
2) Liquid fuel	1,962	kg/h

6.2 Installation materials (data from ASPEN ECONOMICS)

			Cost per y	
Purchased equipment	733,000	$/20 y	36,650	$/y
Piping	104,301	$/20 y	5,215	$/y
Steel	36,290	$/20 y	1,814	$/y

Instrumentation	390,707	$/20 y	19,535	$/y
Electrical	529,154	$/20 y	26,458	$/y
Insulation	53,330	$/20 y	2,666	$/y
Other	1,305,217	$/20 y	65,261	$/y
Total cost	3,151,999	$/20 y	157,600	$/y

6.3 Labor cost (data from ASPEN ECONOMICS)

Direct labor man-hour basis		
Operator LV1		
Operators per shift	2	person
Operating Hours per Period	8,766	
LV1 man-hours	17,532	hrs/yr
Operator LV2	8,766	hrs/yr
Operator LV3		
Operators per shift	2	
Operating Hours per Period	8,766	
LV3 man-hours	17,532	hrs/yr
Total	43,830	hrs/yr

6.4 Indirect labor

Project indirect costs	3,958,150	$
Project lifetime	20	y
	197,908	$/y

6.5 Product(s)

1) Liquid fuels (2 grades)	1,920	kg/h		
2) Fuel gas (to A200)	134	kg/h		
LHV of liquid fuels calculated from Aspen plus			Amount(kg/h)	%
C5-C12	47,439	kJ/kg	1,011	53%
C12+	46,956	kJ/kg	910	47%
average LHV	37,710	kJ/kg		

Note from Table IV.10.

7 Methanol synthesis

7.1 Reactants

1) Fuel gas	134	kg/h
2) MT steam	8.38×10^{8}	J/h
Utilities		
1) Cooling water	1.67×10^{9}	kg/h

7.2 Installation materials (data from ASPEN ECONOMICS)

			Cost per y	
Purchased equipment	7,538,100	$/20 y	376,905	$/y
Piping	889,865	$/20 y	44,493	$/y
Steel	44,244	$/20 y	2,212	$/y
Instrumentation	1,218,150	$/20 y	60,907	$/y
Electrical	867,830	$/20 y	43,391	$/y
Insulation	120,460	$/20 y	6,023	$/y
Other	4,826,443	$/20 y	241,322	$/y
Total cost	15,505,092	$/20 y	775,255	$/y

7.3 Labor cost (data from ASPEN ECONOMICS)

Direct labor man-hour basis

Operator LV1		
Operators per shift	4	person
Operating Hours per Period	8,766	
LV1 man-hours	35,064	hrs/yr
Operator LV2	8,766	hrs/yr
Operator LV3		
Operators per shift	4	
Operating Hours per Period	8,766	
LV3 man-hours	35,064	hrs/yr
Total	<u>78,894</u>	hrs/yr

7.4 Indirect labor

Project indirect costs	22,492,600	$
Project lifetime	20	y
1,124,630	$/y	

7.5 Product(s)

1) Methanol	7,603	kg/h
(energy content = 30.29 MJ/kg)	2.30×10^{11}	J/h

<u>Note from Table IV.11.</u>

8 Waste water treatment process

Calculation data refered from (Arbault et al., 2013) which was assumed that the organic matter from the process has the same concentration as the reference's.

*Waste water produced in this study =20,418 kg ww/h = 1.79×10^8 kg ww/y

assume 95% water recovered 19,397 kg treated water/h

		Amount	Units		
	Capacity	3.71×10^7	m^3		
8.1	Electricity	1.91×10^7	kWh	3.32×10^{11}	J/y
8.2	Activated carbon	1.52×10^5	kg	733.3	kg/y
8.3	Regenerated activated carbon	9.78×10^4	kg	471.8	kg/y
8.4	Acrylic acid	6.07×10^3	kg	29.3	kg/y
8.5	Al2SO4	8.79×10^5	kg	4,240.6	kg/y
8.6	Cl2 gas	4.91×10^4	kg	236.9	kg/y
8.7	Lime	2.63×10^5	kg	1,268.8	kg/y
8.8	H3PO4, 85%	3.06×10^3	kg	14.8	kg/y
8.9	Caustic soda	4.09×10^5	kg	1,973.2	kg/y
8.10	H2SO4	2.43×10^5	kg	1,172.3	kg/y
	Labor and services (S)				
8.11	Purchased inputs and labor	2.00×10^6	Euro	1.08×10^4	$/y
8.12	Material transport (truck)	5.37×10^3	tkm	25.9	tkm/y

Appendix C

SIMULATION RESULTS: PROCESS FLOW DIAGRAM

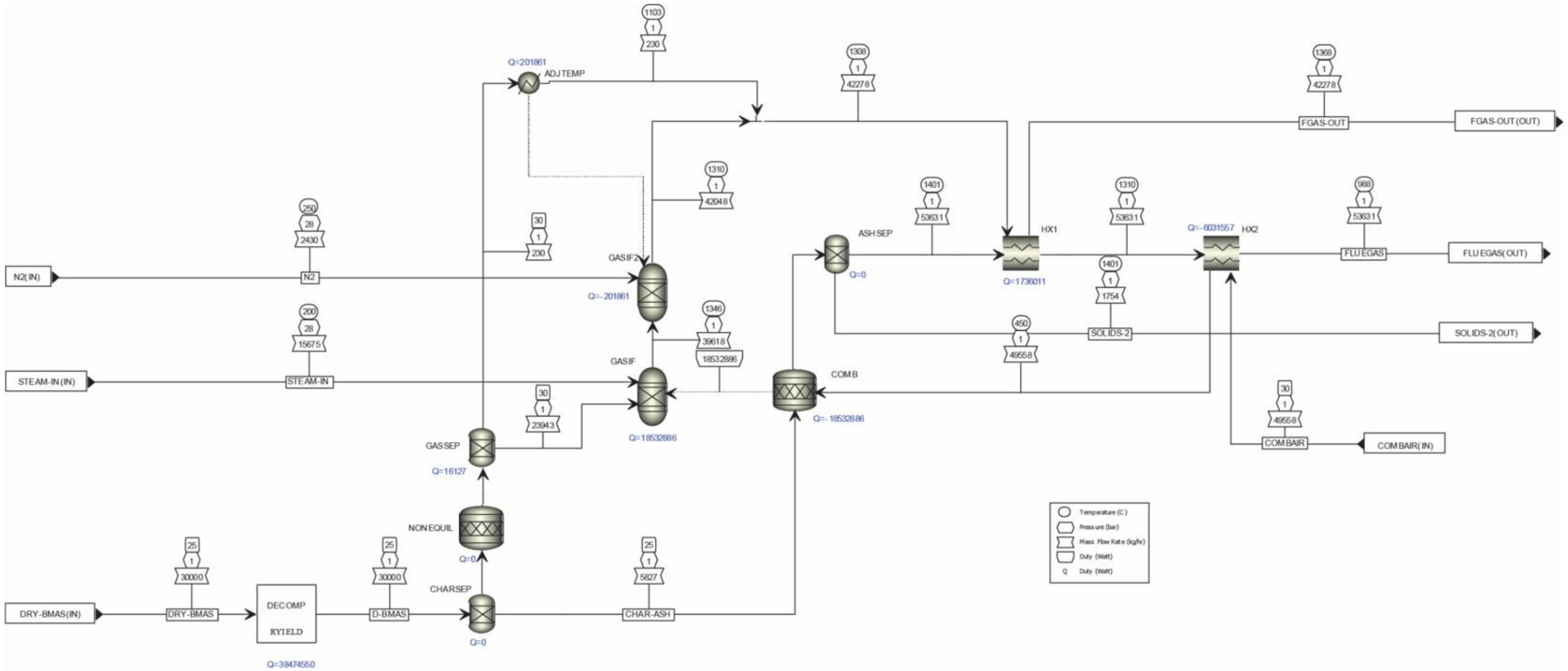

Figure C.1. Process flow diagram of gasification

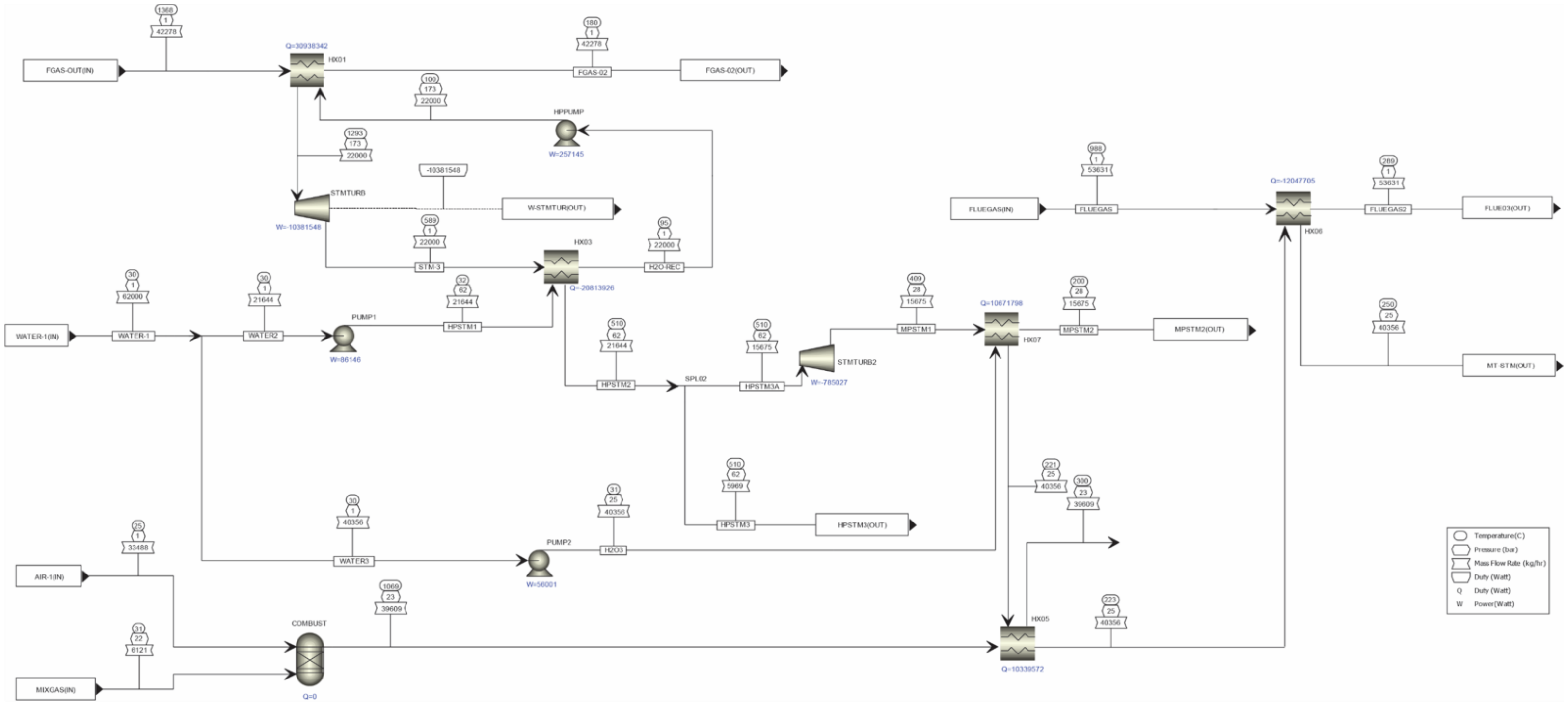

Figure C.2. Process flow diagram of CHP

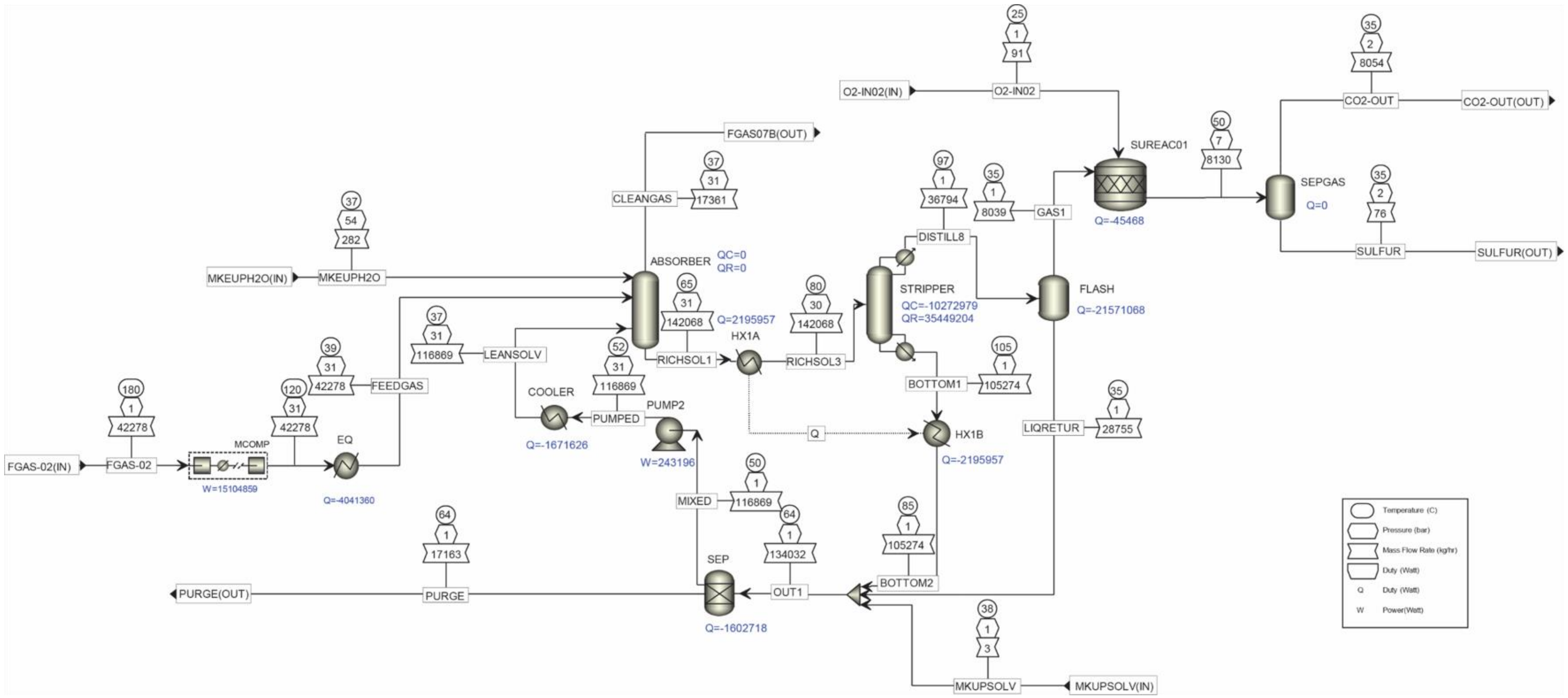

Figure C.3. Process flow diagram of syngas cleaning

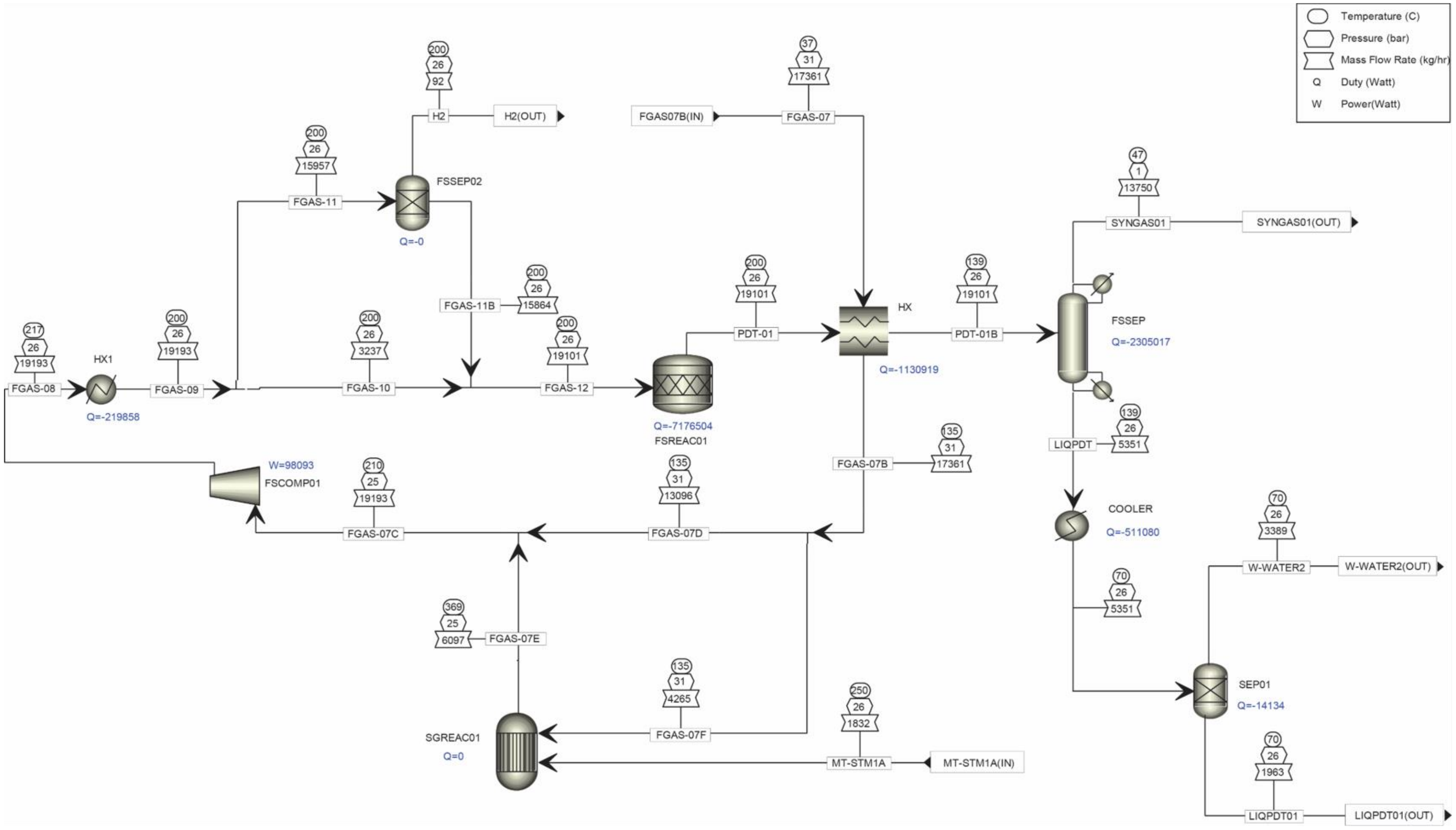

Figure C.4. **Process flow diagram of fuelsynthesis**

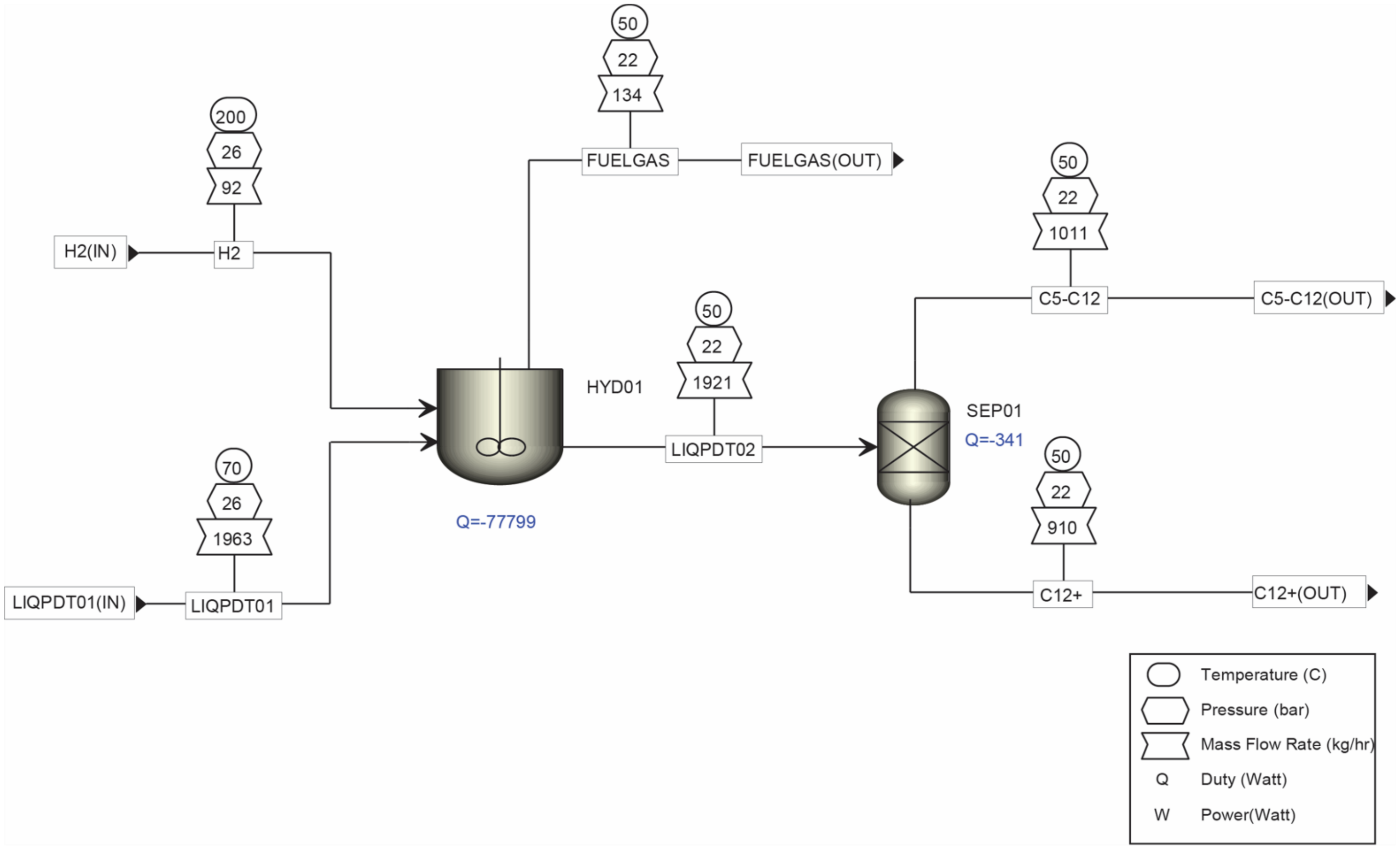

Figure C.5. **Process flow diagram of HDP**

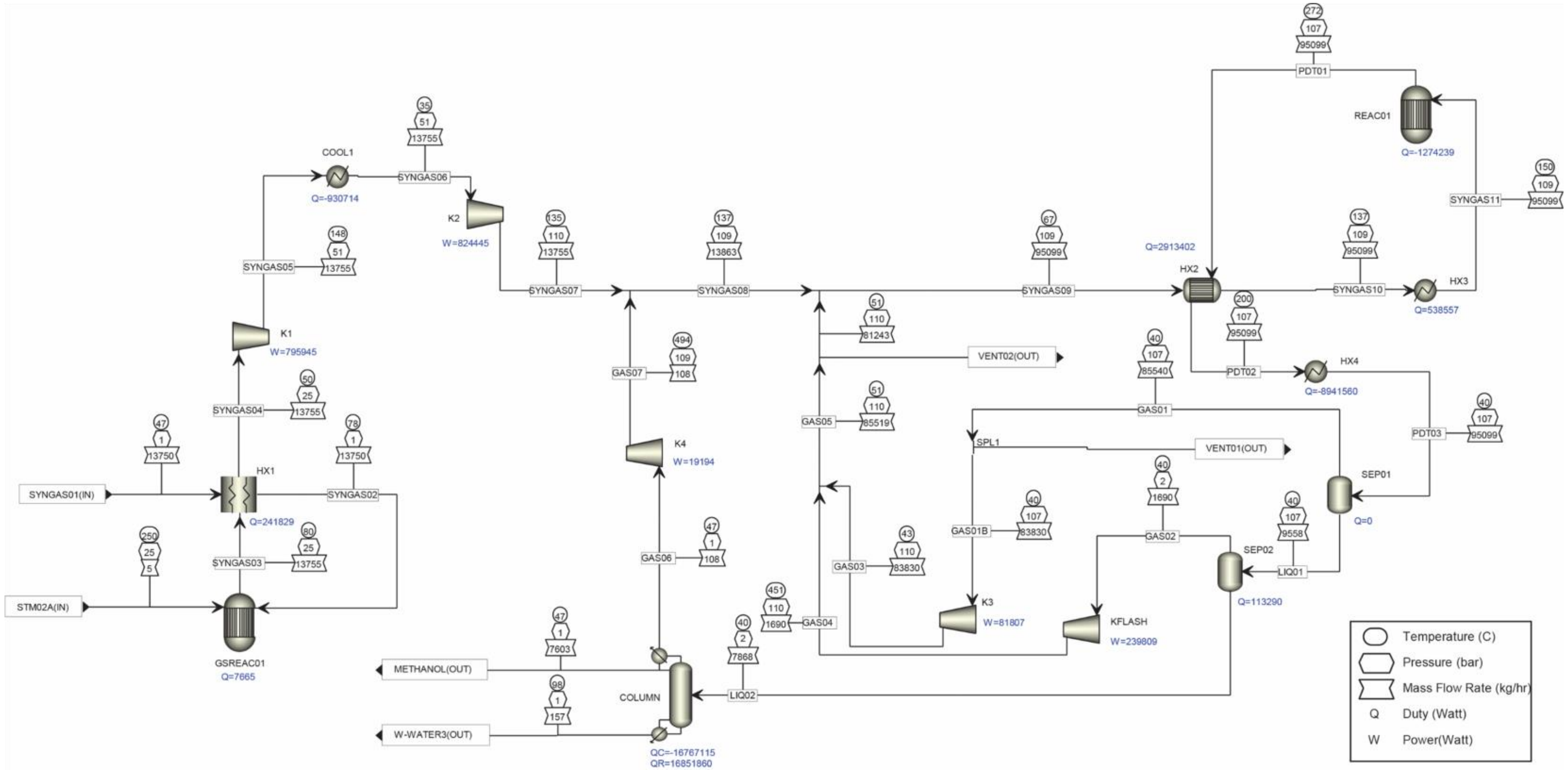

Figure C.6. Process flow diagram of methanol synthesis

SIMULATION RESULTS: STREAM TABLE

Table C.1. Stream table of gasification

	Units	COMBAIR	COMB-AIR	D-BMAS	ELEM2	ELEM3	FGAS-2	FGAS-OUT	FLUE01	FLUE2
Temperature	C	30	450	25	25	30	1,308	1,368	1,401	1,310
Pressure	bar	1	1	1	1	1	1	1	1	1
Mass Flows	kg/hr	49,558	49,558	30,000	24,173	23,943	42,278	42,278	53,631	53,631
Average MW		29	29	13	13	13	17	17	31	31
Mole Flows	kmol/hr	1,718	1,718	1,277	1,277	1,250	2,530	2,530	1,718	1,718
H2O	kmol/hr	0	0	216	216	216	937	937	0	0
CO	kmol/hr	0	0	0	0	0	470	470	0	0
H2	kmol/hr	0	0	715	715	695	845	845	0	0
CO2	kmol/hr	0	0	0	0	0	178	178	339	339
O2	kmol/hr	361	361	338	338	338	0	0	22	22
N2	kmol/hr	1,357	1,357	6	6	0	87	87	1,357	1,357
AR	kmol/hr	0	0	0	0	0	0	0	0	0
CL2	kmol/hr	0	0	0	0	0	0	0	0	0
NO2	kmol/hr	0	0	0	0	0	0	0	0	0
H2S	kmol/hr	0	0	0	0	0	0	0	0	0
NH3	kmol/hr	0	0	0	0	0	13	13	0	0

Table C.1. (cont.) Stream table of gasification

	Units	FLUEGAS	GASOUT	GASOUT2	N2	NONEQ1	NONEQ2	STEAM-IN	TOASHSEP	TOGASSEP
Temperature	C	988	1,346	1,310	250	30	1,103	200	1,401	30
Pressure	bar	1	1	1	28	1	1	28	1	1
Mass Flows	kg/hr	53,631	39,618	42,048	2,430	230	230	15,675	55,385	24,173
Average MW		31	16	17	28	17	17	18	31	13
Mole Flows	kmol/hr	1,718	2,430	2,517	87	13	13	870	1,718	1,264
H2O	kmol/hr	0	942	937	0	0	0	870	0	216
CO	kmol/hr	0	475	470	0	0	0	0	0	0
H2	kmol/hr	0	840	845	0	0	0	0	0	695
CO2	kmol/hr	339	173	178	0	0	0	0	339	0
O2	kmol/hr	22	0	0	0	0	0	0	22	338
N2	kmol/hr	1,357	0	87	87	0	0	0	1,357	0
AR	kmol/hr	0	0	0	0	0	0	0	0	0
CL2	kmol/hr	0	0	0	0	0	0	0	0	0
NO2	kmol/hr	0	0	0	0	0	0	0	0	0
H2S	kmol/hr	0	0	0	0	0	0	0	0	0
NH3	kmol/hr	0	0	0	0	13	13	0	0	13

Table C.2. Stream table of CHP

	Units	AIR-1	FGAS-02	FGAS-OUT	FLUE01	FLUE02	FLUE03	FLUEGAS	FLUEGAS2	H2O3
Temperature	C	25	180	1,368	1,069	300	294	988	289	31
Pressure	bar	1	1	1	23	23	1	1	1	25
Mass Flows	kg/hr	33,488	42,278	42,278	39,609	39,609	93,240	53,631	53,631	40,356
Average MW		29	17	17	29	29	30	31	31	18
Mole Flows	kmol/hr	1,161	2,530	2,530	1,381	1,381	3,099	1,718	1,718	2,240
H2O	kmol/hr	0	937	937	133	133	133	0	0	2,240
CO	kmol/hr	0	470	470	0	0	0	0	0	0
H2	kmol/hr	0	845	845	0	0	0	0	0	0
CO2	kmol/hr	0	178	178	105	105	444	339	339	0
O2	kmol/hr	244	0	0	139	139	161	22	22	0
N2	kmol/hr	917	87	87	1,004	1,004	2,361	1,357	1,357	0
AR	kmol/hr	0	0	0	0	0	0	0	0	0
CL2	kmol/hr	0	0	0	0	0	0	0	0	0
H2S	kmol/hr	0	0	0	0	0	0	0	0	0
NH3	kmol/hr	0	13	13	0	0	0	0	0	0
MEA	kmol/hr	0	0	0	0	0	0	0	0	0
METHANOL	kmol/hr	0	0	0	0	0	0	0	0	0
CH4	kmol/hr	0	0	0	0	0	0	0	0	0
C2H6	kmol/hr	0	0	0	0	0	0	0	0	0
C3	kmol/hr	0	0	0	0	0	0	0	0	0
C4	kmol/hr	0	0	0	0	0	0	0	0	0
C5	kmol/hr	0	0	0	0	0	0	0	0	0
C6	kmol/hr	0	0	0	0	0	0	0	0	0

Table C.2. (cont.) Stream table of CHP

	Units	H2O-IN2	H2O-REC	HPSTM1	HPSTM2	HPSTM3	HPSTM3A	MIXGAS	MPSTM1	MPSTM2
Temperature	C	95	95	32	510	510	510	31	409	200
Pressure	bar	1	1	62	62	62	62	22	28	28
Mass Flows	kg/hr	22,000	22,000	21,644	21,644	5,969	15,675	6,121	15,675	15,675
Average MW		18	18	18	18	18	18	22	18	18
Mole Flows	kmol/hr	1,221	1,221	1,201	1,201	331	870	278	870	870
H2O	kmol/hr	1,221	1,221	1,201	1,201	331	870	0	870	870
CO	kmol/hr	0	0	0	0	0	0	31	0	0
H2	kmol/hr	0	0	0	0	0	0	99	0	0
CO2	kmol/hr	0	0	0	0	0	0	51	0	0
O2	kmol/hr	0	0	0	0	0	0	0	0	0
N2	kmol/hr	0	0	0	0	0	0	87	0	0
AR	kmol/hr	0	0	0	0	0	0	0	0	0
CL2	kmol/hr	0	0	0	0	0	0	0	0	0
H2S	kmol/hr	0	0	0	0	0	0	0	0	0
NH3	kmol/hr	0	0	0	0	0	0	0	0	0
MEA	kmol/hr	0	0	0	0	0	0	0	0	0
METHANOL	kmol/hr	0	0	0	0	0	0	2	0	0
CH4	kmol/hr	0	0	0	0	0	0	2	0	0
C2H6	kmol/hr	0	0	0	0	0	0	2	0	0
C3	kmol/hr	0	0	0	0	0	0	2	0	0
C4	kmol/hr	0	0	0	0	0	0	2	0	0
C5	kmol/hr	0	0	0	0	0	0	0	0	0
C6	kmol/hr	0	0	0	0	0	0	0	0	0

Table C.2. (cont.) Stream table of CHP

	Units	MT-STM	STM-1	STM-2	STM-3	WATER-1	WATER2	WATER3	WATER4	WATER5
Temperature	C	250	100	1,293	589	30	30	30	223	221
Pressure	bar	25	173	173	1	1	1	1	25	25
Mass Flows	kg/hr	40,356	22,000	22,000	22,000	62,000	21,644	40,356	40,356	40,356
Average MW		18	18	18	18	18	18	18	18	18
Mole Flows	kmol/hr	2,240	1,221	1,221	1,221	3,442	1,201	2,240	2,240	2,240
H2O	kmol/hr	2,240	1,221	1,221	1,221	3,442	1,201	2,240	2,240	2,240
CO	kmol/hr	0	0	0	0	0	0	0	0	0
H2	kmol/hr	0	0	0	0	0	0	0	0	0
CO2	kmol/hr	0	0	0	0	0	0	0	0	0
O2	kmol/hr	0	0	0	0	0	0	0	0	0
N2	kmol/hr	0	0	0	0	0	0	0	0	0
AR	kmol/hr	0	0	0	0	0	0	0	0	0
CL2	kmol/hr	0	0	0	0	0	0	0	0	0
H2S	kmol/hr	0	0	0	0	0	0	0	0	0
NH3	kmol/hr	0	0	0	0	0	0	0	0	0
MEA	kmol/hr	0	0	0	0	0	0	0	0	0
METHANOL	kmol/hr	0	0	0	0	0	0	0	0	0
CH4	kmol/hr	0	0	0	0	0	0	0	0	0
C2H6	kmol/hr	0	0	0	0	0	0	0	0	0
C3	kmol/hr	0	0	0	0	0	0	0	0	0
C4	kmol/hr	0	0	0	0	0	0	0	0	0
C5	kmol/hr	0	0	0	0	0	0	0	0	0
C6	kmol/hr	0	0	0	0	0	0	0	0	0

Table C.3. Stream table of syngas cleaning

	Units	BOTTOM1	BOTTOM2	CLEANGAS	CO2-OUT	DISTILL8	FEEDGAS	FGAS-02	FGAS-07	GAS1
Temperature	C	105	85	37	35	97	39	180	37	35
Pressure	bar	1	1	53	2	1	54	1	53	1
Mass Flows	kg/hr	105,274	105,274	17,361	8,054	36,794	42,278	42,278	17,361	8,039
Average MW		24	24	12	43	21	17	17	12	43
Mole Flows	kmol/hr	4,412	4,412	1,404	188	1,782	2,530	2,530	1,404	189
H2O	kmol/hr	3,789	3,789	2	5	1,589	937	937	2	8
CO	kmol/hr	0	0	470	0	0	470	470	470	0
H2	kmol/hr	0	0	845	0	0	845	845	845	0
CO2	kmol/hr	62	62	0	178	178	178	178	0	178
O2	kmol/hr	0	0	0	3	0	0	0	0	0
N2	kmol/hr	0	0	87	0	0	87	87	87	0
AR	kmol/hr	0	0	0	0	0	0	0	0	0
CL2	kmol/hr	0	0	0	0	0	0	0	0	0
SO2	kmol/hr	0	0	0	0	0	0	0	0	0
SO3	kmol/hr	0	0	0	0	0	0	0	0	0
NO2	kmol/hr	0	0	0	0	0	0	0	0	0
H2S	kmol/hr	0	0	0	0	0	0	0	0	0
NH3	kmol/hr	0	0	0	2	13	13	13	0	2
MEA	kmol/hr	561	561	0	0	1	0	0	0	0
SULFUR	kmol/hr	0	0	0	0	0	0	0	0	0

Table C.3. (cont.) Stream table of syngas cleaning

	Units	GAS2	LEANSOLV	LIQRETUR	MIXED	MKEUPH2O	MKUPSOLV	O2-IN02	OUT1	PUMPED
Temperature	C	50	37	35	50	37	38	25	64	52
Pressure	bar	7	54	1	1	54	1	1	1	54
Mass Flows	kg/hr	8,130	116,869	28,755	116,869	282	3	91	134,032	116,869
Average MW		42	23	18	23	18	61	32	22	23
Mole Flows	kmol/hr	192	5,053	1,594	5,053	16	0	3	6,006	5,053
H2O	kmol/hr	9	4,428	1,581	4,428	16	0	0	5,370	4,428
CO	kmol/hr	0	0	0	0	0	0	0	0	0
H2	kmol/hr	0	0	0	0	0	0	0	0	0
CO2	kmol/hr	178	62	0	62	0	0	0	62	62
O2	kmol/hr	3	0	0	0	0	0	3	0	0
N2	kmol/hr	0	0	0	0	0	0	0	0	0
AR	kmol/hr	0	0	0	0	0	0	0	0	0
CL2	kmol/hr	0	0	0	0	0	0	0	0	0
SO2	kmol/hr	0	0	0	0	0	0	0	0	0
SO3	kmol/hr	0	0	0	0	0	0	0	0	0
NO2	kmol/hr	0	0	0	0	0	0	0	0	0
H2S	kmol/hr	0	0	0	0	0	0	0	0	0
NH3	kmol/hr	2	0	11	0	0	0	0	11	0
MEA	kmol/hr	0	562	1	562	0	0	0	562	562
SULFUR	kmol/hr	0	0	0	0	0	0	0	0	0

Table C.3. (cont.) Stream table of syngas cleaning

	Units	**PURGE**	**RICHSOL1**	**RICHSOL3**	**SULFUR**
Temperature	C	64	65	80	35
Pressure	bar	1	53	53	2
Mass Flows	kg/hr	17,163	142,068	142,068	76
Average MW		18	23	23	20
Mole Flows	kmol/hr	953	6,195	6,195	4
H2O	kmol/hr	942	5,378	5,378	3
CO	kmol/hr	0	0	0	0
H2	kmol/hr	0	0	0	0
CO2	kmol/hr	0	240	240	0
O2	kmol/hr	0	0	0	0
N2	kmol/hr	0	0	0	0
AR	kmol/hr	0	0	0	0
CL2	kmol/hr	0	0	0	0
SO2	kmol/hr	0	0	0	0
SO3	kmol/hr	0	0	0	0
NO2	kmol/hr	0	0	0	0
H2S	kmol/hr	0	0	0	0
NH3	kmol/hr	11	13	13	0
MEA	kmol/hr	0	562	562	0
SULFUR	kmol/hr	0	0	0	0

Table C.4. Stream table of fuelsynthesis

	Units	FGAS-07	FGAS-07B	FGAS-07C	FGAS-07D	FGAS-07E	FGAS-07F	FGAS-08	FGAS-09	FGAS-10
Temperature	C	37	135	210	135	369	135	217	200	200
Pressure	bar	53	53	25	53	25	53	26	26	26
Mass Flows	kg/hr	17,361	17,361	19,193	13,096	6,097	4,265	19,193	19,193	3,237
Average MW		12	12	13	12	14	12	13	13	13
Mole Flows	kmol/hr	1,404	1,404	1,506	1,059	447	345	1,506	1,506	254
H2O	kmol/hr	2	2	30	2	29	1	30	30	5
CO	kmol/hr	470	470	397	355	42	115	397	397	67
H2	kmol/hr	845	845	918	637	281	208	918	918	155
CO2	kmol/hr	0	0	73	0	73	0	73	73	12
N2	kmol/hr	87	87	87	65	21	21	87	87	15
CL2	kmol/hr	0	0	0	0	0	0	0	0	0
CH4	kmol/hr	0	0	0	0	0	0	0	0	0
C2H6	kmol/hr	0	0	0	0	0	0	0	0	0
C3	kmol/hr	0	0	0	0	0	0	0	0	0
C4	kmol/hr	0	0	0	0	0	0	0	0	0
C5	kmol/hr	0	0	0	0	0	0	0	0	0
C6	kmol/hr	0	0	0	0	0	0	0	0	0
C7	kmol/hr	0	0	0	0	0	0	0	0	0
C8	kmol/hr	0	0	0	0	0	0	0	0	0
C9	kmol/hr	0	0	0	0	0	0	0	0	0
C10	kmol/hr	0	0	0	0	0	0	0	0	0

Table C.4. (cont.) Stream table of fuelsynthesis

	Units	FGAS-11	FGAS-11B	FGAS-12	H2	LIQPDT	LIQPDT01	MT-STM1A	PDT-01	PDT-01B
Temperature	C	200	200	200	200	139	70	250	200	139
Pressure	bar	26	26	26	26	26	26	26	26	26
Mass Flows	kg/hr	15,957	15,864	19,101	92	5,351	1,963	1,832	19,101	19,101
Average MW		13	13	13	2	27	148	18	17	17
Mole Flows	kmol/hr	1,252	1,206	1,460	46	201	13	102	1,144	1,144
H2O	kmol/hr	25	25	30	0	188	0	102	188	188
CO	kmol/hr	330	330	397	0	0	0	0	239	239
H2	kmol/hr	763	718	872	46	0	0	0	535	535
CO2	kmol/hr	61	61	73	0	0	0	0	73	73
N2	kmol/hr	72	72	87	0	0	0	0	87	87
CL2	kmol/hr	0	0	0	0	0	0	0	0	0
CH4	kmol/hr	0	0	0	0	0	0	0	2	2
C2H6	kmol/hr	0	0	0	0	0	0	0	2	2
C3	kmol/hr	0	0	0	0	0	0	0	2	2
C4	kmol/hr	0	0	0	0	0	0	0	2	2
C5	kmol/hr	0	0	0	0	2	2	0	2	2
C6	kmol/hr	0	0	0	0	1	1	0	1	1
C7	kmol/hr	0	0	0	0	1	1	0	1	1
C8	kmol/hr	0	0	0	0	1	1	0	1	1
C9	kmol/hr	0	0	0	0	1	1	0	1	1
C10	kmol/hr	0	0	0	0	1	1	0	1	1
C11	kmol/hr	0	0	0	0	1	1	0	1	1
C12	kmol/hr	0	0	0	0	1	1	0	1	1
C13	kmol/hr	0	0	0	0	1	1	0	1	1
C14	kmol/hr	0	0	0	0	1	1	0	1	1
C15	kmol/hr	0	0	0	0	1	1	0	1	1
C16	kmol/hr	0	0	0	0	1	1	0	1	1

Table C.4. (cont.) Stream table of fuelsynthesis

	Units	**SYNGAS01**	**W-WATER2**
Temperature	C	47	70
Pressure	bar	1	26
Mass Flows	kg/hr	13,750	3,389
Average MW		15	18
Mole Flows	kmol/hr	943	188
H2O	kmol/hr	0	188
CO	kmol/hr	239	0
H2	kmol/hr	535	0
CO2	kmol/hr	73	0
N2	kmol/hr	87	0
CL2	kmol/hr	0	0
CH4	kmol/hr	2	0
C2H6	kmol/hr	2	0
C3	kmol/hr	2	0
C4	kmol/hr	2	0
C5	kmol/hr	0	0
C6	kmol/hr	0	0
C7	kmol/hr	0	0
C8	kmol/hr	0	0
C9	kmol/hr	0	0
C10	kmol/hr	0	0

Table C.5. Stream table of HDP

	Units	C12+	C5-C12	FUELGAS	H2	LIQPDT01	LIQPDT02
Temperature	C	50	50	50	200	70	50
Pressure	bar	22	22	22	26	26	22
Mass Flows	kg/hr	910	1,011	134	92	1,963	1,921
Average MW		216	111	3	2	148	144
Mole Flows	kmol/hr	4	9	46	46	13	13
H2O	kmol/hr	0	0	0	0	0	0
CO	kmol/hr	0	0	0	0	0	0
H2	kmol/hr	0	0	45	46	0	0
CO2	kmol/hr	0	0	0	0	0	0
CH4	kmol/hr	0	0	0	0	0	0
C3	kmol/hr	0	0	0	0	0	0
C4	kmol/hr	0	0	0	0	0	0
C5	kmol/hr	0	1	0	0	2	1
C6	kmol/hr	0	1	0	0	1	1
C7	kmol/hr	0	1	0	0	1	1
C8	kmol/hr	0	2	0	0	1	2
C9	kmol/hr	0	0	0	0	1	0
C10	kmol/hr	0	1	0	0	1	1
C11	kmol/hr	0	1	0	0	1	1
C12	kmol/hr	0	1	0	0	1	1
C13	kmol/hr	1	0	0	0	1	1
C14	kmol/hr	1	0	0	0	1	1
C15	kmol/hr	1	0	0	0	1	1
C16	kmol/hr	2	0	0	0	1	2
C17	kmol/hr	0	0	0	0	0	0
C18	kmol/hr	0	0	0	0	0	0
C19	kmol/hr	0	0	0	0	0	0
C20	kmol/hr	0	0	0	0	0	0

Table C.6. Stream table of methanol synthesis

	Units	GAS01	GAS01B	GAS02	GAS03	GAS04	GAS05	GAS06	GAS07	GAS08
Temperature	C	40	40	40	43	451	51	47	494	51
Pressure	bar	107	107	2	110	110	110	1	109	110
Mass Flows	kg/hr	85,540	83,830	1,690	83,830	1,690	85,519	108	108	81,243
Average MW		26	26	41	26	41	26	40	40	26
Mole Flows	kmol/hr	3,332	3,265	41	3,265	41	3,306	3	3	3,141
H2O	kmol/hr	1	1	0	1	0	1	0	0	1
CO	kmol/hr	447	438	0	438	0	439	0	0	417
H2	kmol/hr	775	759	0	759	0	760	0	0	722
CO2	kmol/hr	716	701	28	701	28	729	1	1	692
O2	kmol/hr	0	0	0	0	0	0	0	0	0
N2	kmol/hr	1,253	1,228	3	1,228	3	1,231	0	0	1,169
AR	kmol/hr	0	0	0	0	0	0	0	0	0
CL2	kmol/hr	2	2	0	2	0	2	0	0	2
SO2	kmol/hr	0	0	0	0	0	0	0	0	0
SO3	kmol/hr	0	0	0	0	0	0	0	0	0
NO2	kmol/hr	0	0	0	0	0	0	0	0	0
H2S	kmol/hr	0	0	0	0	0	0	0	0	0
NH3	kmol/hr	0	0	0	0	0	0	0	0	0
MEA	kmol/hr	0	0	0	0	0	0	0	0	0
METHANOL	kmol/hr	24	24	6	24	6	30	1	1	28
CH4	kmol/hr	34	34	0	34	0	34	0	0	32
C2H6	kmol/hr	31	30	1	30	1	31	0	0	29
C2H4	kmol/hr	0	0	0	0	0	0	0	0	0
C2H2	kmol/hr	0	0	0	0	0	0	0	0	0
C3	kmol/hr	27	27	1	27	1	28	0	0	26
C4	kmol/hr	21	21	2	21	2	23	0	0	21

Table C.6. (cont.) Stream table of methanol synthesis

	Units	LIQ01	LIQ02	METHANOL	PDT01	PDT02	PDT03	STM02A	SYNGAS01	SYNGAS02
Temperature	C	40	40	47	272	200	40	250	47	78
Pressure	bar	107	2	1	107	107	107	25	1	1
Mass Flows	kg/hr	9,558	7,868	7,603	95,099	95,099	95,099	5	13,750	13,750
Average MW		32	31	31	26	26	26	18	15	15
Mole Flows	kmol/hr	295	254	243	3,627	3,627	3,627	0	943	943
H2O	kmol/hr	22	22	14	23	23	23	0	0	0
CO	kmol/hr	0	0	0	448	448	448	0	239	239
H2	kmol/hr	0	0	0	775	775	775	0	535	535
CO2	kmol/hr	29	2	1	745	745	745	0	73	73
O2	kmol/hr	0	0	0	0	0	0	0	0	0
N2	kmol/hr	3	0	0	1,256	1,256	1,256	0	87	87
AR	kmol/hr	0	0	0	0	0	0	0	0	0
CL2	kmol/hr	1	0	0	3	3	3	0	0	0
SO2	kmol/hr	0	0	0	0	0	0	0	0	0
SO3	kmol/hr	0	0	0	0	0	0	0	0	0
NO2	kmol/hr	0	0	0	0	0	0	0	0	0
H2S	kmol/hr	0	0	0	0	0	0	0	0	0
NH3	kmol/hr	0	0	0	0	0	0	0	0	0
MEA	kmol/hr	0	0	0	0	0	0	0	0	0
METHANOL	kmol/hr	235	229	228	259	259	259	0	0	0
CH4	kmol/hr	0	0	0	34	34	34	0	2	2
C2H6	kmol/hr	1	0	0	32	32	32	0	2	2
C2H4	kmol/hr	0	0	0	0	0	0	0	0	0
C2H2	kmol/hr	0	0	0	0	0	0	0	0	0
C3	kmol/hr	1	0	0	28	28	28	0	2	2
C4	kmol/hr	2	0	0	23	23	23	0	2	2

Table C.6. (cont.) Stream table of methanol synthesis

	Units	SYNGAS03	SYNGAS04	SYNGAS05	SYNGAS06	SYNGAS07	SYNGAS08	SYNGAS09	SYNGAS10	SYNGAS11
Temperature	C	80	50	148	35	135	137	67	137	150
Pressure	bar	25	25	51	51	110	109	109	109	109
Mass Flows	kg/hr	13,755	13,755	13,755	13,755	13,755	13,863	95,099	95,099	95,099
Average MW		15	15	15	15	15	15	23	23	23
Mole Flows	kmol/hr	943	943	943	943	943	946	4,087	4,087	4,087
H2O	kmol/hr	0	0	0	0	0	0	1	1	1
CO	kmol/hr	238	238	238	238	238	238	655	655	655
H2	kmol/hr	535	535	535	535	535	535	1,257	1,257	1,257
CO2	kmol/hr	74	74	74	74	74	75	767	767	767
O2	kmol/hr	0	0	0	0	0	0	0	0	0
N2	kmol/hr	87	87	87	87	87	87	1,256	1,256	1,256
AR	kmol/hr	0	0	0	0	0	0	0	0	0
CL2	kmol/hr	0	0	0	0	0	0	3	3	3
SO2	kmol/hr	0	0	0	0	0	0	0	0	0
SO3	kmol/hr	0	0	0	0	0	0	0	0	0
NO2	kmol/hr	0	0	0	0	0	0	0	0	0
H2S	kmol/hr	0	0	0	0	0	0	0	0	0
NH3	kmol/hr	0	0	0	0	0	0	0	0	0
MEA	kmol/hr	0	0	0	0	0	0	0	0	0
METHANOL	kmol/hr	0	0	0	0	0	1	29	29	29
CH4	kmol/hr	2	2	2	2	2	2	34	34	34
C2H6	kmol/hr	2	2	2	2	2	2	32	32	32
C2H4	kmol/hr	0	0	0	0	0	0	0	0	0
C2H2	kmol/hr	0	0	0	0	0	0	0	0	0
C3	kmol/hr	2	2	2	2	2	2	28	28	28
C4	kmol/hr	2	2	2	2	2	2	23	23	23

Table C.6. (cont.) Stream table of methanol synthesis

	Units	VENT01	VENT02	W-WATER3
Temperature	C	40	51	98
Pressure	bar	107	110	1
Mass Flows	kg/hr	1,711	4,276	157
Average MW		26	26	18
Mole Flows	kmol/hr	67	165	9
H2O	kmol/hr	0	0	8
CO	kmol/hr	9	22	0
H2	kmol/hr	15	38	0
CO2	kmol/hr	14	36	0
O2	kmol/hr	0	0	0
N2	kmol/hr	25	62	0
AR	kmol/hr	0	0	0
CL2	kmol/hr	0	0	0
SO2	kmol/hr	0	0	0
SO3	kmol/hr	0	0	0
NO2	kmol/hr	0	0	0
H2S	kmol/hr	0	0	0
NH3	kmol/hr	0	0	0
MEA	kmol/hr	0	0	0
METHANOL	kmol/hr	0	1	0
CH4	kmol/hr	1	2	0
C2H6	kmol/hr	1	2	0
C2H4	kmol/hr	0	0	0
C2H2	kmol/hr	0	0	0
C3	kmol/hr	1	1	0
C4	kmol/hr	0	1	0

References for appendix

Aemkulwat, C., 2010. Labor force structure change and Thai labor market, 1990-2008, Proceedings of the Second Annual Conference of the Academic Network for Development in Asia (ANDA), pp. 1-19.

Brown, M.T., Protano, G., Ulgiati, S., 2011. Assessing geobiosphere work of generating global reserves of coal, crude oil, and natural gas. Ecological Modelling 222, 879-887.

Chimres, N., Wongwises, S., 2016. Critical review of the current status of solar energy in Thailand. Renewable and Sustainable Energy Reviews 58, 198-207.

Cohen, M.J., Brown, M.T., Shepherd, K.D., 2006. Estimating the environmental costs of soil erosion at multiple scales in Kenya using emergy synthesis. Agriculture, ecosystems & environment 114, 249-269.

Liese, B., Isvilanonda, S., Nguyen, K., Nguyen, L., Pananurak, P., Romnea, P., Shwe, T., Sombounkhanh, K., Möllmann, T., Zimmer, Y., 2014. Economics of Southeast Asian rice production. Agri Benchmark: Braunschweig, Germany) Available at http://www.agribenchmark.org/fileadmin/Dateiablage/B-Cash-Crop/Reports/Report-2014-1-rice-FAO.pdf [Verified 26 September 2016].

Morandi, F., Perrin, A., Østergård, H., 2016. Miscanthus as energy crop: Environmental assessment of a miscanthus biomass production case study in France. Journal of Cleaner Production 137, 313-321.

Norsuwan, T., Marohn, C., Jintrawet, A., 2014. Effects of irrigation treatments and nitrogen applications on Napier grass planted in dry season as energy crop at Chiang Mai province.

Pansak, W., Hilger, T., Dercon, G., Kongkaew, T., Cadisch, G., 2008. Changes in the relationship between soil erosion and N loss pathways after establishing soil conservation systems in uplands of Northeast Thailand. Agriculture, Ecosystems & Environment 128, 167-176.

VITA

Miss Prathana Nimmanterdwong was born on 10th August 1988 at Mueng Udonthani, Thailand. She received her Bachelor and Master degree in Chemical Technology, Faculty of Science, Chulalongkorn University. Then, she started her doctorate program in the 2012 academic year, again, in the Department of Chemical Technology Faculty of Science, Chulalongkorn University.